Universität Rostock

Traditio et Innovatio

Evaluation of the Post-Accident Load Carrying Performance of Hatch Covers and an Innovative Design Proposal

Dissertation

zur
Erlangung des akademischen Grades

Doktor-Ingenieur (Dr.-Ing.)

Fakultät für Maschinenbau und Schiffstechnik
Universität Rostock

vorgelegt von

M.Sc. Özlem Akkuş

geb. am 24.01.1986 in Zile, Türkei

Rostock
17.06.2022

https://doi.org/10.18453/rosdok_id00004103

Gutachter

Prof. Dr.Eng./Hiroshima Univ. Patrick Kaeding

Lehrstuhl für Schiffstechnische Konstruktionen
Fakultät für Maschinenbau und Schiffstechnik
Universität Rostock

Assoc. Prof. Dr. Ertekin Bayraktarkatal

Fakultät für Schiffbau und Meerestechnik
Istanbul Technische Universität

Datum der Einreichung

17.06.2022

Datum der mündlichen Prüfung

09.12.2022

to the precious memory of my beloved grandmother Türkan Başar…

ABSTRACT

One of the major topics to be investigated in the marine industry is accidents, considering their serious consequences on human life, the environment and the economy. Despite the developments in accident prevention methods and techniques, accidents continue to occur. In this regard, the evaluation of the post-accidental state of vessels becomes significantly important. By a prompt and accurate assessment, the residual structural capacity can be judged and necessary actions can be taken to save lives, avoid environmental hazards and minimise financial loss.

In this thesis, the post-accident load carrying performance of a damaged hatch cover is evaluated through a number of simulations. Dropped object case is selected as the accidental event where the dominant load type is impact. Three individual dropped object simulations are conducted. Although the geometry and properties of the object are kept the same, analysis settings and impact type are applied differently. In the first case, the object falls onto the hatch cover under the effect of gravity and at the end of the simulation, the failed elements are preserved within the structure. The second case is almost identical to the first one, however, element erosion due to failure is allowed. The third simulation focuses on the influence of impact type, thus the dropped object is in a projectile motion which means it has a horizontal velocity in addition to the gravity effect.

In further static analyses, after the transfer of the deformed geometry together with residual stresses and strains, a uniform lateral pressure is applied to the damaged structures and their performances are compared to the intact structure. Results confirm that accurate and sufficiently detailed damage modelling is crucial for post-accident evaluations.

Finally, an innovative design hatch cover design concept is proposed for a competitive structural performance regarding impact load and post-accidental behaviour. Through a section modulus based iterative approach, optimum dimensions are determined and the abovementioned analysis procedure is applied.

This thesis presents a more realistic assessment of the post-accident load carrying performance of hatch covers. The applicability of the use of a single engineering environment is verified for an accurate, prompt and practical post-accident evaluation. Furthermore, the thesis proposes an alternative hatch cover design concept that promises a competitive structural performance while ensuring weight reduction and maintenance ease.

ACKNOWLEDGEMENTS

"*Science is the only true guide for civilization, for life and for success in the world*."

This quote belongs to Mustafa Kemal Atatürk, the founder of secular, modern Turkey and a great reformist. I have found my inspiration and motivation in his vision and achievements since the early years of my life. Therefore, I would like to commemorate him, when I am approaching the end of a meaningful challenge and my most extensive scientific work. His vision, which is predicated on education and science, always enlightens my path.

I am particularly grateful to my academic supervisor, Prof. Dr. Eng. Patrick Kaeding for sharing his valuable expertise and experience. Thanks to his advice, guidance and continuous support, this work could be accomplished. I highly appreciate the freedom and flexibility that he provided, which enabled me to pursue this research even in hard conditions, including the pandemic times. I wish to extend my sincere thanks to Assoc. Prof. Dr. Ertekin Bayraktarkatal, for his contribution and endorsement during my studies. My research significantly benefitted from his comments and feedback. Also, I would like to thank Dr.-Ing. Thomas Lindemann for his guidance and assistance.

Furthermore, I am indebted to Prof. Dr. Ömer Belik, Assist. Prof. Dr. Nermin Tekogul, Assist. Prof. Dr. Yalçın Ünsan, Mr. Neculai Craita and M.Sc. Nilüfer Haftacı, from whom I received a great deal of knowledge regarding naval architecture and structural mechanics, in addition to their meaningful mentorship.

I would also like to thank all my colleagues at Friendship Systems AG, for their valuable support during my preparation phase for the dissertation.

My deepest gratitude and appreciation go to each member of my extended family:

> Mustafa Başar, Türkan Başar, Nermin Akkuş, Hüseyin Akkuş, Solmaz Başar, Elmas Özkan, Engin Başar, Hatice Başar; for giving me a wonderful life, endless love and support.
>
> Didem Akkuş, Barış Deniz Başar and Egemen Başar; for bringing joy to my life.
>
> Georg Pehl; for his very precious love, patience and encouragement.

Özlem Akkuş
Berlin, 2022

Declaration of Authorship

I hereby declare, that I am the sole author and composer of my thesis and that no other sources or learning aids, other than those listed, have been used. Furthermore, I declare that I have acknowledged the work of others by providing detailed references of said work. I also hereby declare that my thesis has not been prepared for another examination or assignment, either in its entirety or excerpts thereof.

Özlem Akkuş

17.06.2022

CONTENTS

1. Introduction 1

1.1 Background 1
1.2 Literature Review 2
1.3 Objective of the Thesis and Methodology 5
1.4 Thesis Structure 7

2. Validation 9

2.1 The Reference Study 9
2.2 Dropped Object Simulation in Ansys Explicit Dynamics 10
2.2.1 Geometry of the Simulation Bodies 10
2.2.2 FE Model 11
2.3 Comparison of the Results and Conclusion 12

3. Geometry and FE Model of the Reference Structure 14

3.1 General Information About Steel Hatch Covers 14
3.2 M/V Derbyshire 15
3.3 Hatch Covers of M/V Derbyshire 17
3.4 Calculated Loads on Hatch Covers 18
3.4.1 Design Load 18
3.4.2 Wave Loads 18
3.4.2.1 Hydrostatic loads 18
3.4.2.2 Hydrodynamic loads 19
3.5 FE Model 20
3.5.1 Modelling Techniques 20
3.5.1.1 Software 20
3.5.1.2 Mesh size 21
3.5.2 The Hatch Cover 21
3.5.3 The Dropped Object 22
3.5.4 Boundary Conditions 23

4. Dropped Object Case – Explicit Dynamic Analysis 25

4.1 Impact Load 25
4.2 Nonlinear FEA and the Selected Software 27
4.3 Material Modelling 28
4.3.1 Bilinear Isotropic Hardening Model 29
4.3.2 Cowper-Symonds Strength Model 29
4.3.3 Material Model of the Simulations 30
4.4 Failure Criteria 30
4.5 Dropped Object Case-1 31
4.6 Dropped Object Case-2 33
4.7 Dropped Object Case-3 35
4.8 Comparison of the Results 37

5. Post-Impact Load Carrying Performance 40

5.1 Load and Failure Types 40
5.2 Post-Accident Performance Evaluation 41
5.2.1 Performance Evaluation Methodology 42
5.2.1.1 Transfer of the Deformed Structure and Residual Stresses 42
5.2.1.2 Nonlinear Static Analysis 43
5.2.2 Analysis Settings 45
5.3 Results and Discussions 46
5.3.1 Deformation Results 48
5.3.2 Equivalent Stress Results 52
5.3.3 Equivalent Total and Plastic Strain Results 55

6. A New Hatch Cover Design Proposal 60

6.1 Previous Hatch Cover Design Optimisation Studies 61
6.1.1 Alternative Materials 61
6.1.2 Alternative Configurations 62
6.2 New Hatch Cover Design Concept 63
6.2.1 Structural Properties of Corrugated Plates 65
6.3 Geometric Details of the Proposed Hatch Cover 67
6.4 Structural Behaviour under Impact Load 70
6.5 Post-Accident Performance 74
6.6 Review and Discussion 79

7. Conclusion and future work 80

References 82

LIST OF FIGURES

Figure 1.1: Casualty types between 2014-2020 [2] 1
Figure 1.2: Bulk carrier loss scenarios [4] 2
Figure 1.3: Methodology 6
Figure 2.1: Dropped object test facility [23] 9
Figure 2.2: Dimensions of the steel plate and the jig 10
Figure 2.3: Meshed structures 11
Figure 2.4: Comparison of experiment and simulation deformation results 12
Figure 2.5: Deformation after impact 13
Figure 3.1: Hatch cover types 14
Figure 3.2: M/V Derbyshire [31] 15
Figure 3.3: Loading condition on the final voyage [32] 16
Figure 3.4: Derbyshire cargo hold-1 port side hatch cover sketch 17
Figure 3.5: Water pressure-time [15] 19
Figure 3.6: Geometry of SHELL 181 and SOLID 186 elements [38] 22
Figure 3.7: Meshed hatch cover and dropped object 23
Figure 3.8: Boundary conditions 24
Figure 4.1: Dissipation of strain energy [35] 26
Figure 4.2: Effective stress – effective strain curve [46] 29
Figure 4.3: Dropped object Case-1 32
Figure 4.4: Dropped object Case-2 35
Figure 4.5: Dropped object Case-3 37
Figure 4.6: Plastic strain results comparison 37
Figure 4.7: Case-1 and Case-2 plastic strain 38
Figure 4.8: Deformation form of Case-2 and Case-3 38
Figure 4.9: Deformation results comparison 39
Figure 5.1: Hinge lines [54] 41
Figure 5.2: Transfer of the results from damage simulation 43
Figure 5.3: Newton-Raphson iterations [60] 45
Figure 5.4: Nodal displacements 49
Figure 5.5: Deformation results 51
Figure 5.6: Equivalent stress results of the plate 52
Figure 5.7: Equivalent stress results of the stiffeners 53
Figure 5.8: Equivalent stress results 55
Figure 5.9: Equivalent plastic strain results of the plates 56
Figure 5.10: Equivalent plastic strain results of the stiffeners 56
Figure 5.11: Equivalent total strain results of the plates 57
Figure 5.12: Equivalent total strain results of the stiffeners 57
Figure 5.13: Equivalent plastic strain results 59
Figure 6.1: Stronger support members [39] 62
Figure 6.2: U-profiles of hatch cover top plate [21] 63
Figure 6.3: Corrugated bulkhead [66, 67] 64
Figure 6.4: 3-D sketch of the corrugated cover concept 64
Figure 6.5: Corrugated hatch cover with PVC foam 65
Figure 6.6: Corrugated bulkhead main dimensions [70] 65
Figure 6.7: Collapse pattern of a corrugated panel [69] 66
Figure 6.8: Single Corrugation under Lateral Pressure [69] 66
Figure 6.9: One-bay model cross-section 67

Figure 6.10: Deformation results of different design proposals 69
Figure 6.11: Comparative deformation results under impact load..... 71
Figure 6.12: Comparative equivalent stress results under impact load..... 72
Figure 6.13: Comparative equivalent plastic strain results under impact load 73
Figure 6.14: Post-accident nodal deformation results..... 75
Figure 6.15: Post-accident equivalent stress results..... 76
Figure 6.16: Post-accident equivalent plastic strain results 77
Figure 6.17: : Post-accident equivalent total strain results 78

LIST OF TABLES

Table 2.1: Maximum deformation results 12
Table 3.1: Main particulars [15] 15
Table 3.2: Pressure heads 19
Table 3.3: Properties of the dropped object 22
Table 4.1: Material properties 30
Table 4.2: Analysis results of dropped object Case-1 31
Table 4.3: Analysis results of dropped object Case-2 33
Table 4.4: Analysis results of dropped object Case-3 35
Table 5.1: Load application 45
Table 5.2: Load carrying performance results – 0.01743 MPa 46
Table 5.3: Load carrying performance results – 0.05403 MPa 47
Table 5.4: Load carrying performance results of middle node – 0.01743 MPa 47
Table 5.5: Load Carrying Performance Results of Middle Node-0.05403 MPa 48
Table 5.6: Z-coordinates of the Middle Node 49
Table 6.1: Geometric properties of the hatch cover 67
Table 6.2: Cross-sections of corrugated segments 68
Table 6.3: Comparison of different design options 69
Table 6.4: Analysis of drooped object case – Corrugated hatch cover 70
Table 6.5: Post-accident performance comparison 74

NOMENCLATURE

C	Cowper-Symond coefficient
C	Hatch coaming height
C	Damping matrix
$E_{kinetic}$	Kinetic energy
E_s	Strain energy
$E_{s,i}$	Strain energy for impacted component
$E_{s,o}$	Strain energy for dropped object
E_t	Effective strain-effective stress second curve slope
F	Freeboard
F_{ext}	External forces
F_{int}	Internal forces
h	Drop height
h	Maximum head
H	Wave length
h_b	Average head
g	Gravity
L	Hatch cover length
l_e	Element length
m	Mass of the object
m	Mean slope of the crest
M	Mass matrix
q	Cowper-Symond coefficient
R	Contact force
R_i	Contact force for dropped object
R_o	Contact force for impacted component
Rot_x Rot_y Rot_z	Rotational constraints about respective axes
t	Plate thickness
t	Time
u	Displacement vector
U_x U_y U_z	Displacement constraints in respective x,y,z directions
w	Deformation
w_i	Deformation for dropped object
w_o	Deformation for impacted component
v	Velocity
Z	Section modulus

$\{F^a\}$	Vector of applied loads
$\{F_i^{nr}\}$	Vector of restoring loads corresponding to the element internal loads
$[K_i^T]$	Jacobian matrix (tangent matrix)
$\{u_i\}$	Displacement vector
$\{\Delta u_i\}$	Displacement increments

α	Nonlinear wave ratio
ε	Strain
ε_e	Necking
ε_f	Failure strain
ε_{eff}	Effective strain
ε_g	Uniform strain rate
ε_{xx} ε_{yy} ε_{zz}	Normal strain components
ε_{xy} ε_{yz} ε_{zx}	Shear strain components
λ	Load factor
σ_y	Static yield stress
σ_{yd}	Dynamic yield stress

[Blank page]

1. INTRODUCTION

1.1 Background

According to the United Nations Conference on Trade and Development (UNCTAD) review in 2020, more than 80% of world trade volume is transported by the shipping industry [1]. Therefore, the safety of ships is a very critical subject, which is mainly threatened by accidental events. European Maritime Safety Agency (EMSA) states that between the years 2014 and 2020, 19418 accidental events were reported, 162 vessels were totally lost and 2137 vessels were considered unfit to proceed [2].

Although a large number of researches and projects concerning accident prevention have been conducted over the last decades, accidents are still inevitable. Thus, post-accidental evaluation of ship condition is also a crucial topic in terms of life saving, prevention of environmental hazards and financial loss. For post-accident evaluation of the structure and to determine the safety actions, two major topics must be considered. Those are the type of accidents and the affected structure of the vessel.

The type of accident is important to understand the accidental load and determine the relevant assessment method. Annual Overview of Marine Causalities and Incidents 2021 Report of EMSA [2] revealed that 43% of causalities between 2014-2020 were caused by collision, contact and grounding/stranding, as seen in Fig. 1.1. The dominant accidental load regarding the listed causality types is impact load. Therefore, impact load is of interest in this study.

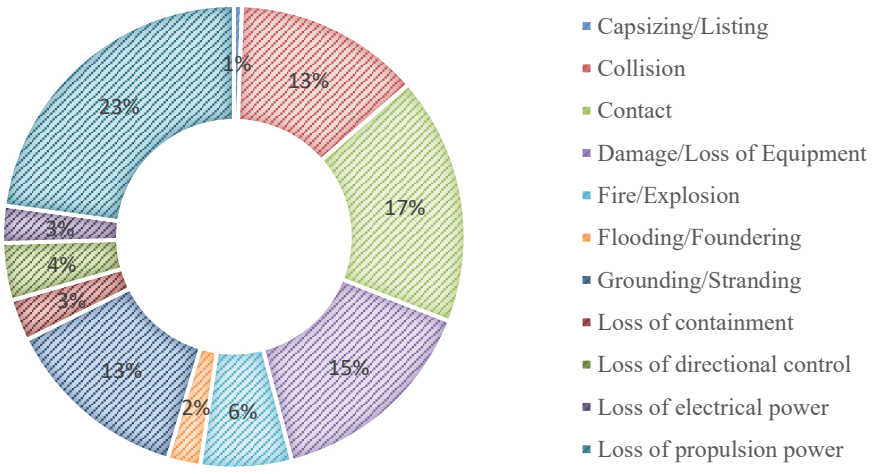

Figure 1.1: Casualty types between 2014-2020 [2]

On the other hand, while accidental damage is crucial for the overall structure, the particular importance of individual structural elements is another topic to be investigated. For instance, the loss of bulk carrier M/V Derbyshire with 44 people on board, drew considerable attention to the catastrophic consequences of hatch cover failure, since it is one of the most probable loss scenarios [3]. Paik and Thayamballi [4] presented a schematic demonstration of bulk carrier loss scenarios, as seen in Fig. 1.2. This schema further supports the argument about role of hatch cover failure, in vessel loss.

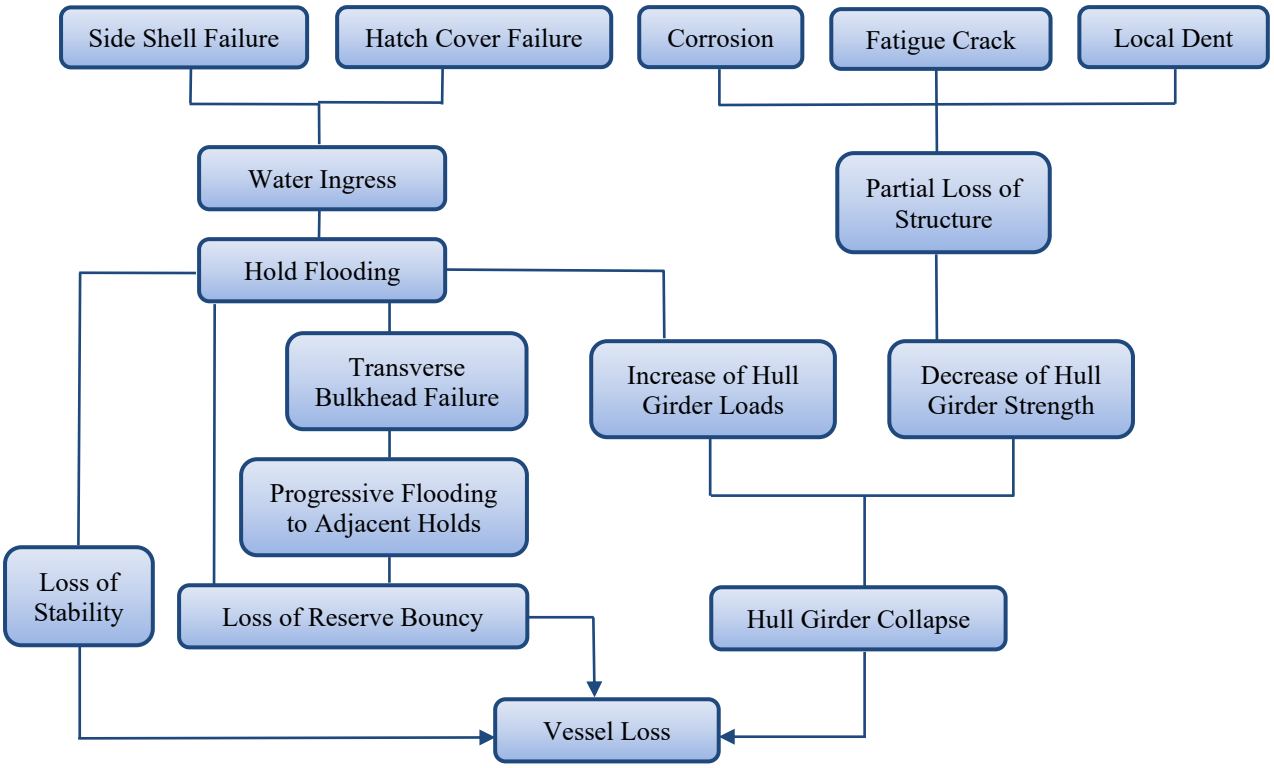

Figure 1.2: Bulk carrier loss scenarios [4]

Considering the criticality of hatch cover failure for vessel safety and high risk of impact load as a failure cause, the overall aim of this thesis is to investigate the post-accident load carrying performance of a hatch cover and propose an improved design alternative.

1.2 Literature Review

A considerable body of literature exists on the impact load and residual strength of ships. Paik et. al [5] aimed to develop a prompt method to assess the collapse of the hull girder due to collision and grounding damage. Respectively, section modulus and ultimate bending strength based, residual strength indexes were defined. Later in another study, Paik et. al [6] proposed a new method for the assessment of ship safety after grounding. The method defines "Residual Strength – Damage (R-D) Index Diagram" as a function of the location and extent

of the damage. It was suggested that R-D diagrams could be utilised for the safety level judgement of the damaged vessel. Underwood [7] focused on improving the modelling of damaged structures for rapid salvage operations in emergency cases. The study demonstrated a better understanding of the influence of damage on the failure mechanism of the structure. Alie et. al [8] investigated the influence of asymmetrical damage on the hull girder ultimate strength by analysing three-cargo-hold model of a bulk carrier with damage on the side shell due to collision. Soares et. al [9] carried out an assessment of the useability of simplified structural analysis methods based on Smith's formulation, for the prediction of damaged ship ultimate strength. A benchmark study was performed, first on the intact structure and later on the same structure with damage modelling. Saad-Eldeen et. al [10] analysed the ultimate compressive strength of highly damaged plates due to impact loads such as dropped objects, grounding or collision which could cause an indentation in forms of hemisphere, cube and prism. Witlowska and Soares [11] focused on compressive behaviour and ultimate strength of locally damaged plate panels, affected by fall or strike of an object, as well.

The common feature of the abovementioned studies is their conventional damage modelling technique. In conventional damage modelling, the damage is represented either by removal of the relevant structural elements in the affected area or the application of different slenderness ratios. However, the conventional method remains inadequate for a realistic representation of the effect of the accidental damage. Because geometric distortion is not the only influencing factor on residual strength, besides residual stresses resulting from plastic deformation must be taken into account [12]. In this respect, Smith and Dow [12] proposed a two-phased method that consists of an initial simulation of the damage by applying and removing lateral load and consequently applying axial compressive load. In this way, residual stresses can be obtained from the first phase and residual strength can be analysed more accurately in the second phase. Authors highlighted that including damage process simulation might be vital to fully calculate the damage effects in residual strength analysis. In the same manner, Nikolov [13] conducted a damage simulation to obtain residual deflection and stresses by loading and unloading a plate with forced lateral displacements. Then, compressive load was applied to the deformed structure and ultimate strength is calculated. The study revealed that ultimate strength could be overestimated without consideration of residual stresses. Also, Cai et.al [14] performed a two-phase analysis that concerned a stiffened plate under impact forces. After damage simulation, the deformed structure was exported into the static analysis phase together with the residual stresses. In order to analyse the residual strength, uniaxial load was applied to the damaged structure.

The studies which took residual stress into account, are more advanced in comparison to the studies in which conventional damage modelling was employed. However, a closer look reveals some drawbacks. The key problem regarding the realistic representation of accidental cases is that damage simulations were not extensively conducted. Moreover, the boundary conditions were defined differently in damage and ultimate strength assessment simulations, which cause discrepancies. Besides, the damaged structure export techniques were not addressed.

On the other hand, hatch cover design and strength assessment are among widely discussed topics in literature. Historically, “An Independent Assessment of the Sinking of the M/V Derbyshire” by Faulkner [15] is one of the studies which comprehensively involved the subject of hatch cover loads and collapse possibilities. Dallinga and Gaillarde [16] performed experiments with the scaled model of M/V Derbyshire in order to define the hatch cover loads during the typhoon Orchid which caused the loss of the vessel. Yao et.al [17] proposed a simple method to evaluate the collapse strength of hatch covers that are exposed to lateral pressure load. For this aim, folding type and sliding type hatch covers were examined through a series of elastoplastic large deflection analyses. Also, the influence of different designs, such as according to ICLL and IACS rules, on the structural performance of hatch cover was observed. Mohammadrahimi and Sayebani [18] presented the failure probability and reliability of hatch covers by using MATLAB.

Furthermore, hatch cover design improvement has been explored in prior studies. For instance, Li et.al [19] suggested FRP composite as an alternative material for hatch covers, to achieve weight reduction and corrosion resistance while keeping high strength. Tawfik et.al [20] replaced steel with E-Glass composite, again for weight reduction and better structural performance. Studies revealed that despite the weight and strength advantages of alternative materials, the acquisition cost of steel hatch cover is still more profitable. Alongside, optimisation of steel hatch cover design was of interest to some patented researches, such as replacing typical stiffeners with U-Type profiles [21]. Correspondingly, a program to determine the optimal dimensions of U-Type profiles of a hatch cover was developed by Um and Roh [22]. In addition, Shi and Gao [23] compared the ultimate strength of U-Type profiles with bulb profiles of a selected panel.

1.3 Objective of the Thesis and Methodology

After reviewing the literature, it can be concluded that although residual strength of damaged structures and ultimate strength of hatch covers were deeply investigated in previous studies, there are still some gaps and shortcomings which can be summarised as below:

- In the studies which follow conventional damage modelling by removing the elements in the affected area and neglecting residual stresses, representation of real accidental cases is not possible.
- Although the studies which involves damage simulations to obtain deformation and residual stresses, are relatively more comprehensive; the use of different boundary conditions for the same structure in damage and ultimate strength calculation simulations, is unreasonable. Those studies offer no explanation for the transfer of the deformed structure from damage simulation to ultimate strength calculation. Moreover, the effect of residual strains is not examined.
- The studies that concern damaged hatch covers, exclusively focus on the calculation of residual strength under the effect of in-plane loads, whereas lateral loads remain to be addressed.

As stated earlier, the main goal of the current thesis is to examine the post-accident load carrying performance of a hatch cover and propose an alternative design. Together with the deductions from the literature review in mind, the research aim is:

- To investigate post-accident lateral load carrying performance of a hatch cover that is impacted by a dropped object, through a simulation chain:
    - dropped object simulation
    - transfer of the deformed structure, residual stresses and residual strains
    - static analysis by application of lateral pressure
- To demonstrate a practical and prompt calculation approach in a single tool, by verifying the capabilities of the selected engineering environment for the abovementioned chain of analyses.
- To propose an alternative steel hatch cover design configuration, for a competitive structural performance especially against accidental loads, while securing weight and maintenance benefits.

Prior publications of the author regarding some of the aspects of the research aims, which were published during the course of this work, are referenced properly throughout the thesis.

The methodology which is used within the framework of this thesis involves three stages: explicit dynamic analysis, transfer of the damaged structure and nonlinear static analysis.

Dropped object case is chosen as the accidental event and three individual explicit dynamic analysis systems are employed, namely Case-1, Case-2 and Case-3. Although the same geometry and boundary conditions are assigned in each simulation, there are slight differences between the analysis settings. Case-1 and Case-2 are almost identical except for the use of element erosion function. Failed elements, which exceed the element distortion value, are removed from the system in Case-2, while they are kept in Case-1. In this way, the influence of more realistic damage representation is investigated. On the other hand, in Case-3 the dropped object has horizontal velocity, in addition to the gravity effect in other cases. Element erosion is also allowed in Case-3. Details of each case are given in Chapter-4.

During the transfer phase, the deformed body from Case-1 is exported directly to the further analysis system, while the bodies from Case-2 and Case-3 require an additional process to transfer the eroded elements data. Moreover, residual stresses and strains are obtained from the dynamic analyses and assigned to the deformed bodies for static analyses separately.

Post-accident structural performances of deformed structures are examined in nonlinear static systems. Following the order of the transfer phase, two sub-cases (A and B) are defined for each deformed structure. In the sub-cases with notation A, simulations are conducted on deformed structures, with only residual stresses assigned. Whereas, the sub-cases with notation B, involve residual strains additionally. Fig. 1.3 illustrates the schematic representation of the methodology. More details regarding the transfer and static analyses phases can be found in Chapter-5.

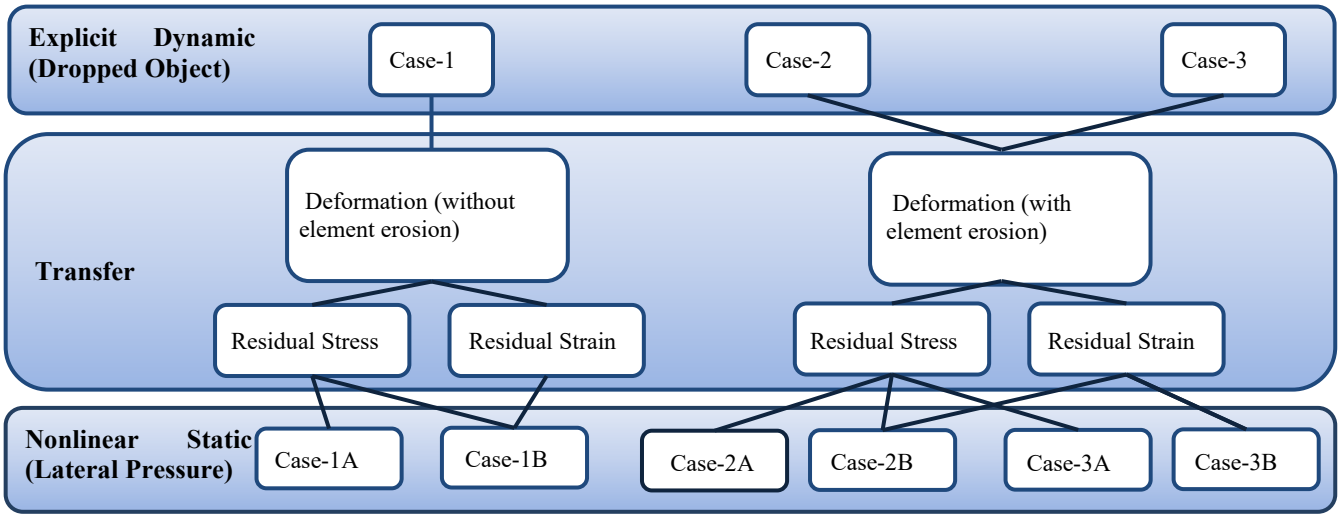

Figure 1.3: Methodology

1.4 Thesis Structure

This thesis is structured as follows:

- Chapter 1 gives a brief overview of the topic, presents the state of art and describes the overall aim of the research together with the methodology.
- Chapter 2 verifies the simulation process of dropped object events, by referencing an experimental study. Although explicit dynamic and nonlinear static simulations are included in this thesis, it is considered sufficient to present validation of only the explicit dynamic method due to its higher complexity and relatively less predictability.
- Chapter-3 presents a general information about steel hatch covers and a brief history of the loss of M/V Derbyshire which arose more attention to the cruciality of hatch cover structure for vessel safety. Also, this chapter details the geometry, calculated loads and FE model of M/V Derbyshire's hatch cover, since it is selected as the reference structure in this thesis.
- Chapter-4 provides information about impact load, calculation methods and nonlinear finite element analysis. Moreover, the details of the material models and failure criteria are described. In this chapter, which focuses on damage simulation, three different dropped object analyses are conducted in explicit dynamic systems. Element erosion function for distorted elements and different impact types such as free-fall and projectile motion are explored. By comparative studies, it is demonstrated that accurate and realistic accident simulation is essential and simplifications should be avoided for the assessment of residual state of the damaged structure.
- Chapter-5 addresses the load and failure types, the theoretical background of nonlinear calculations and the applied analysis settings of the simulations. The post-accident load carrying performances of the deformed hatch covers, under lateral pressure load are examined through six nonlinear static analyses. Deformed geometry, residual stresses and residual strains are transferred from explicit dynamic analysis systems to nonlinear static systems for further analyses. The influence of impact type and accident simulation method on evaluation of post-accident behaviour of the structure is observed. On the other hand, the capabilities of the selected engineering environment to be able to execute accurate and rapid calculations for a sophisticated chain of events are verified.
- Chapter-6 summarises the prior studies on hatch cover design optimisation and proposes an innovative design concept that promises a competitive structural performance while achieving weight reduction and maintenance ease. Scantlings of

the proposed concept are determined by an iterative approach based on section modulus and the structural performance under static design load. The claimed advantages of the new design concept are proven via a series of simulations. A dynamic analysis is conducted to examine the behaviour of the proposed structure against impact load. The post-accident performance is evaluated by a static analysis and compared with the original structure`s.

- Chapter-7 presents a summary of findings and draws conclusions based on the obtained results. Recommendations for future work are given.

2. VALIDATION

In this thesis, a dropped object scenario is simulated as an accidental case. It is conducted in an explicit dynamic analysis system. In order to validate the simulation method in the preferred engineering environment, “An experimental and numerical study on nonlinear impact responses of steel-plated structures in an Arctic environment” by Kim et. al [24] is considered to be the proper reference, due to the similar analysis case.

2.1 The Reference Study

In the reference study [24] a series of experiments were conducted in a dropped object test facility which consists of a cone-shaped striker, a rigid jig and the steel specimens as Type-1 (unstiffened) and Type-2 (with cross-shaped flat bar stiffeners). The specimens were welded to the rigid jig at the edges. The experiments were conducted at room temperature and at -60° C separately. To simulate the drop case, the striker hit the centre of the steel test specimen from different drop heights as 3 m and 5 m. A high-speed camera and strain gauges were used to measure the velocity and strains. The test facility is shown in Fig. 2.1 [24].

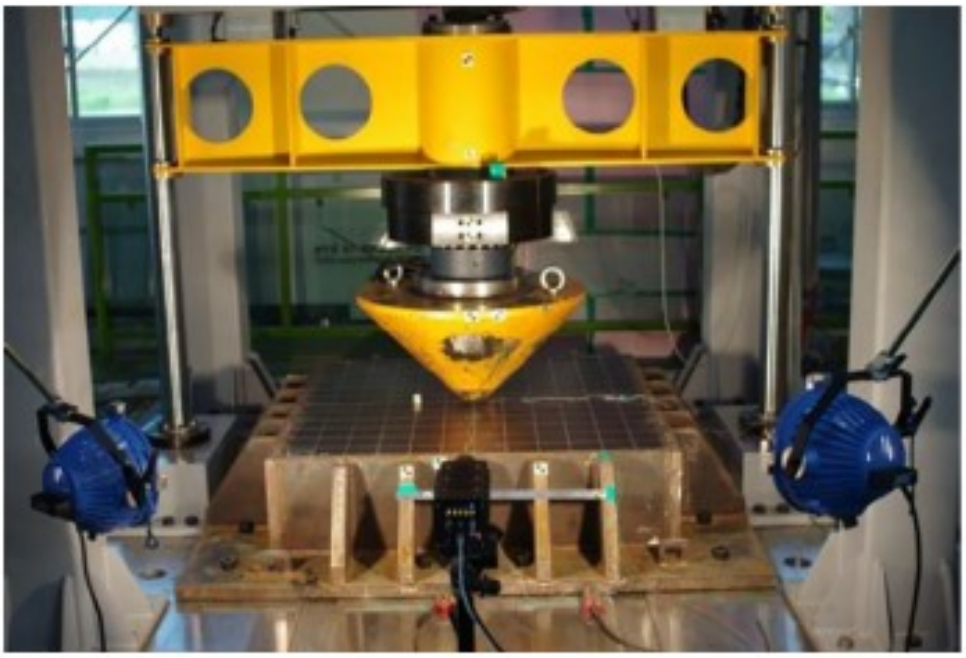

Figure 2.1: Dropped object test facility [24]

Respectively, the drop cases were simulated in LS-Dyna 3D to compare the results. Shell elements with a mesh size of 20 mm were assigned to the test structure, after a mesh-convergence test to determine the best mesh size which has a strong effect on the accuracy of the results and the computation time. The material model was chosen as piecewise linear

plasticity and strain rate effects were also considered. Therefore, C=3200 /q=5 and C=40.4 / q=5 were defined as Cowper-Symonds coefficients in two different analyses for comparison. Simulations were conducted at both room temperature and -60° C as well [24].

2.2 Dropped Object Simulation in Ansys Explicit Dynamics

2.2.1 Geometry of the Simulation Bodies

As stated in the previous part, the dropped object experiment of the reference study is simulated in Ansys Explicit Dynamics, for the validation of the methodology and calculation tools of this thesis. The experiment scenario Case-1 [24] is taken as the reference which is conducted at room temperature with Type-1 non-stiffened steel plate and 3 m of drop height. Dimensions of the plate are 1200 x 1200 x 6 mm, while the weight of the striker is about 11.5 kN, together with the striker holder.

The simulation bodies are modelled in Ansys Workbench Design Modeler, based on the data received from the authors of the reference study. The steel plate, which is exposed to the impact load, is placed on a solid jig. The dimensions and the configuration of the setup are presented in Fig. 2.2.

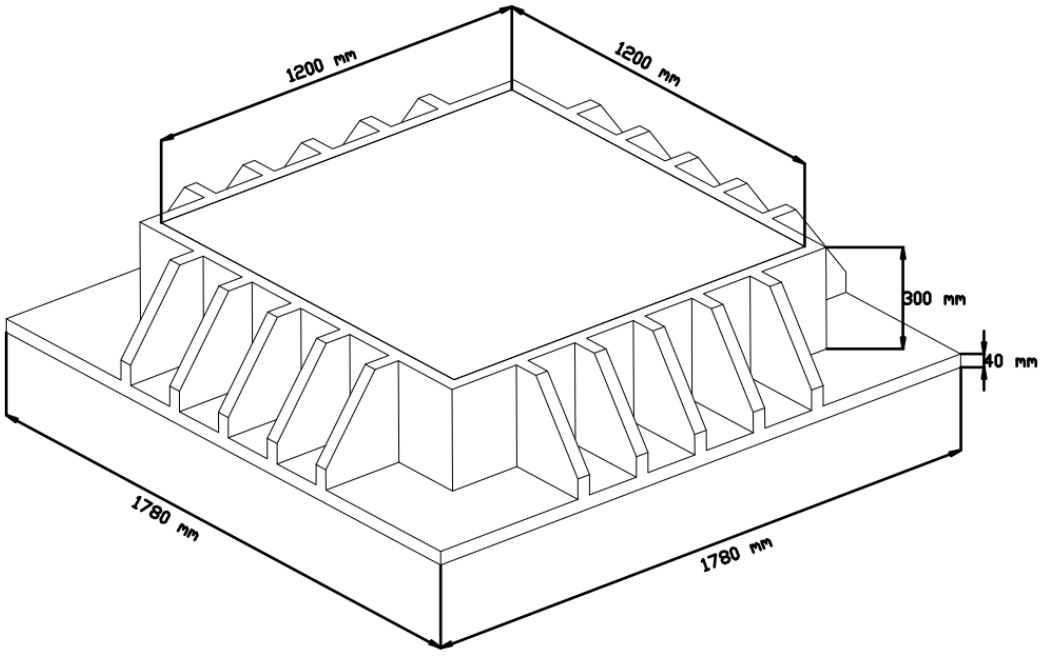

Figure 2.2: Dimensions of the steel plate and the jig

2.2.2 FE Model

While solid elements are chosen for the jig and the striker, shell elements are used for the test plate. Those are assigned as SOLID 186 and SHELL 181 element types respectively in ANSYS Workbench, by default [25]. The details of element properties are given in Chapter 4.

Between the test plate and the upper edges of the jig, “bonded contact type” is defined to represent the welding in reality. Moreover, Ansys Workbench defines “body interactions” by default in explicit dynamic analysis system, which is the proper contact type for the dropped object simulations [26]. Body interaction type is defined as frictional with 0.3 friction coefficient, as in the reference.

The mesh element size of the test plate is defined as 20 mm, in compliance with the reference study, also by considering the element size dependency of the plastic strain results. 3600 shell elements are generated for the test plate mesh. The striker and the jig are formed of 3803 solid elements in total, with a minimum edge length of 40 mm. Coarser mesh is thought proper for those solid structures, as the main objective is to analyse the behaviour of only the test plate. Meshed structures can be seen in Fig. 2.3. Cowper-Symonds coefficients are defined as C=3200 and q=5. Material models are discussed in Chapter 4 and the constitutive equation of Cowper-Symonds model is presented in Eq. 4.4.

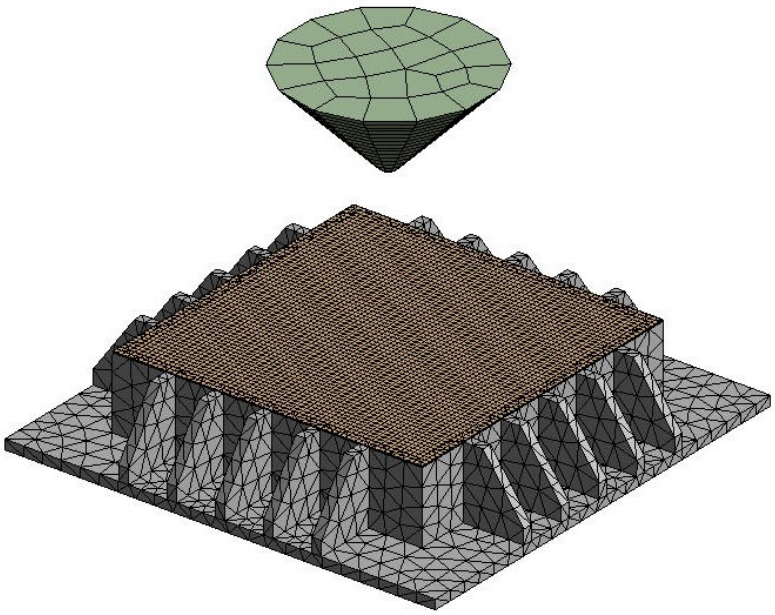

Figure 2.3: Meshed structures

The bottom surface of the jig is fixed in the vertical direction and the specified bolt locations are fixed in the horizontal direction, in order to represent the real conditions of the experimental setup. To validate the method which is used in this study, only Standard Earth Gravity with a default magnitude of 9806.6 mm/s^2 is applied to the rigid striker. Hence the free-fall of the solid object by the effect of the gravity is simulated.

2.3 Comparison of the Results and Conclusion

To verify the accuracy of the dropped object simulation which is conducted in Ansys Explicit Dynamics environment, the deformation results of the simulation and experiment are compared. As it can be seen in Table 2.1 the results of the FE analysis in the selected engineering environment are in good agreement with the experiment results. The insignificant error magnitude of circa 1.7% could be attributed to modelling limitations, as it is indicated also by the authors of the reference study [24].

Table 2.1: Maximum deformation results

Deformation	Experiment	Ansys Explicit Dynamics	Error
	109.28 mm	107.42 mm	~0.017

For a more detailed look, Fig. 2.4 presents a comparative deformation plot over time. The moment of impact of the striker on the plate is set as t_0=0 (s). Apart from the slight discrepancy after the moment of impact, the deformation graphs of the results from the experiment and the simulation are almost identical.

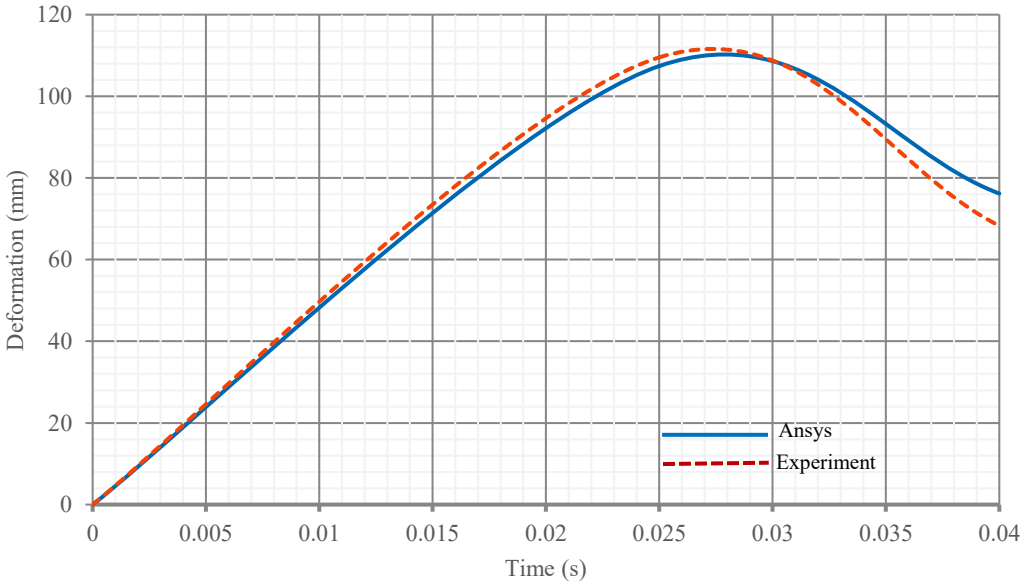

Figure 2.4: Comparison of deformation results of the experiment and simulation

Moreover, the deformation pattern of the test plate can be seen in Fig. 2.5(a) and (b) which are obtained from the experiment and FE simulation respectively. The similarity of the deformation patterns constitutes further evidence for the validity of the explicit dynamic analysis methodology.

To sum up, verification of explicit solutions is only possible by comparison to experimental results. In this chapter, dropped object simulation method in Ansys Explicit Dynamics is validated by comparison of the deformation magnitudes and pattern with the results of the experiment by Kim et. al [24]. The findings confirm the accuracy and the reliable use of the method in the preferred engineering environment for dropped object simulation.

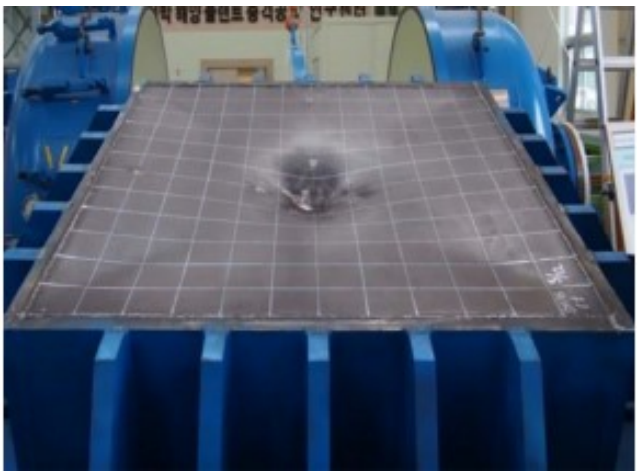

(a) Experiment

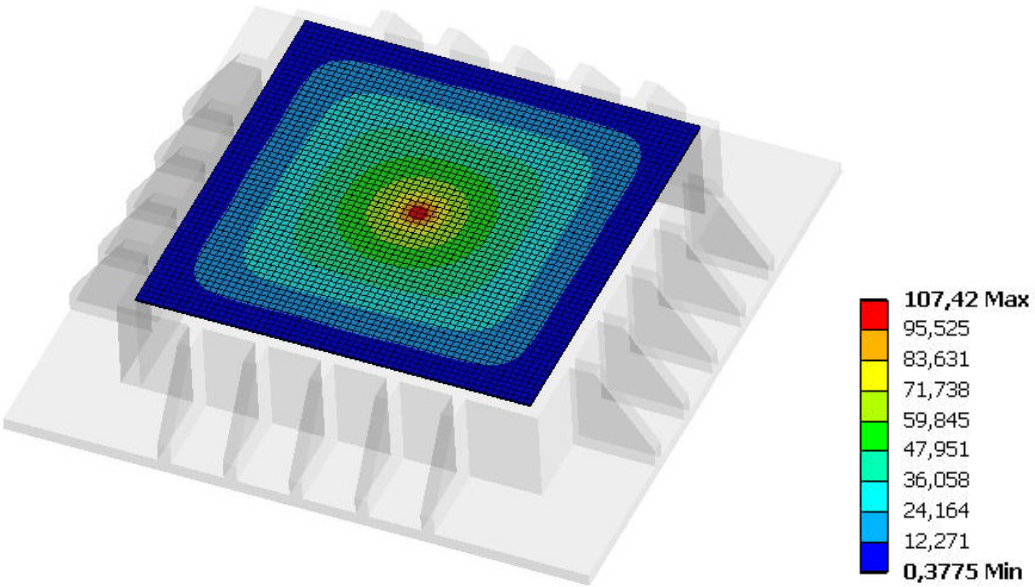

(b) Simulation

Figure 2.5: Deformation after impact

3. GEOMETRY AND FE MODEL OF THE REFERENCE STRUCTURE

3.1 General Information About Steel Hatch Covers

Hatch covers are one of the critical structural elements of cargo ships due to their direct influence on cargo safety, cargo hold safety and consequently structural integrity of the vessel. Moreover, hatch cover type and operation method strongly affect cargo handling practices and the time spent in the ports. Definition of the hatch cover is given as "A large steel structure fitted over a hatch opening to prevent the ingress of water into the cargo hold. It may also be the supporting structure for deck cargo." by Jan Babicz [27].

To fulfil the purpose of maintaining watertightness for the cargo hold and resistance against green water, various types of hatch covers with different materials have been designed over the years. The first steel hatch cover was developed by Robert and Joseph MacGregor and patented in 1929 due to the aroused concerns after the preventable loss of North Sea coal miners in the 1920s [28]. Today, hatch covers are designed by taking many factors into consideration such as ship type, cargo type, voyage type, geometric restrictions, operation methods, water-weathertightness requirements, production techniques and cost.

International Load Line Convention [29] and IACS UR S21 [30] are the main regulatory documents which concern hatch cover design. Alongside, classification societies generate their rules for hatch cover design and requirements, in accordance with the two documents mentioned above.

To be able to describe the main characteristics of different hatch cover types systematically, Buxton et. al grouped hatch covers into five categories based on their operation methods [31], as given in Fig. 3.1:

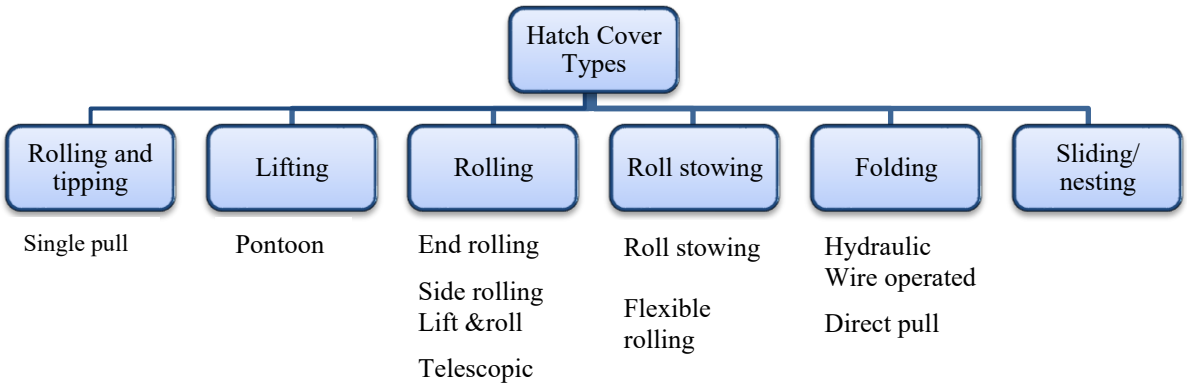

Figure 3.1: Hatch cover types

On the other hand, IACS categorises hatch covers according to their structural configuration [30]. Those are:

- **Single skin cover:** Continuous top and side plating, open underneath with the stiffening structure exposed.
- **Double skin cover:** Continuous top, side and bottom plating, stiffening structure and internals are protected from the environment.
- **Pontoon type cover:** A special type of portable cover, secured weathertight by tarpaulins and battening devices. However, modern lift-away hatch covers are called as pontoon, although it does not fit to this description. Those modern lift –away hatch covers should be considered as single or double skin covers. [30].

The category of the hatch cover which is used in this study is a lift-away single skin cover.

3.2 M/V Derbyshire

The loss of capsize bulk carrier M/V Derbyshire with 44 people on board, had great importance on carrying the topic of safety of bulk carriers onto the international platform. After this accident, international organisations and classification societies examined the structural weaknesses of bulk carriers with higher sensitivity and revised the design criteria and limitations.

M/V Derbyshire was an OBO carrier, as seen in Fig. 3.2 which was built among the 6 sister ships in the period 1970-1976 at Haverton Hill Shipyard in the UK. It was one of the largest and safest ships of its era. The main particulars of the ship are given in Table 3.1 [15]:

Table 3.1: Main particulars [15]

L	B	D	C_B	$T_{SERVICE}$	T_{SUMMER}	Δ_{MAX}	DWT_{MAX}
281.94 m	44.20 m	24.99 m	0.84	17.04 m	18.46 m	203.80 t	173.20 t

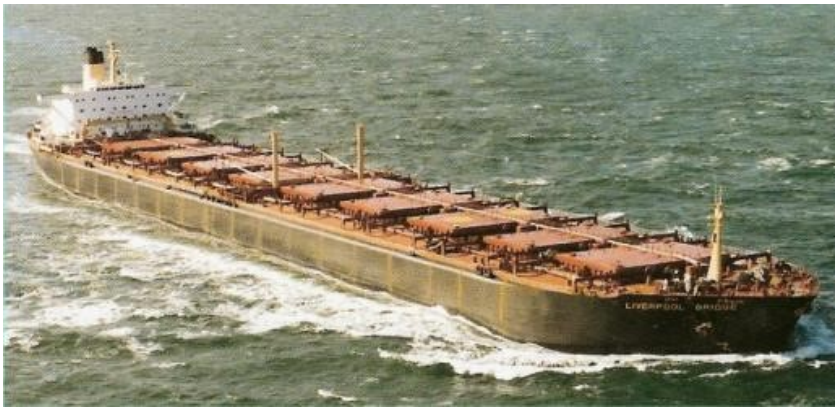

Figure 3.2: M/V Derbyshire [32]

The vessel was classed with Lloyd`s Register and the hull was double skinned with a double bottom and categorised as B-60 type according to the ICLL [29] which allowed 60 cm reduced freeboard in comparison to regular B class. M/V Derbyshire was loaded 158000 tonnes of ore concentrates, which were distributed in 7 of the 9 holds as seen in Fig. 3.3, during its final voyage to Yokohama/Japan with an estimated mean draught T≈18.0 m and freeboard F≈7.0 m. On 9th-10th September 1980, during the typhoon Orchid, M/V Derbyshire was lost around 400 miles away from Shikoku Island/Japan, with 44 people on board [15].

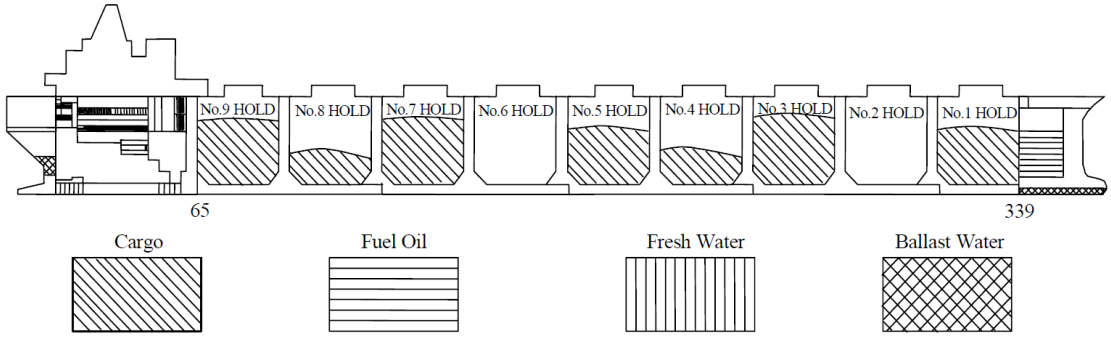

Figure 3.3: Loading condition on the final voyage [33]

There were limitations for obtaining concrete evidence due to the late start of investigations and the fact that the ship was immersed. Therefore, accident scenarios were developed based on sister ships. Although the official investigation in 1994 could not conclude on clear explanations for the exact reason of the accident, among 13 loss scenarios, the two most probable causes were emphasised [34]. Those are:

- Hatch cover collapse
- Deck fracture at Frame 95 due to fatigue

A considerable number of studies have been conducted which investigated loss scenarios of M/V Derbyshire; hence the details of the possible causes are not presented repetitively in this study. However, M/V Derbyshire accident is a valuable case which highlighted the importance of hatch covers for vessel safety and that initiated more extensive and sensitive hatch cover design considerations. Therefore, the hatch cover of M/V Derbyshire is chosen as the reference hatch cover to conduct the simulations in this study. This choice also provides an opportunity to analyse the investigated cases on a real structure.

3.3 Hatch Covers of M/V Derbyshire

M/V Derbyshire had 9 cargo holds and each hold had 2 hatch covers at port and starboard sides. According to the most probable loss scenario, hatch cover of Cargo Hold 1 collapsed first and caused flooding in the hold [35]. In this study, port side pair of Cargo Hold 1 hatch cover is modelled and investigated for the computation time efficiency. A two-dimensional Autocad sketch of this pair is presented in Fig. 3.4 and the geometric properties are listed below [35]:

- Panel breadth: 11,000 mm
- Panel length: 14,680 mm
- Plate thickness: 10.5 mm
- Center transverse girder: T 920 x 10.5 x 75 x 25 mm
- 2 side girders: T 560 x 10.5 x 100 x 25 mm
- 10 longitudinal stiffeners: T 635 x 10.5 x 280 x 25 mm (spacing b=994 mm)

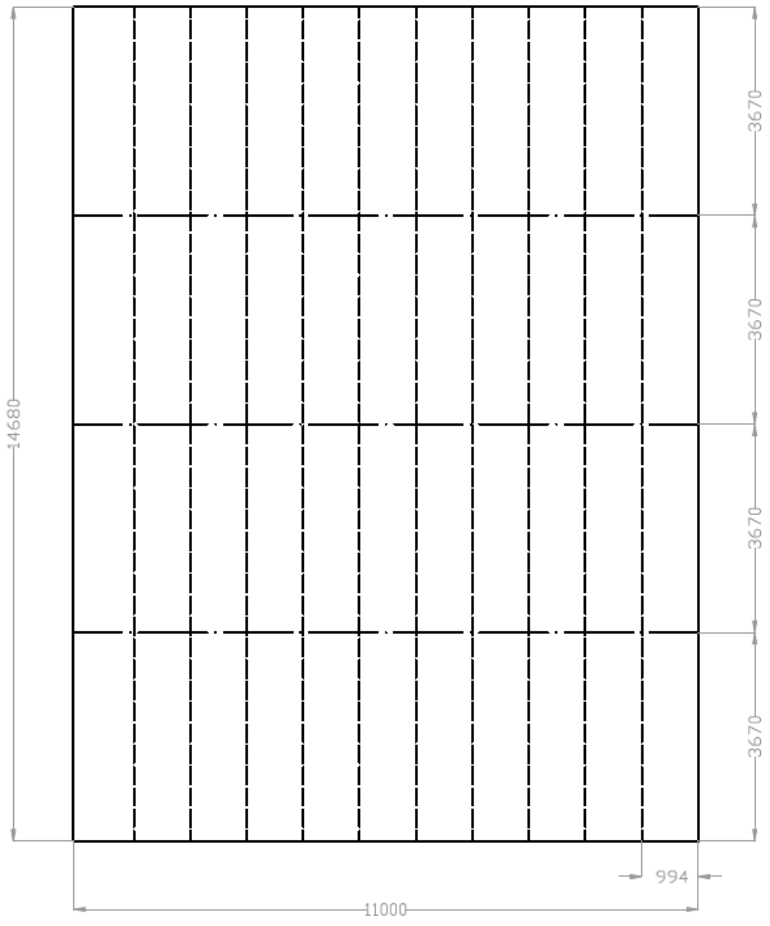

Figure 3.4: Derbyshire cargo hold-1 port side hatch cover sketch

3.4 Calculated Loads on Hatch Covers

3.4.1 Design Load

Faulkner [15] stated that M/V Derbyshire hatch covers were designed according to ICLL 1966 [29] which requires the following strength criteria for hatch covers located at a quarter length from the forward perpendicular (0.25 L) and made of mild steel:

- Design load, uniform static pressure should be not less than 1.75 tonne/m^2
- Maximum stress should not exceed Ultimate Tensile Strength/4.25
- Steel plate thickness should be not less than 1% of the stiffener spacing or 6 mm

Moreover, Faulkner [15] calculated the maximum head on the hatch cover by using UTS criterion, thus allowable maximum stress value Ultimate Tensile Strength/4.25 equals $0.40\sigma_y$ for mild steel and Ultimate Stress could be assumed as $1.25\sigma_y$. Here, 1.25 is the value of shape factor for T-beams. Then load factor is calculated by using Eq. (3.1)

$$Load\ factor(\lambda) = \frac{Ultimate\ stress}{Design\ stress} = \frac{1.25\sigma_y}{0.4\sigma_y} = 3.125 \tag{3.1}$$

Consequently, collapse load can be calculated by the applications of load factor as in Eq. (3.2)

$$Load\ factor(\lambda) = \frac{Collapse\ load}{Design\ load}$$

$$3.125 = \frac{Collapse\ load}{1.75\ tonne/m^2} \tag{3.2}$$

$$Collapse\ load = 5.47\ tonne/m^2$$

3.4.2 Wave Loads

3.4.2.1 Hydrostatic loads

Accident scenarios also investigated extreme wave height probabilities which might have led to the collapse of forward hatch covers during the Typhoon Orchid. Due to the longer natural pitch period of the ship than the wave period, it was assumed that instead of rising on the wave crests, the ship was plunging through the steep waves [35].

By using a quasi-static wave profile and the characteristic equations, Faulkner [15] presented the most probable extreme wave heights and pressure heights as in Eq. (3.3).

$$h = \alpha H - (F + C)$$
$$h_b = h(1 - \frac{mL}{4h}) \quad (3.3)$$

where;

H=wave height *C = coaming height, 2.0 m*

h = maximum head *F = freeboard, 6.9 m*

h_b=average head *L= hatch cover length, 14.68 m*

α= nonlinear wave ratio, 0.65 *m = mean slope of the crest (for typhoon Orchid), 0.5*

Table 3.2 presents the pressure heads for the assumed wave height range of the nonlinear waves [15].

Table 3.2: Pressure heads

H [m]	**20**	**22**	**24**	**26**	**28**	**30**
H[m]	4.1	5.4	6.7	8.0	9.3	10.6
h_b[m]	2.3	3.6	4.9	6.2	7.5	8.8

3.4.2.2 Hydrodynamic loads

In Derbyshire wreckage, brittle fracture evidence was found on the hatch covers especially along with the welding. For mild steel, brittle fracture could be caused by very steep pressure impulses which are called gifle peak, due to the breaking or plunging waves. Water particles can reach a very high velocity in milliseconds and create a strong impact force when they hit. Fig. 3.5 illustrates the gifle peak pressure which reaches 200 kN/m^2 [35].

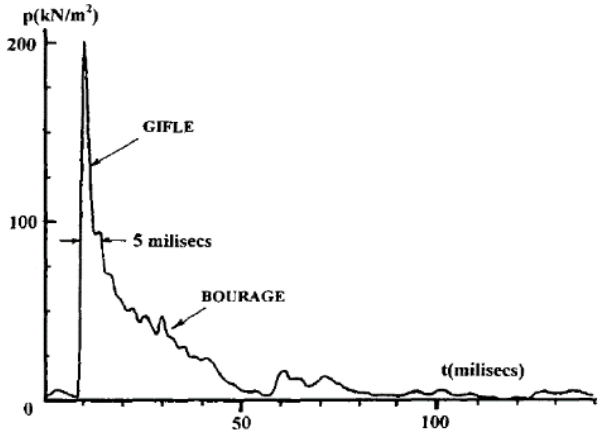

Figure 3.5: Water pressure-time [15]

Design loads and the most probable wave loads that Cargo Hold 1 hatch cover of M/V Derbyshire could have been exposed to, were explained above. Considering the aim of this study, it is not necessary to conduct analysis for each load case. However, the most relevant of those loads are applied to the structure, to be compliant with the real case.

3.5 FE Model

As it is stated before, the loss of M/V Derbyshire drew attention and initiated reviews regarding the importance of hatch cover design principles for ship safety. Thus, hatch cover geometry of M/V Derbyshire is used to generate the reference hatch cover model in this study, which concerns the behaviour of hatch covers under different loads and proposes a new structural configuration. The scantlings of the cover are given in detail in section 3.3.

On the other hand, accidental cases have been widely investigated for the safety of marine structures. DNVGL-RP-C204 [36] is a recommended practice document which is focused on achieving the design which enables the structure to withstand loads caused by accidental events. According to this recommended practice, one of the most prescriptive accidental events is dropped object case, based on risk studies and experience [36]. Considering merchant ships, hatch covers are one of the structures which are most frequently exposed to dropped object cases, especially during loading and unloading operations.

Therefore, in this thesis, it is assumed that a prismatic rigid object drops onto M/V Derbyshire`s hatch cover and the behaviour of the hatch cover under this impact load is investigated.

3.5.1 Modelling Techniques

In finite element analysis, modelling is an important pre-processing step which influences the results directly and should be accomplished accurately and sensitively. On the other hand, this process should be fast and efficient [25].

3.5.1.1 Software

Akkus and Kaeding [37] investigated the relation between different modelling techniques and analysis results in their study which also concerns dropped object case. First of all, they studied the modelling efficiency and import compatibility of three different commercial software packages which are Ansys Design Modeller, Autocad and Solidworks; due to the importance of import capabilities, when it comes to the performance of the engineering environment for practical implementations. Authors concluded that the influence of different

software packages is inconsiderable on modelling, so import and the selection of the software package was entrusted to user preference [37]. In this study, all models are generated in Ansys Design Modeller, due to the modification flexibility within the software environment.

3.5.1.2 Mesh size

Failure strain limit is the main criteria for such analysis and is dependent on mesh element size [38] which is explained in the Chapter 4. Therefore, Akkus and Kaeding [37] conducted a mesh convergence study to determine the mesh size and performed simulations with 200, 150, 125 and 100 mm element sizes. The findings revealed that equivalent plastic strain result increased inversely proportional to element size, in a similar manner the limit value also increased due to its dependency on the element size. As a result, it was observed that with mesh refinement, the study converged, however smaller element size led to longer computational time.

Based on the evaluation above, in order to keep the computation time reasonable, it is decided to assign 200 mm mesh element size to the structure. 200 mm is the upper limit which is recommended by Zhang et. al [38], for the determination of realistic failure of elements in impact studies.

3.5.2 The Hatch Cover

The reference hatch cover model is generated in Ansys Design Modeller and shell elements are chosen for the structural components. SHELL 181 element type is assigned by the software for shell elements [25], which is suitable for the analysis. As seen in Figure 3.6, SHELL 181 is a 4-node element that is appropriate for the analysis of moderately-thick shell structures. It has 6-degrees of freedom, as 3 translations in x, y and z directions and 3 rotations about x, y and z-axes, at each node. Employing SHELL 181 is proper, especially in case of nonlinearities, large deformations and rotations. In nonlinear analyses, shell thickness change is also considered automatically [39]. Logarithmic strain and true stress measures are the base of the element formulation. To ensure a congruent mesh at the intersecting surfaces, “Joint” operation is applied to all components of the hatch cover structure and a multibody part is formed [37]. In this case, additional contact definition for the connection of the components is not required because nodes are shared in the multibody [26]. Mild steel is assigned as material type which is explained in section 4.2 in detail. The shell body that represents the hatch cover consists of 9012 nodes and 8906 elements, with 200 mm element size and adaptive sizing.

3.5.3 The Dropped Object

The rigid object which dropped onto the hatch cover model was assumed as a component of a wind turbine and modelled as a rectangular prism with the dimensions of 1m x 1m x 2 m, in the study of Akkus and Kaeding [37]. Similarly in this study, a hypothetical case is investigated, thus it is acceptable to model the dropped object as a simple solid rectangular prism made of Mild Steel, with the same dimensions; while keeping in mind that geometry simplification could have an influence on results in finite element analysis and should be done carefully. The object is located at 6.5 m height from the upper surface of the hatch cover, which is assumed as z=0. Moreover, it is aimed to land the object approximately in the middle of the hatch cover, so –x and -y coordinates are adjusted accordingly in different drop scenarios. Ansys Workbench assigns SOLID 186 element type for solid objects, by default [25]. SOLID 186 is a 3-D solid element with 20 nodes which has 3-degrees of freedom on each, as translations in x, y and z directions. It shows a quadratic displacement behaviour. Plasticity, hyperelasticity, creep, stress stiffening, large deflection and large strain capabilities are supported by SOLID 186. Either uniform reduced integration method or full integration method is used. The geometry the of element can be seen in Figure 3.6.

The mesh element size of the dropped object is also assigned as 200 mm for the coherence. The object consists of 396 Nodes and 250 elements. The properties of the object are listed in Table 3.3. Fig. 3.7 illustrates the meshed structure of the hatch cover and the dropped object.

Table 3.3: Properties of the dropped object

Dimensions [mm]	Mass [t]	Centre of Gravity [mm]	
		case-1 & case-2	case-3
x= 1000, y= 1000, z= 2000	18	x= 7300, y= 5000, z= 7500	x= 2573.5, y= 5000, z= 7500

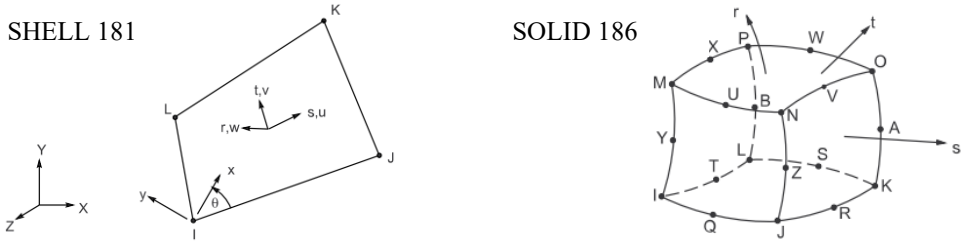

Figure 3.6: Geometry of SHELL 181 and SOLID 186 elements [39]

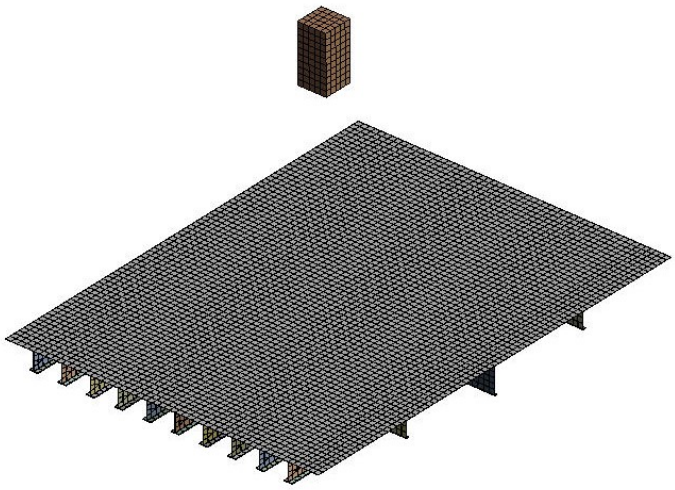

Figure 3.7: Meshed hatch cover and dropped object

3.5.4 Boundary Conditions

As explained in the previous section, the analysed model is in this study is the whole structure of a hatch cover. In reality, this structure rests on the hatch coaming. In M/V Derbyshire case, the hatch covers were attached to the coaming by cleats and the hatch cover pairs had securing catches between port and starboard covers. However, in this study, in order to avoid complications boundary conditions are simplified, while confirming that they represent the real condition accurately. The boundary conditions are summarised below and shown in Fig. 3.8:

- Port and Starboard edges: displacements in y- and z- directions; rotation around z- axis are constrained.
- Aft and Forward edges: displacements in x- and z- directions; rotations around z- axis are constrained.
- Standard earth gravity of -9806.6 mm/s^2 in z- direction is applied.

Free-fall of the rigid object is actualised by the gravity effect in all simulations. Later, in section 4.5 horizontal speed is assigned to the dropped object, which is explained in the relevant part.

“Body interactions” is automatically defined by the software in explicit dynamics analysis system as contact type for two bodies; the hatch cover and the dropped object which are interacting. The friction coefficient is set as 0.3 in compliance with previous studies [24].

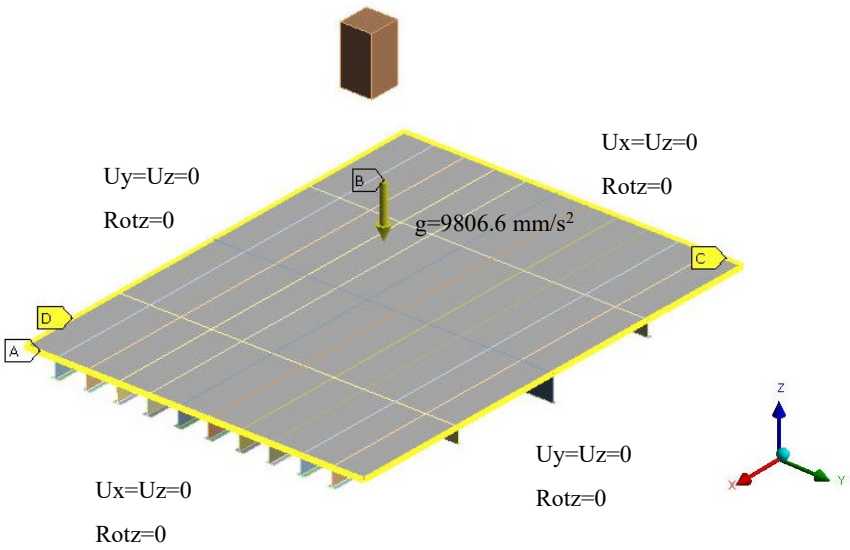

Figure 3.8: Boundary conditions

4. DROPPED OBJECT CASE –EXPLICIT DYNAMIC ANALYSIS

4.1 Impact Load

Marine structures are subjected to loads during their operational life. The load types are categorised by Paik and Thayamballi [40] in four groups according to their origin and characteristics:

- Dead loads (permanent loads) the position and magnitude of dead loads are independent of time and this load type is dominated by the gravity, such as the weight of the structures or permanent components which are immobile.
- Live loads are also dominated by the gravity; however, the magnitude and position may vary in time during the operation, i.e. human on board, mobile equipment, consumable goods.
- Environmental loads are caused by natural events such as wind, waves, currents, snow and earthquake. They are mostly time-dependent and might have recurring patterns.
- Accidental loads originate as a result of accidents which could be defined as undesired events and technical failures. Accidental loads are highly time-dependent. For marine structures, relevant accidental events could be listed as collision, grounding, explosion, fire and dropped objects [40].

On the other hand, Pauling [41] classified loads that impose on marine structures according to their time variability characteristics and grouped them as: static loads, low-frequency dynamic loads, high-frequency dynamic loads and impact loads.

This study investigates a dropped object case; therefore accidental loads are of interest. Accidental loads can be dynamic or impact loads, depending on their time variance. Dropped object loads are considered as impact loads [42].

The main characteristic of dropped object load is the kinetic energy which is associated with the mass of the object and the velocity at the moment of impact [36]. Kinetic energy of a free-falling object is calculated as in Eq. (4.1)

$$E_{kinetic} = \frac{1}{2}mv^2 , \qquad v = \sqrt{2gh} \tag{4.1}$$

where;

m=mass of the object *h= drop height* *v= velocity* *g= gravity*

A significant amount of kinetic energy is dissipated as strain energy in the structure which is subjected to impact and also in the dropped object. Therefore, large plastic strains and structural damage occur. In order to estimate the strain energy dissipation, force-deformation relationships are examined. Those relationships can be shown as in Fig. 4.1 [36].

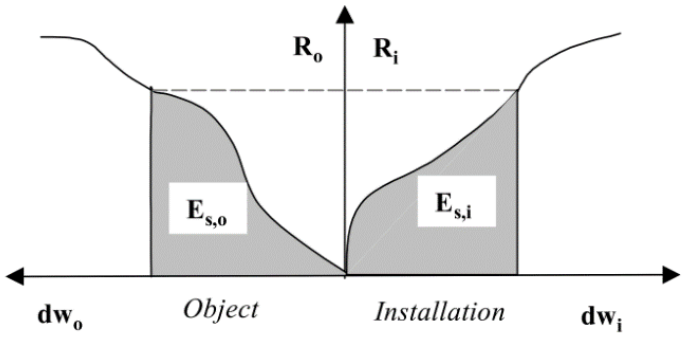

Figure 4.1: Dissipation of strain energy [36]

The total area under the curve equals to the dissipated strain energy and could be formulated as in the Eq. (4.2):

$$E_s = E_{s,o} + E_{s,i} = \int_0^{w_{o,max}} R_o dw_o + \int_0^{w_{i,max}} R_i dw_i \tag{4.2}$$

where;

E_s= Strain energy ($E_{s,o}$= for the dropped object; $E_{s,i}$= for the impacted component)
R= Contact force (R_o=for the dropped object; R_i=for the impacted component)
w= Deformation (w_o=for the dropped object, w_i=for the impacted object)

Generally, the dropped object is assumed to be rigid, thus dissipated energy is relevant only for the impacted component [36].

Since the mechanical response of the structures to accidental loads involves energy dissipation, large deformations and strains which are beyond the elastic range, plasticity methods should be used for the analyses of such loads. Similarly, in dropped object cases, the structural effect due to the impact, can be determined by nonlinear dynamic finite element analysis [36].

4.2 Nonlinear FEA and the Selected Software

After stating that nonlinear finite element analysis is the suitable method to analyse dropped object case; the fundamentals of nonlinear analysis and the features of the selected software Ansys are briefly discussed in this section.

The nonlinear structural behaviour is related to 3 main causes:

- Geometric nonlinearities, due to large deformations and stress stiffening
- Material nonlinearities; which could be characterised by plasticity, creep, nonlinear elasticity, viscoelasticity and hyper elasticity
- Changing status nonlinearities, which represent the change in the physical status of the system through the contact and boundary conditions [43].

In order to solve the nonlinear problems, either implicit or explicit methods could be used; however the method should be selected carefully according to the nature and the requirements of the problem. The equation of motion Eq. (4.3) is expressed by matrix equation for dynamic problems and this is also the governing equation for both implicit and explicit methods [44]:

$$M\ddot{u}(t) + C\dot{u}(t) + F_{int}(t) = F_{ext}(t) \tag{4.3}$$

where;

M= mass matrix F_{int}*= internal forces*

u= displacement vector F_{ext}*= external forces*

C= damping matrix *t= time*

Both methods divide the process into time increments and apply the load through those time steps.

There have been numerous studies to compare the advantages and the efficiency of those methods for different type of problems. Concisely, implicit methods utilize matrix inversions and iterations to solve the equation. State of the current time increment is defined based on the data of the same time increment together with the previous time increment. Accuracy is ensured by convergence criterion. Implicit method is stable even for large time steps. The iterations and matrix inversions lead quite long computational time, in case of very large deformations, due to the much bigger size of stiffness matrix [44,45,46].

On the other hand, explicit methods solve the equation for the current time increment, based on the data only from the previous time increment. Therefore, there is no need for iteration.

Also, no convergence check is required because of uncoupled equations. Inversion of stiffness matrix is not needed. To ensure the accuracy, size of time steps is limited. Due to the smaller time steps, explicit methods are more suitable for highly time dependent, short duration events such as impact or explosion analysis, while implicit methods are suitable for much slower events [44,45,46].

Thus, in this study Ansys Workbench Explicit Dynamics suite is chosen for the impact simulations.

4.3 Material Modelling

The response of the material to an applied load is mathematically represented by the material models and it is another important aspect in FEA, which has direct effect on simulation results.

Initially when the deformation is proportional to loading, metals show elastic behaviour which recovers deformation upon the removal of the load. In case of further loading beyond the elastic limit, deformation is not recoverable which means plastic strain develops within the structure. For instance, under highly dynamic loading, structures can quickly reach their elastic limit and deform plastically. For such structures which are subjected to loading beyond the elastic limit, plasticity models is used to define the material. Important characteristics of the plastic material models are [47]:

- Yield criterion: Material state when plastic strains initiate. For steel materials, generally Von Mises theory.
- Flow rule: Correlation between the increment of plastic strain and load.
- Hardening rule: Evaluation of yield surface during plastic deformation. Two types of hardening are defined. Those are: isotropic hardening in which the yield surface equally expands in every direction and kinematic hardening in which the shape of yield surface remains same while the origin of the surface shifts (Baushinger effect) [48].

To determine the material properties, experiments and tests are conducted or the data from previous experiments and standard tables can be used. There are many constitutive plasticity models to represent the elasto-plastic behaviour [47]. Within Ansys Explicit Dynamics eight different plasticity models are available currently: Bilinear Isotropic Hardening, Multilinear Isotropic Hardening, Kinematic Isotropic Hardening, Kinematic Multilinear Hardening, Johnson-Cook Strength, Cowper-Symonds Strength, Steinberg-Guinan Strength, Zerili-

Armstrong Strength. Bilinear Isotropic Hardening and Cowper-Symonds models are two of the most widely used material models for impact studies in this field.

4.3.1 Bilinear Isotropic Hardening Model

Bilinear isotropic hardening is defined by a bilinear curve of effective stress-effective strain curve as illustrated in Fig. 4.2. The first slope of the curve represents the elastic modulus up to the initial yield stress. In the plastic range where the plastic strains occur, the relationship between stress and strain is defined by E_T which is the second slope of the curve [47].

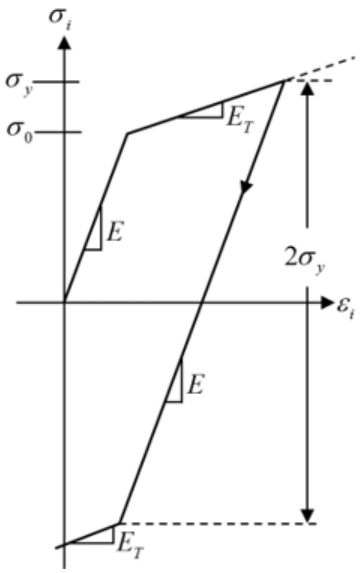

Figure 4.2: Effective stress – effective strain curve [47]

4.3.2 Cowper-Symonds Strength Model

The mechanical properties of the material could be influenced by environmental conditions and loading pattern. For instance, loading speed affects the properties of structural steel which indicates that strain rate is an important parameter [40]. Eq. (4.4) is the constitutive equation of Cowper-Symond model that includes strain rate parameters [24,49]:

$$\frac{\sigma_{Yd}}{\sigma_Y} = 1 + \left(\frac{\dot{\varepsilon}}{C}\right)^{\frac{1}{q}} \tag{4.4}$$

where;

σ_{Yd}= *dynamic yield stress* σ_Y= *static yield stress*

$\dot{\varepsilon}$ = *strain rate* C= *coefficient* q= *coefficient*

The coefficients C and q are determined based on experiment results [24]. For mild steel, C=40.4 and q=5 [49].

4.3.3 Material Model of the Simulations

Akkus and Kaeding [37] investigated the behaviour of hatch covers made out of mild and high tensile steel under impact load. Also, the study evaluates the strain rate effect by comparing bilinear isotropic hardening and Cowper-Symonds material models. As a result, it is observed that mild steel is more sensitive to strain rate effect, in compliance with the previous studies in the literature [50]. Since Cowper-Symonds material model is highly dependent on experiment results and it is possible to get different results for the same material in different conditions, material properties should be defined very carefully [51]. It is concluded that in lack of sufficient experimental data, Cowper-Symonds model is not reliable and it is preferred to use more conservative approach such as bilinear isotropic material model to define the plastic properties [37].

Similarly, in this thesis bilinear isotropic material model is applied in all simulations. The material is assigned as mild steel and the material properties of the structure can be seen in Table 4.1.

Table 4.1: Material properties

Density	Elasticity Modulus	Poissons`Ratio	Yield Strength	Tangent Modulus
7850 kg/m^3	210 GPa	0.3	235 MPa	672 MPa

4.4 Failure Criteria

When the accidental loads are of interest, energy dissipation related failure criteria is preferred to assess the structural capacity [40]. The amount of energy dissipation, which is equivalent to straining, is limited by fracture [36]. Fracture is characterised as the critical situation in finite element analysis and very large strain values are reached at the time of initial fracture [38]. Thus, it could be concluded that the plastic strain is the essential parameter to evaluate the failure in nonlinear analysis, in plastic range.

In the literature, some approaches have been suggested for the determination of critical plastic strain value [52,53,54]. Akkus and Kaeding [37] compared the results of dropped object simulations to the failure criteria presented by Scharrer et.al [52] as in Eq. (4.5):

$$\varepsilon_f(l_e) = \varepsilon_g + \varepsilon_e \frac{t}{l_e} \tag{4.5}$$

where;

ε_f= *failure strain* ε_g= *uniform strain rate* ε_e= *necking*

t= *plate thickness* l_e= *element length*

Uniform strain rate and necking are taken 0.056 and 0.54 respectively for shell elements [52]. Due to the dependency of the formulation on mesh element size, the failure strain value decreases, as the element length increases. In this study the applied mesh element length is 200 mm and the plate thickness is 10.5 mm, thus the critical strain value ε_{cr} can be calculated in Eq. (4.6):

$$0.056 + 0.54\frac{10.5}{200} = 0.08435 \tag{4.6}$$

4.5 Dropped Object Case-1

After modelling the geometry, material and boundary conditions as described in section 1.3, the system is solved only under the gravity effect. Erosion of the elements which exceed the plastic strain limit is not allowed, thus the collapsed elements are kept in the structure. The response of the hatch cover to the impact load is presented as maximum deformation, equivalent stress and plastic strain results over the simulation time in Table 4.2 and Fig. 4.3.

Table 4.2: Analysis results of dropped object Case-1

Case-1	Deformation [mm]	Equivalent Stress [MPa]	Equivalent Plastic Strain [-]
Plate	239.86	231.44	0.0130
Stiffener	233.87	266.91	0.1251

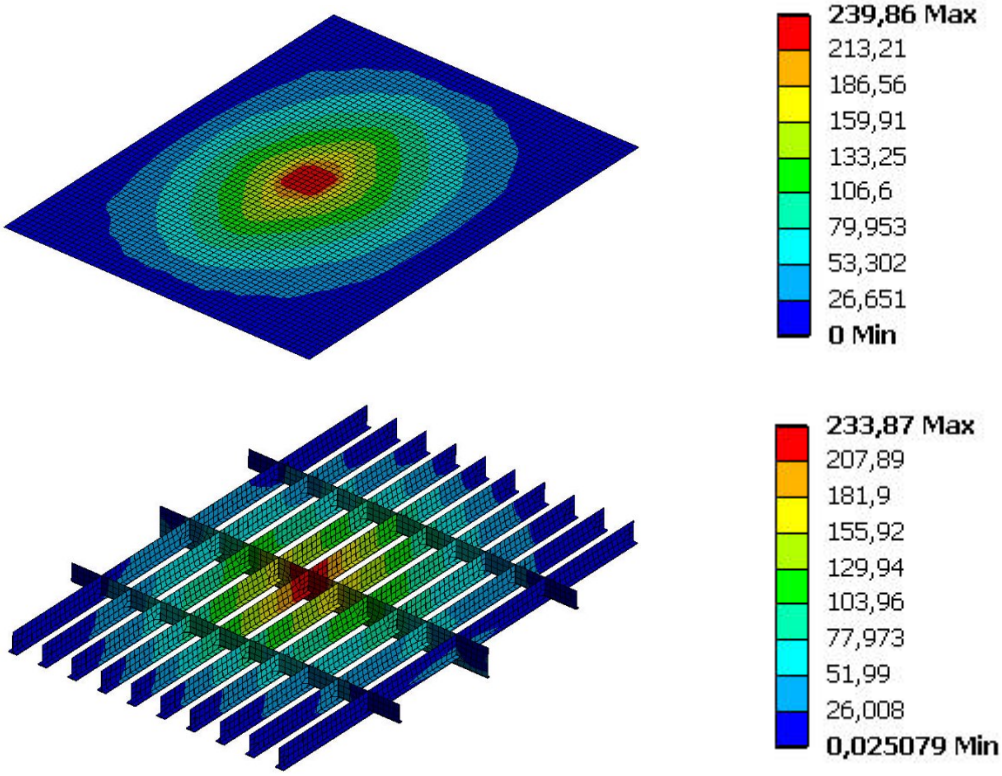

(a) Deformation

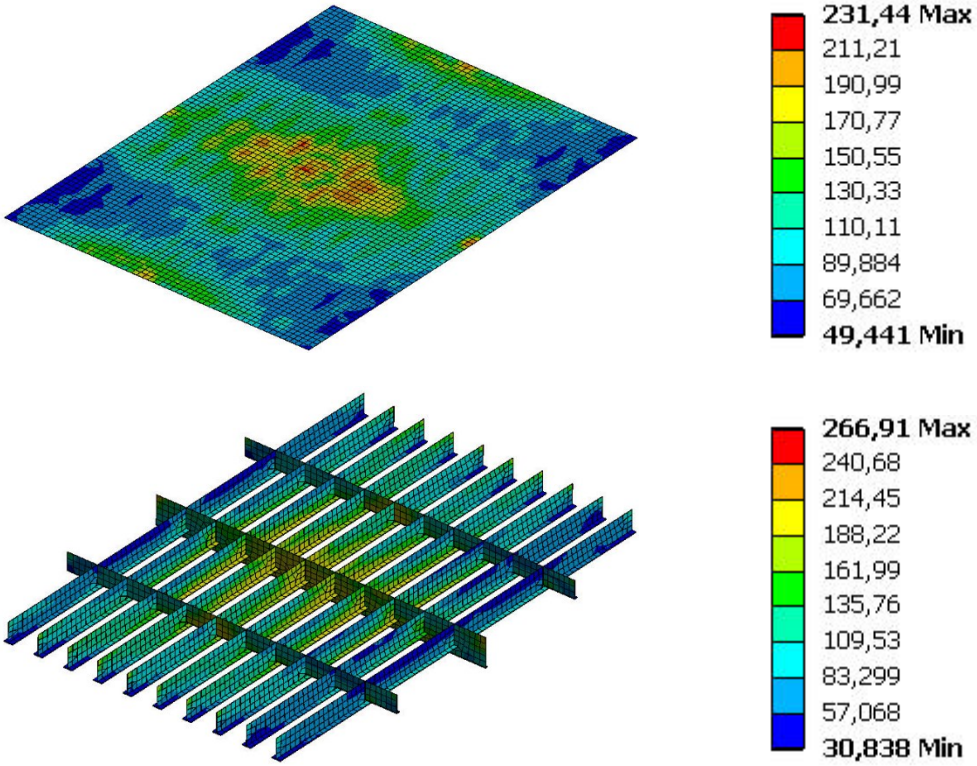

(b) Equivalent Stress

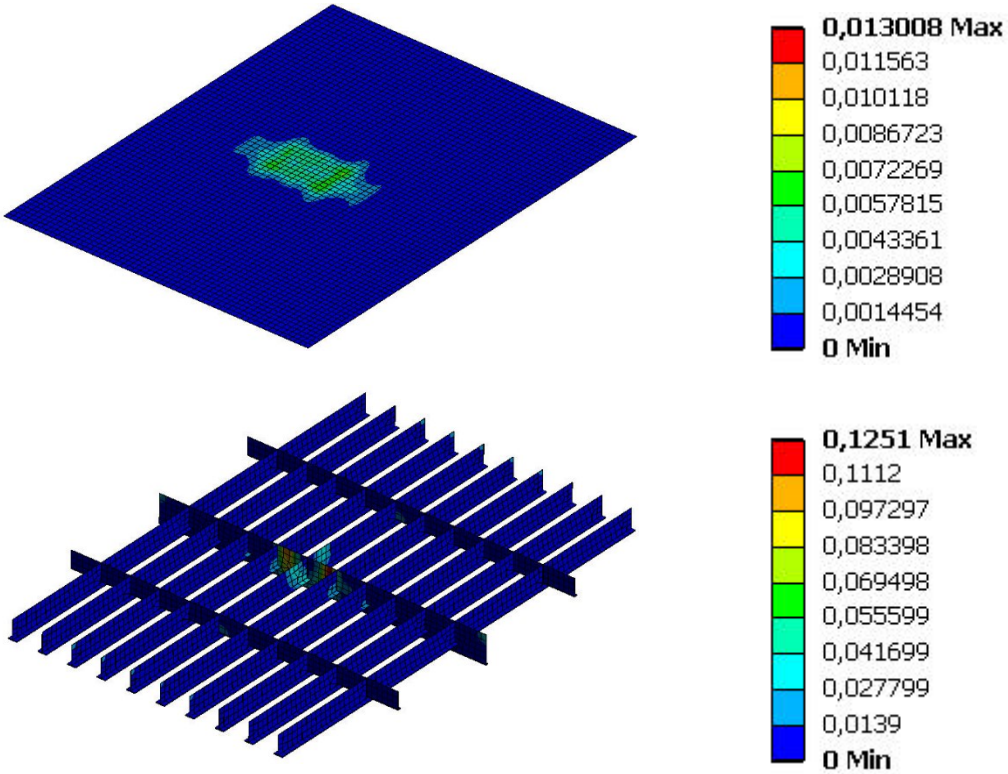

(c) Equivalent Plastic Strain

Figure 4.3: Dropped object Case-1

4.6 Dropped Object Case-2

In order to obtain a more realistic damage form and compare the influence of element removal on the results, Case-2 is simulated. This case is a duplication of Case-1 with the activated element erosion function. This function can be described as the physical separation of the distorted element from the rest of the mesh [45]. Because, very distorted elements might become degenerated if they are not removed from the simulation. By removing those elements, a reasonable stability timestep level is ensured, so the simulation can terminate at the desired time. One of the criteria to initiate element erosion is setting a Geometric Strain Limit which is a measure of the distortion of an element. It is calculated from the global strain components as shown in Eq. (4.7) [45].

$$\varepsilon_{eff} = \frac{2}{3}\left[\left|\left(\varepsilon_{xx}^2 + \varepsilon_{yy}^2 + \varepsilon_{zz}^2\right) - \left(\varepsilon_{xx}\varepsilon_{yy} + \varepsilon_{yy}\varepsilon_{zz} + \varepsilon_{zz}\varepsilon_{yy}\right) + 3\left(\varepsilon_{xy}^2 + \varepsilon_{yz}^2 + \varepsilon_{zx}^2\right)\right|\right]^{1/2} \tag{4.7}$$

When the measure of local element distortion exceeds the limit value which is represented by failure strain 0.08435 in this study, those elements are removed from the structure. The maximum results over the simulation time are presented in Table 4.3 and Fig. 4.4.

Table 4.3: Analysis results of dropped object Case-2

Case-2	Deformation [mm]	Equivalent Stress [MPa]	Equivalent Plastic Strain [-]
Plate	279.75	233.89	0.039175
Stiffener	269.11	256.73	0.075384

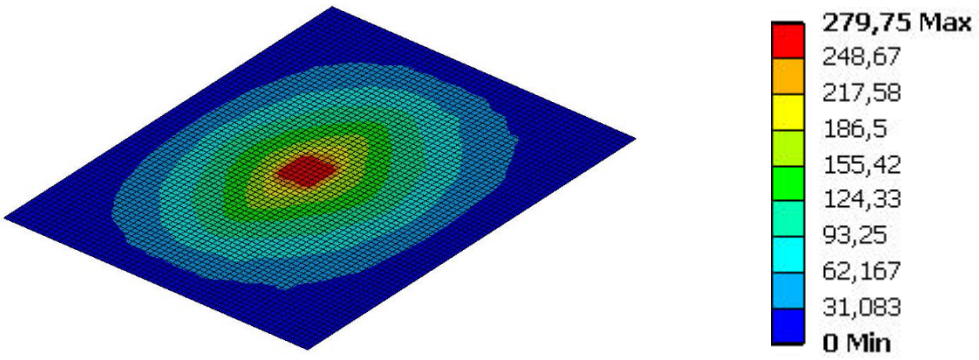

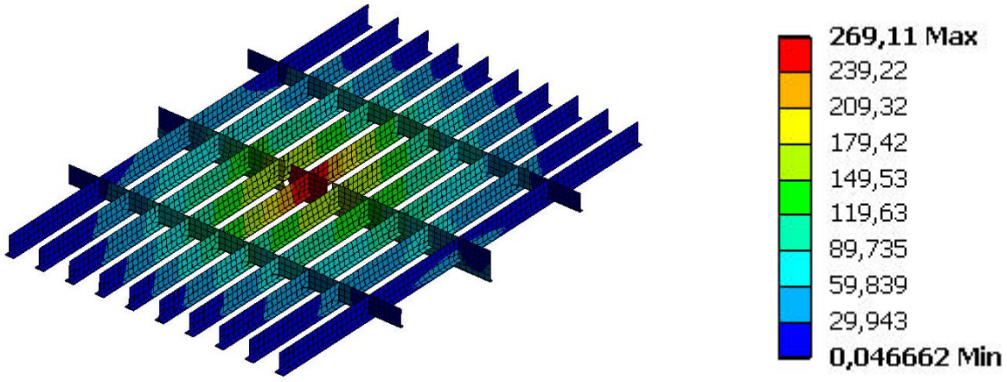

(a) Deformation

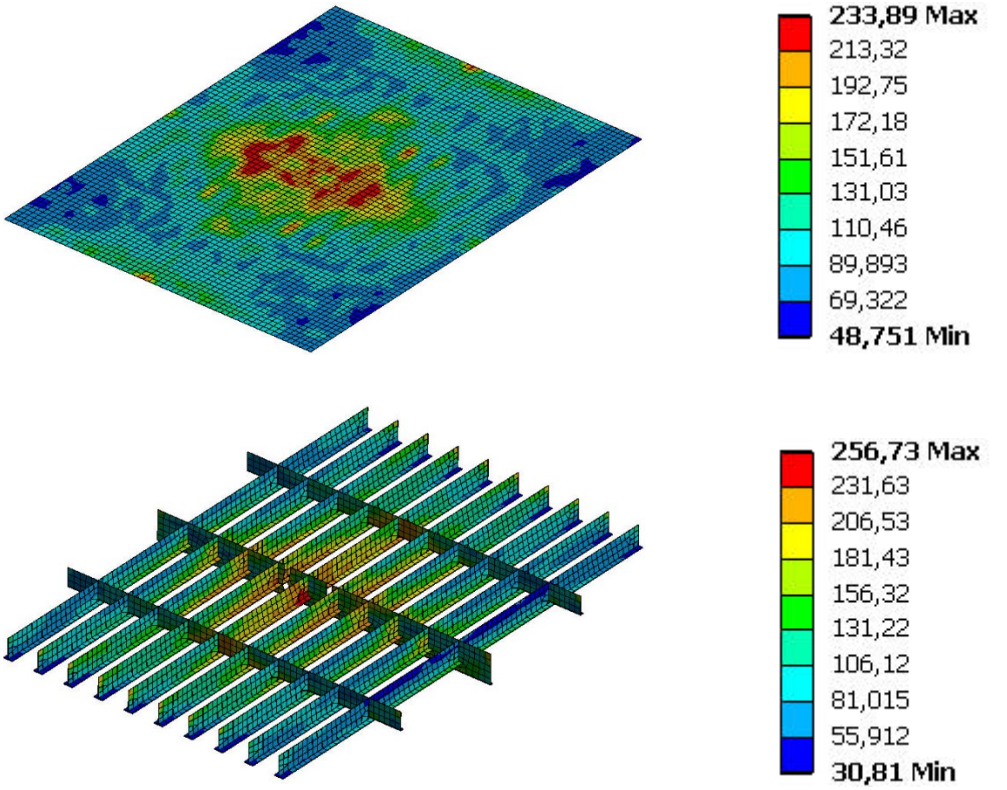

(b) Equivalent Stress

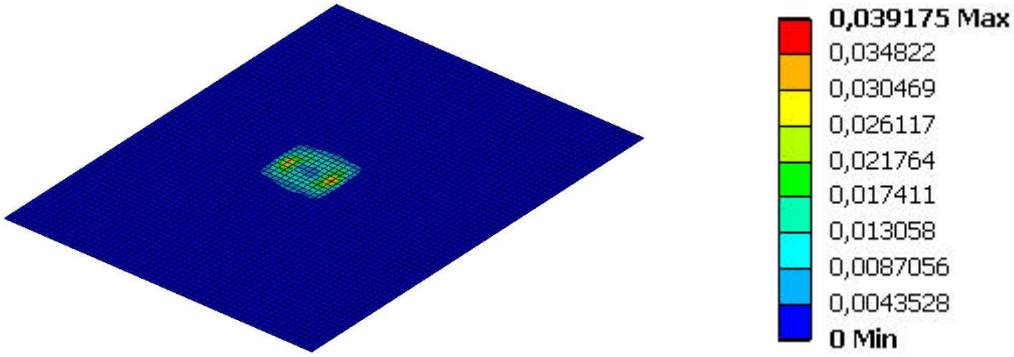

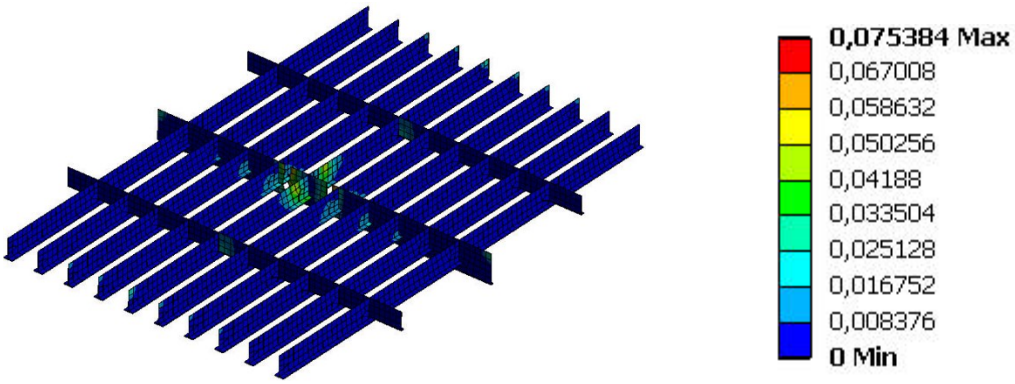

(c) Equivalent Plastic Strain

Figure 4.4: Dropped object Case-2

4.7 Dropped Object Case-3

In the third case, the response of the hatch cover is investigated when the dropped object has also horizontal velocity, in addition to free-fall motion due to the gravity. This object might drop from a moving system or from a stationary system onto a ship under way.

In this section, it is assumed that the object falls onto the hatch cover while the speed of the vessel is 8 knots. Hence, the horizontal speed of the object is 4.11 m/s in –x direction. Moreover the –x coordinate of the object position is shifted 4726.6 mm, in order to land the object approximately in the same area as in Case-1 and 2, for a more coherent comparison of the results. The rest of the analysis settings are kept same and element erosion is allowed. The results are presented in Table 4.4 and Fig. 4.5.

Table 4.4: Analysis results of dropped object Case-3

Case-3	Deformation [mm]	Equivalent Stress [MPa]	Equivalent Plastic Strain [-]
Plate	3955.7	253.16	0.0401
Stiffener	3945.7	261.82	0.0740

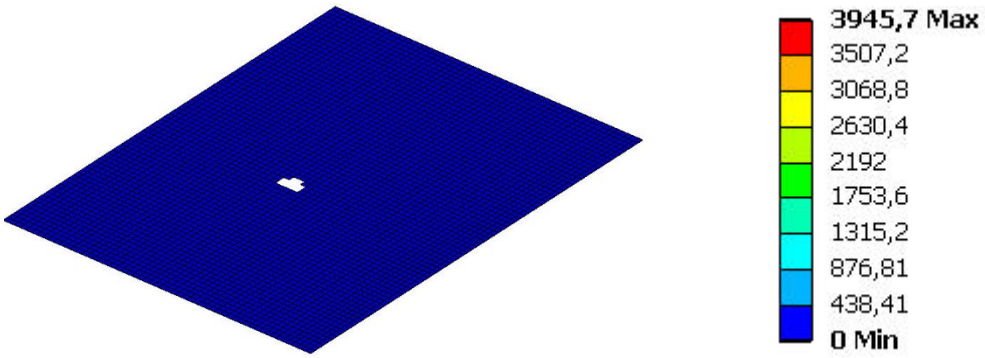

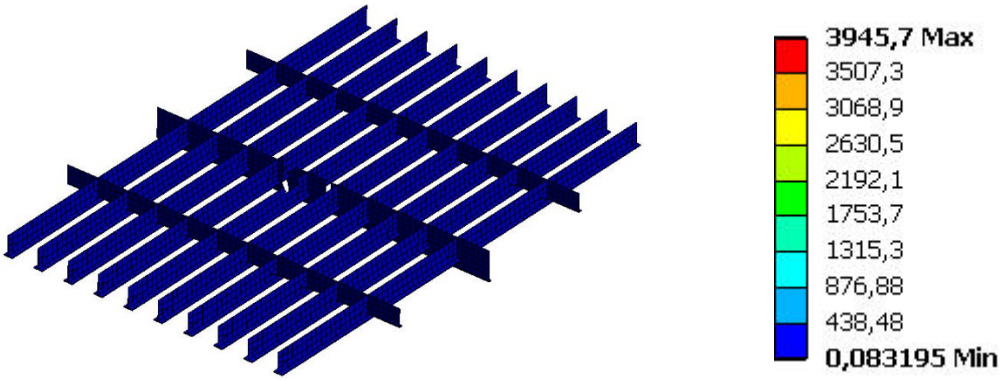

(a) Deformation

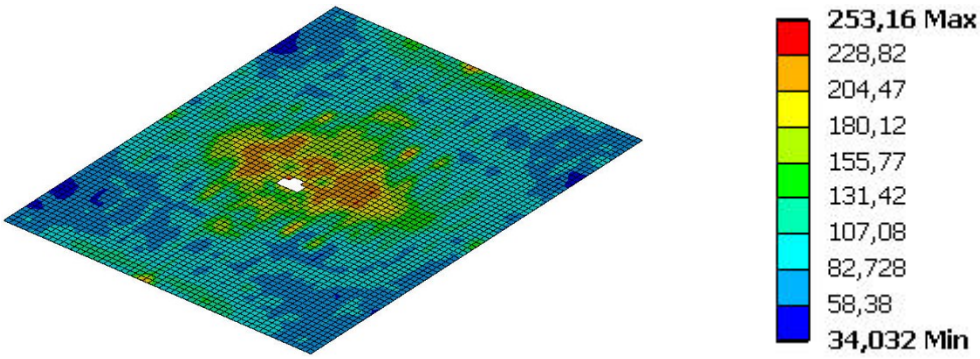

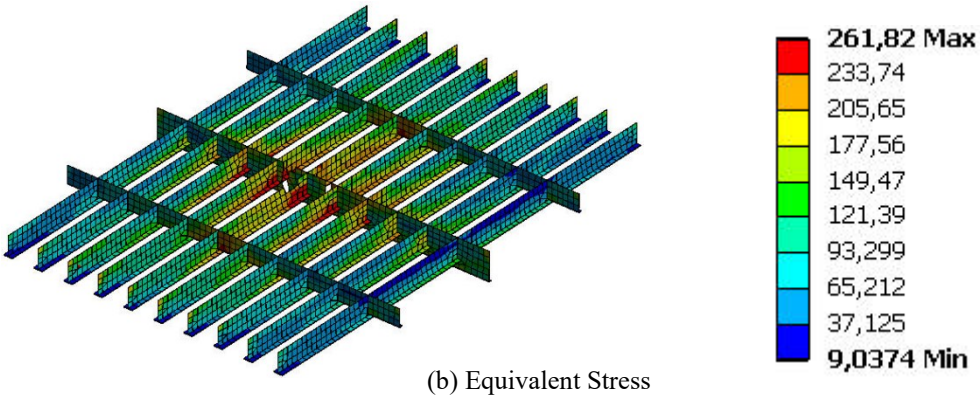

(b) Equivalent Stress

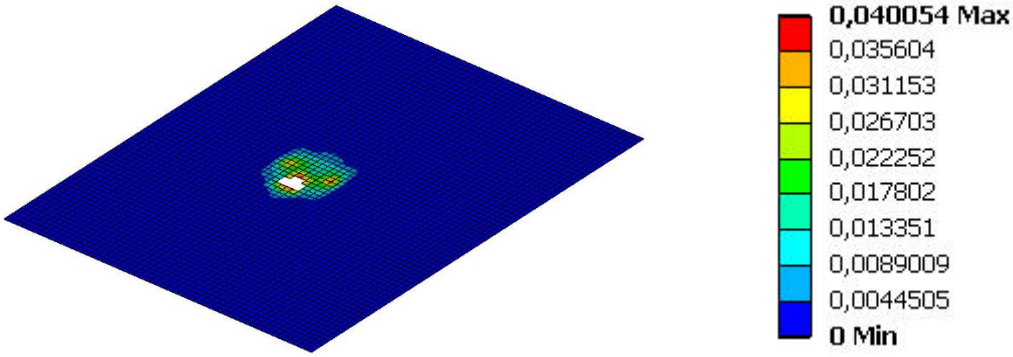

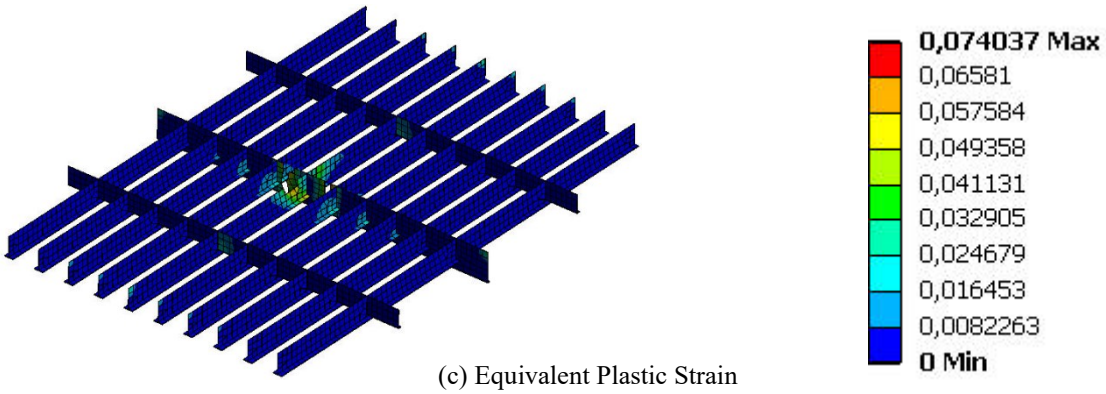

(c) Equivalent Plastic Strain

Figure 4.5: Dropped object Case-3

4.8 Comparison of the Results

One of the most important findings is that activating element erosion in the analysis, leads to more realistic damage form and numeric results. Although Case-1 and Case-2 have identical analysis setup, except for element erosion, the plastic strain result of Case-1 is considerable higher than Case-2 as seen in Fig. 4.6. Therefore, it can be deducted that keeping the failed elements in the structure could cause strongly conservative evaluation of the residual state of the structure.

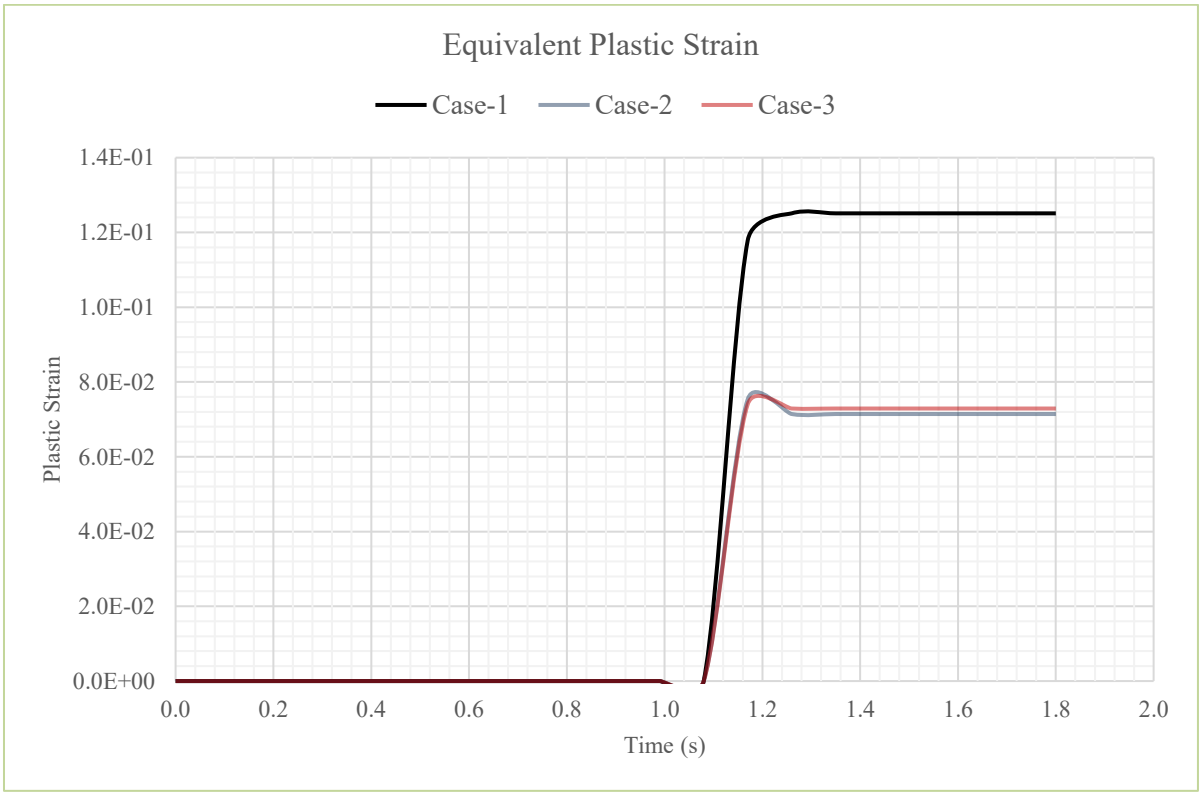

Figure 4.6: Plastic strain results comparison

Fig. 4.7 shows and compares plastic strain results of Case-1 and Case-2, at the location where element erosion occurs.

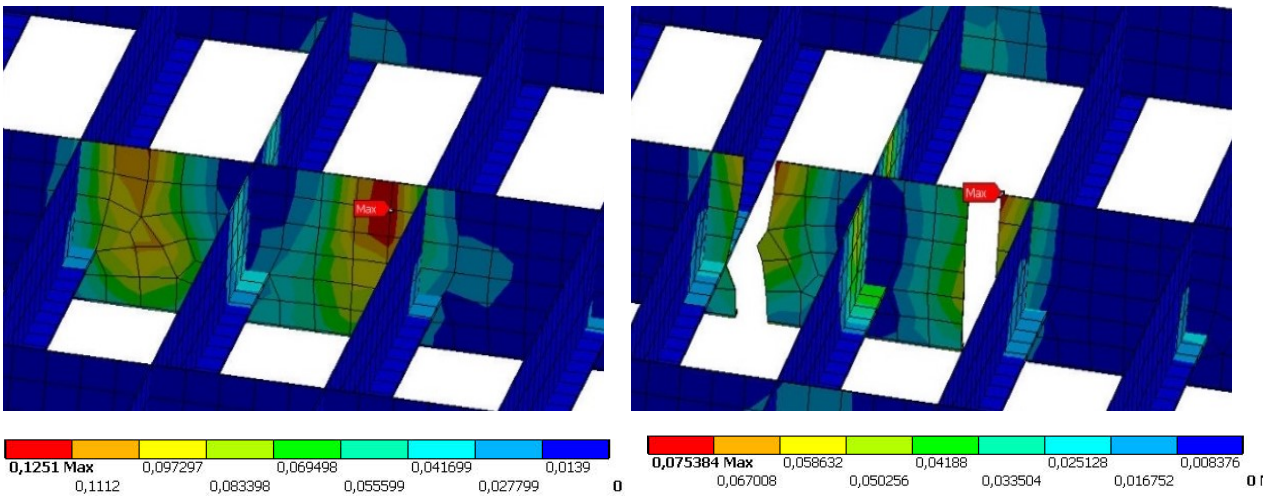

Case-1 Case-2

Figure 4.7: Case-1 and Case-2 plastic strain

On the other hand, comparison of Case-2 and Case-3 highlights the influence of the impact type on results. In Case-2, the pattern of the dropped object motion is free-fall, while it is projectile motion in Case-3. A closer view of the damage area of Case-2 and Case-3 are shown in Fig. 4.8. Projectile motion causes a significant damage in the plate of the hatch cover, which risks the watertightness. The results confirm that when the dropped object has also a horizontal speed, the damage could be catastrophic as it can be seen in Fig. 4.9 where the deformation results of each case are presented.

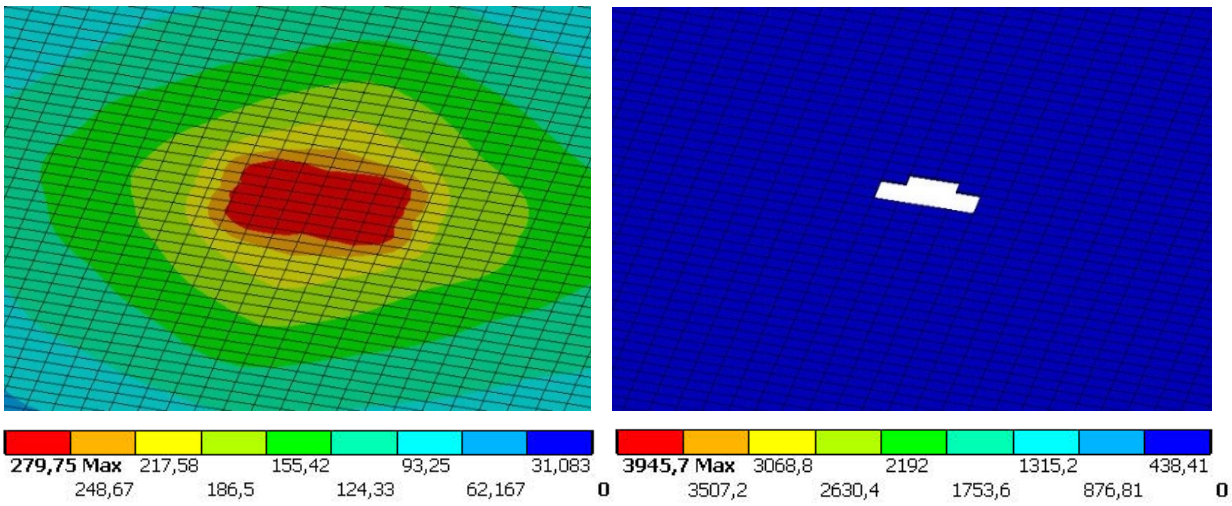

Case-2 Case-3

Figure 4.8: Deformation form of Case-2 and Case-3

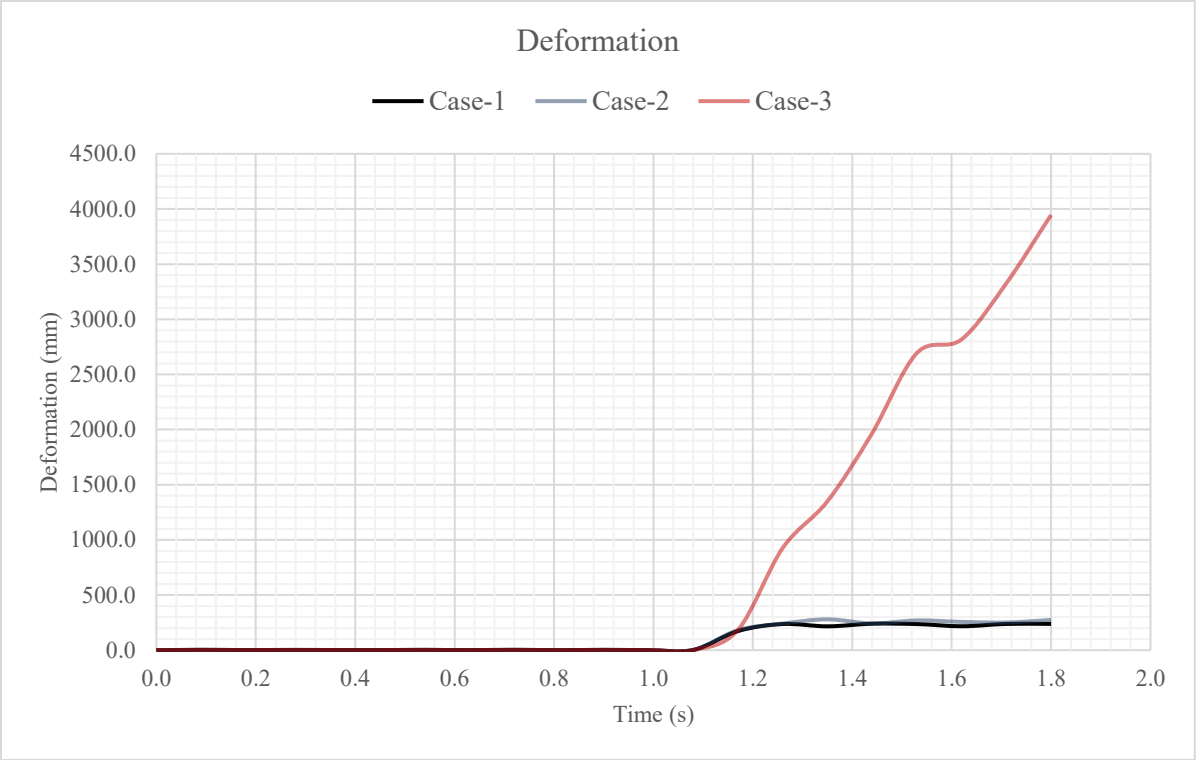

Figure 4.9: Deformation results comparison

5. POST-IMPACT LOAD CARRYING PERFORMANCE

5.1 Load and Failure Types

To evaluate the load carrying performance of a structure, the first step is defining the failure criteria. For ductile steel, failure is related to geometric and/or material nonlinearity [40]. There are many types of structural failure; however some important types for steel structural members can be listed as follows [55]:

- Large local plasticity
- Instability (bifurcation and non-bifurcation)
- Fracture (direct, fatigue, brittle)

The most critical or relevant failure type for a specific structure can be determined according to the configuration of the structure and the exposed load type [40].

A pontoon hatch cover, which is the subject of this thesis and composed of a plate-beam combination, could be called also as “stiffened panel” in terms of structural configuration. Generally, plate-beam combinations within the ship structures are subjected to following loads individually or in a combined way [40]:

- Axial compression/tension
- Concentrated or distributed lateral load
- End moment

In discordance with most ship panel structures, pontoon hatch covers are not affected by the loads that the global structure is exposed to, because the pontoon hatch cover is not connected to the ship hull directly by any connection method. Therefore, the main load is the green sea load that a pontoon hatch cover hatch cover is exposed to and green sea load acts on a hatch cover as a distributed lateral load.

One way to investigate the collapse load of a beam under lateral load is rigid-plastic analysis based on hand calculations. In this method simply if a cross-section reaches yield strength under lateral load, plastic hinge occurs at that point and no more bending moment can be carried. However, it is more complicated for plates. Although it is an approximate approach, “rigid plastic hinge line” method can be used for large deflection calculations of plates under static pressure. In this method, material is considered to be rigid-perfectly plastic and elastic deflections are not taken into account. The plate is divided into four regions. Those regions are assumed rigid and they are separated by hinge lines in order to form a collapse mechanism

as illustrated in Fig. 5.1. Finally, it is assumed that maximum normal stress yield criteria govern the yield [55]. Nevertheless, for efficiency and higher accuracy finite element methods are widely used for such kind of problems.

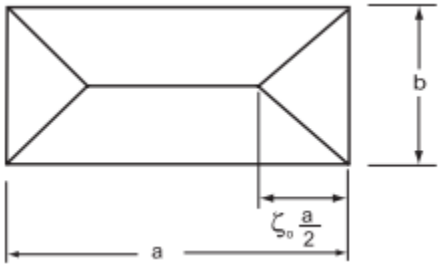

Figure 5.1: Hinge lines [55]

5.2 Post-Accident Performance Evaluation

It is a crucial topic to be able to evaluate the residual strength of a marine structure after an accidental case; in order to take timely action for prevention from loss of life, environmental and financial harms. A review of existing literature on this topic is given in Chapter-1. There are numerous methods to analyse the residual strength of the structure, depending on the accident and load types. For decades, those methods are conducted in different engineering environments, provided by commercial software. On the other hand, accuracy, promptness and practicality of the evaluation method are important factors. Therefore, one of the aims of this thesis is to verify the capabilities of the employed engineering environment for conducting a chain of simulations which consists of the accidental event, transfer of the results and post-accidental performance evaluation.

Likewise, Akkus et al. [56] reviewed the existing literature on residual strength analysis and reported that previous studies in this field are not sufficient enough for reliable results due to conventional damage modelling techniques. Those techniques are implemented mostly by removing the damaged area from the whole structure or applying different slenderness ratio in the assumed damage area and they neglect the effect of residual stresses [7,11,57]. In addition, majority of existing studies on residual strength analysis focus on in-plane loads. However, the dominant load case for pontoon hatch covers is lateral loads. Thus, post-impact, lateral load carrying performance evaluation is a novel topic which is investigated within this thesis, as well as by Akkus et. al [56].

5.2.1 Performance Evaluation Methodology

Implementation of conventional damage modelling, without realistic damage simulation and residual stresses, remains very conservative for the assessment under lateral pressure [56]. So, this study does not include the conventionally modelled damage analysis repetitively, however intact structure is analysed for comparison of the performance before and after the accident. As recommended by previous studies [12,56] residual stresses are also taken into account to achieve higher accuracy of the results.

Damage simulations are conducted in Chapter-4, as Dropped Object Case-1, Case-2 and Case-3. In this chapter, the behaviour of the damaged structure is investigated under static load. To achieve this, the deformed geometries of the hatch covers are transferred with the residual stresses to the further analysis systems.

In addition, the effect of residual plastic strain due to plastic deformation is another interesting topic. Residual plastic strain effect has been explored in prior studies in the scope of fabrication processes and their influence on structural behaviour [58,59]. However, it has not been studied for accidental cases and for the assessment of performance of damaged structure. Therefore in this study, it is considered worthy to examine the effect of residual plastic strain due to the impact of dropped object, on the behaviour of the damaged hatch cover. In this regard, two sub-cases (A and B) are defined for the post-accident assessment of each drop case. A schematic representation of the methodology is given in Chapter-1. To sum up:

- Case-1A, Case-2A, Case-3A assess the behaviour of damaged structure by taking the residual stresses into account.
- Case-1B, Case-2B, Case-3B assess the behaviour of damaged structure by taking the residual stresses and residual strains into account.

To analyse the behaviour of the structure under static lateral load, Static Structural analysis system is employed within Ansys Workbench environment.

5.2.1.1 Transfer of the Deformed Structure and Residual Stresses

The simulations are conducted in Ansys Workbench 2020 R2 which enables data sharing or transfer between two systems for sequential simulation, as aimed in this study [26]. By linking the relevant tabs of the analysis systems, transfer of the deformed geometry is achieved. To be able to export the deformation results of the damage simulation, “Solution” tab of the Explicit Dynamics system is linked to “Model” tab of the Static Structural System. However, when there are eroded elements in the deformed structure, it is not possible yet for

the software to transfer the erosion information to the subsequent analysis only by linking the tabs. In this case, help of APDL interface is needed to delete the eroded elements manually.

On the other hand, residual stresses and strains cannot be transferred via linking of the two systems and additional operations are needed. For this purpose, “External Data” function of the software is employed, that allows data import from text files to a Mechanical system [26]. First of all, within the Explicit Dynamic System, normal and shear stress elemental results for bottom, middle and top faces of shell elements are exported as text files. Then, through the External Data tool, those files are read in Static Structural system and defined as “Initial Stress” for the elements of the deformed structure. Similar procedure is applied for the transfer of residual plastic strain. Equivalent plastic strain elemental results are also exported for bottom, middle and top faces separately and transferred to the Static analysis system as “Initial Strain” through External Data tool. Fig. 5.2 presents the data transfer between the systems for the sequential analyses.

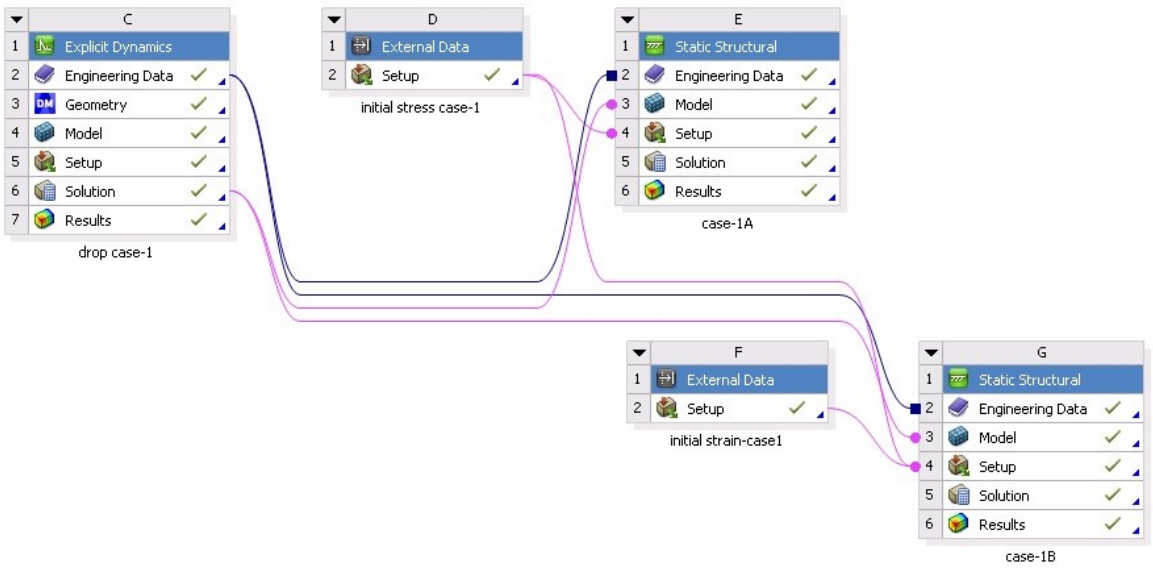

Figure 5.2: Transfer of the results from damage simulation

5.2.1.2 Nonlinear Static Analysis

As stated earlier, green sea load is the main concern in this study, especially by considering that could be the reason for the failure of M/V Derbyshire hatch cover. Yao et. al [17] affirms that although green sea loading has dynamic nature; it can be treated as a static load, when the response of the structure which is exposed to green sea load is investigated. Moreover, it is suggested [17] that the load can be applied as gradually increased static pressure and it seems to be a reliable and practical approach for the aim of the present study as well. Thus, nonlinear

static analysis is used to evaluate the post-impact performance of the hatch cover under green sea loading.

Ansys Workbench "Static Structural" analysis system is utilised for this purpose. Within the system, it is assumed that the loading and response conditions are steady and vary slowly in time. The system enables user to determine displacements, stresses and strains as response to the loads which do not actuate considerable inertia and damping effects [26].

It is possible to conduct linear and nonlinear static analysis within this system. In the post-accident static analyses, nonlinearity is expected especially under higher pressure magnitudes. Newton-Raphson method is used for the solution of the nonlinear system, as default option in the software.

Newton-Raphson method linearizes the solution of nonlinear equations through gradual and iterative processes. First, load is divided into smaller increments and applied gradually. For each small load increment, a linear solution is performed and the convergence is checked. Several iterations are conducted until the convergence criteria are satisfied [60].

The finite element equilibrium equation can be written for Newton-Raphson iterations as in Eq. (5.1):

$$[K_i^T]\{\Delta u_i\} = \{F^a\} - \{F_i^{nr}\}$$
$$\{u_{i+1}\} = \{u_i\} + \{\Delta u_i\} \tag{5.1}$$

where;

$[K_i^T]$ = *Jacobian matrix (tangent matrix)* i = *current equilibrium iteration*

$\{u_i\}$ = *displacement vector,* $\{\Delta u_i\}$ = *displacement increments*

$\{F^a\}$= *vector of applied loads*

$\{F_i^{nr}\}$= *vector of restoring loads corresponding to the element internal loads*

The difference between the restoring forces and applied loads are called as "out of balance loads" and they are evaluated before each solution of the given load. This constitutes the right-hand side of the Eq. 5.1 and basically shows the amount of out of equilibrium. After the linear solution of load increments, the convergence to equilibrium is checked. If the convergence is not sufficient, the out of balance load vector is evaluated again, the stiffness matrix is updated and the process is repeated iteratively until the equilibrium is obtained [60,61]. Fig. 5.3 presents the graphical depiction of the first iteration and the subsequent iteration.

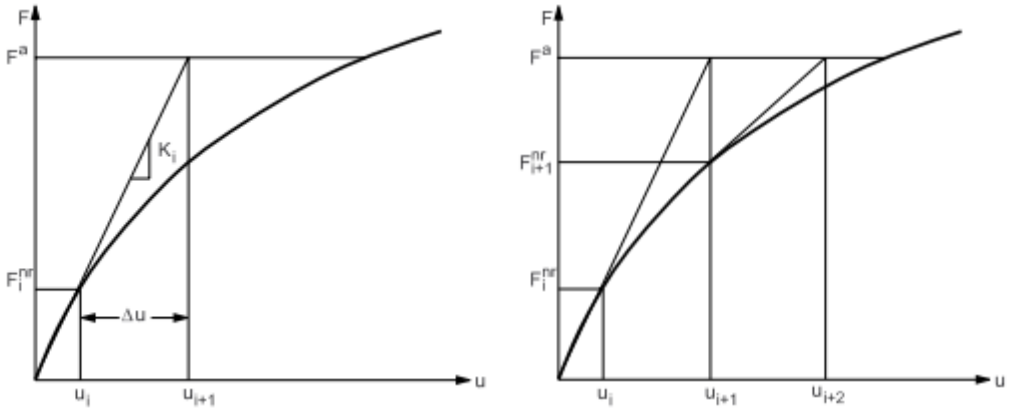

(a) First iteration (b)Next iteration

Figure 5.3: Newton-Raphson iterations [61]

5.2.2 Analysis Settings

To keep the consistency and realistic representation of the event chain, mesh and boundary conditions should be kept as same as in the accident simulations [56]. Therefore, with the help of transfer function of the software, mesh properties imported automatically in the static analysis system. Boundary conditions are defined as described in Chapter- 3. The solid dropped object is excluded from the simulation, since the focus is only hatch cover structure.

It is recommended to turn "Large Deflection" property on, to take into consideration the stiffness changes due to large deformations, rotations, strains and in order to obtain more accurate results [62]. Convergence and stabilisation controls are left to the program controlled option which is sufficiently good for this type of analysis.

Uniformly distributed lateral load is applied as pressure on the top surface of the hatch cover plate. The pressure is defined to the normal of the surface, so homogeneity is achieved in the deformed area. Design load and collapse load of M/V Derbyshire`s hatch cover are chosen as load cases, as explained in Chapter-3. Those loads are 1.75 t/m^2 (0.01743 MPa) and 5.47 t/m^2 (0.05403 MPa) which are applied gradually in 5 equal steps. Table 5.1 presents the load increments through the time for the two load cases.

Table 5.1: Load application

Time [s]	**0**	**1**	**2**	**3**	**4**	**5**
Pressure [MPa]	0	0.003486	0.006972	0.010458	0.013944	0.01743

(a) Design load

Time [s]	**0**	**1**	**2**	**3**	**4**	**5**
Pressure [MPa]	0	0.01743	0.02658	0.03573	0.04488	0.05403

(b) Collapse load

5.3 Results and Discussions

For the comparative study, behaviour of hatch cover models are analysed through the described methodology, in six sub-cases. Maximum deformation, equivalent stress, equivalent total strain and equivalent plastic strain values are obtained at the end of the load application, for the hatch cover panel plate and stiffeners separately, for a coherent comparison. Moreover, in order to avoid the influence of boundary conditions, the maximum values are detected within the area 2 meters inside from the edges.

Table 5.2 and Table 5.3 show the results under the design load 0.01743 MPa and collapse load 0.05403 MPa respectively. Those tables display the maximum values, thus they might not always occur at the same node.

On the other hand, comparison of the results for a specific node could be also beneficial for the assessment from a different perspective. For this purpose, the middle node of the intact structure with the coordinates of x= 7340, y= 5566.4, z=0 is selected. Nodal results for each case are presented in Table 5.4 and Table 5.5.

Table 5.2: Load carrying performance results – 0.01743 MPa

0.01743 MPa		Case-1A	Case-2A	Case-3A	Intact
Plate	Deformation [mm]	5.7986	4.1632	3.5645	13.828
	Eqv. Stress [MPa]	219.14	181.82	207.46	37.492
	Eqv. Total Strain [-]	0.00049956	0.00042149	0.00057593	0.00018748
	Eqv. Plastic Strain [-]	0.00010968	0.0000248	0.000023605	0
Stiffener	Deformation [mm]	4.0352	3.3387	3.1674	12.299
	Eqv. Stress [MPa]	233.13	235.05	235.29	154.91
	Eqv. Total Strain [-]	0.00039711	0.00092258	0.00078974	0.00077558
	Eqv. Plastic Strain [-]	0.000031924	0.000037499	0.00043058	0

(a) Performance of the deformed structure together with residual stresses

0.01743 MPa		Case-1B	Case-2B	Case-3B
Plate	Deformation [mm]	5.7979	4.1633	3.5644
	Eqv. Stress [MPa]	218.3	181.82	207.56
	Eqv. Total Strain [-]	0.00049588	0.00042147	0.0005758
	Eqv. Plastic Strain [-]	0.000095641	0.0000185	0.000013586
Stiffener	Deformation [mm]	4.0331	3.3386	3.1674
	Eqv. Stress [MPa]	233.2	249.23	267.29
	Eqv. Total Strain [-]	0.0003971	0.00089907	0.00078882
	Eqv. Plastic Strain [-]	0.000013444	0.0000019083	0.00027294

(b) Performance of the deformed structure together with residual stresses and strains

Table 5.3: Load carrying performance results – 0.05403 MPa

0.05403 MPa		Case-1A	Case-2A	Case-3A	Intact
Plate	Deformation [mm]	26.283	27.903	28.905	46.83
	Eqv. Stress [MPa]	222.52	222.48	233.54	124.23
	Eqv. Total Strain [-]	0.00064699	0.00060169	0.00085748	0.00062122
	Eqv. Plastic Strain [-]	0.000188	0.0000801	0.00018282	0
Stiffener	Deformation [mm]	23.486	25.366	27.785	42.448
	Eqv. Stress [MPa]	235.32	235.99	237.03	240.86
	Eqv. Total Strain [-]	0.0014437	0.0069741	0.0012574	0.0032254
	Eqv. Plastic Strain [-]	0.00066601	0.005431	0.00055442	0.0020435

(a) Performance of the deformed structure together with residual stresses

0.05403 MPa		Case-1B	Case-2B	Case-3B
Plate	Deformation [mm]	26.127	27.794	28.805
	Eqv. Stress [MPa]	221.9	222.51	234.56
	Eqv. Total Strain [-]	0.00064355	0.00060725	0.00084812
	Eqv. Plastic Strain [-]	0.00017181	0.0000720	0.00016834
Stiffener	Deformation [mm]	23.323	25.289	27.707
	Eqv. Stress [MPa]	266.96	292.4	267.3
	Eqv. Total Strain [-]	0.0015082	0.0071227	0.0012028
	Eqv. Plastic Strain [-]	0.00074398	0.0055662	0.00043572

(b) Performance of the deformed structure together with residual stresses and strains

Table 5.4: Load carrying performance results of middle node – 0.01743 MPa

0.01743 MPa		Case-1A	Case-2A	Case-3A	Intact
Middle Node	Deformation [mm]	4.0352	1.621	0.94598	12.299
	Eqv. Stress [MPa]	188.64	87.529	103.26	26.656
	Eqv. Total Strain [-]	0.00025473	0.0004017	0.00029114	0.00013415
	Eqv. Plastic Strain [-]	0	0	0	0

(a) Performance of the deformed structure together with residual stresses

0.01743 MPa		Case-1B	Case-2B	Case-3B
Middle Node	Deformation [mm]	4.0331	1.621	0.94611
	Eqv. Stress [MPa]	188.66	87.525	100.89
	Eqv. Total Strain [-]	0.000251	0.00040169	0.00029143
	Eqv. Plastic Strain [-]	0	0	0

(b) Performance of the deformed structure together with residual stresses and strains

Table 5.5: Load Carrying Performance Results of Middle Node-0.05403 MPa

0.05403 MPa		Case-1A	Case-2A	Case-3A	Intact
Middle Node	Deformation [mm]	23.43	23.03	26.25	42.448
	Eqv. Stress [MPa]	210.64	235.1	199.41	84.911
	Eqv. Total Strain [-]	0.00039015	0.0013267	0.00091224	0.00042755
	Eqv. Plastic Strain [-]	0.0000228	0.000151	0.0001247	0

(a) Performance of the deformed structure together with residual stresses

0.05403 MPa		Case-1B	Case-2B	Case-3B
Middle Node	Deformation [mm]	23.258	22.936	26.162
	Eqv. Stress [MPa]	211.15	235.11	199.85
	Eqv. Total Strain [-]	0.00038554	0.0013374	0.00091462
	Eqv. Plastic Strain [-]	0.0000210	0.000162	0.0000939

(b) Performance of the deformed structure together with residual stresses and strains

It is observed that the effect of residual strain assignment is not significantly strong on the performance evaluation analyses, regarding deformation and stress results. The difference between the deformation results of A-subcases (Case-1A, Case-2A, Case-3A) and B-subcases (Case-1B, Case-2B, Case-3B) are less than 1% for the plate and the stiffeners. Similarly, the difference between equivalent stress results is less than 1% for the plate, while it is around 6% under the design load and around 16% under the collapse load for the stiffeners in average.

On the contrary, the difference between plastic strain results is higher and might reach up to 97%. Especially, when the plastic strain results are relatively lower, the influence of residual strain assignment is stronger.

This comparative study confirms that in addition to existing post-accident evaluation methods which are focused on deformation and residual stresses, it could be more realistic to consider the residual plastic strains as well. However, future investigations are necessary to validate the findings of this study and draw a precise conclusion. After reviewing the residual strain effect, in order to avoid redundancy and to have a clearer overview, only results of Case-1A, Case-2A and Case-3A will be discussed and given in the graphs, in the rest of this study.

5.3.1 Deformation Results

Deformation values show the magnitude of displacement of a node at the end of the simulation. Therefore, the deformation results for the damaged structures, which are presented above, demonstrate the displacement only due to the static load application. However, if the first displacements due to the accident simulation are considered together with the sequential static analysis, then the total displacements values become higher. In order to clarify the issue,

z-coordinates of the middle node are given in Table 5.6 for the initial state, at the end of the dropped object analysis and at the end of the static analysis; together with the difference values between the two analyses, which correspond to the nodal deformation results given in Table 5.5.

Result plots in terms of nodal displacements during the static analyses are presented in Fig. 5.4. For damaged structures, namely Case-1A, Case-2A and Case-3A, final displacements of the accident simulations are taken as initial values. As seen in the graph, severity of damage has a strong effect on further displacement under static pressure. Although in Case-1A and Case-2A same accident scenario is applied, because of the removal of failed elements, the integrity of the structure is lost in Case-2A, which leads higher deformation. Similarly, the structure in Case-3A has a bigger damage in comparison to Case-2A, thus performance of Case-3A is weaker than Case-2A, in means of displacement. Fig. 5.5 presents illustrations of deformation distribution within the structures under the pressure of 0.05403 MPa.

Table 5.6: Z-coordinates of the Middle Node

	Initial State	After Accident Simulation (Dynamic)	After Pressure Application (Static)	Difference (mm)
Intact	0	-	-42.448	42.448
Case-1A	0	-223.65	-247.08	23.43
Case-2A	0	-253.24	-276.27	23.03
Case-3A	0	-266.77	-293.02	26.25

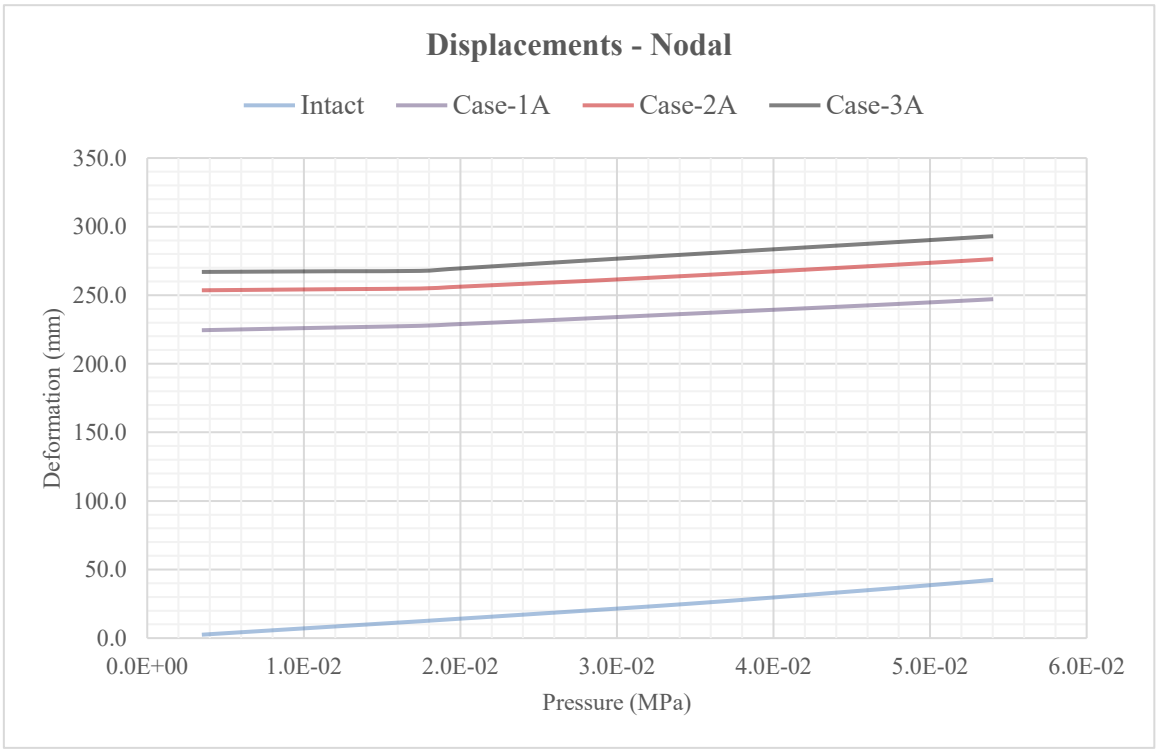

Figure 5.4: Nodal displacements

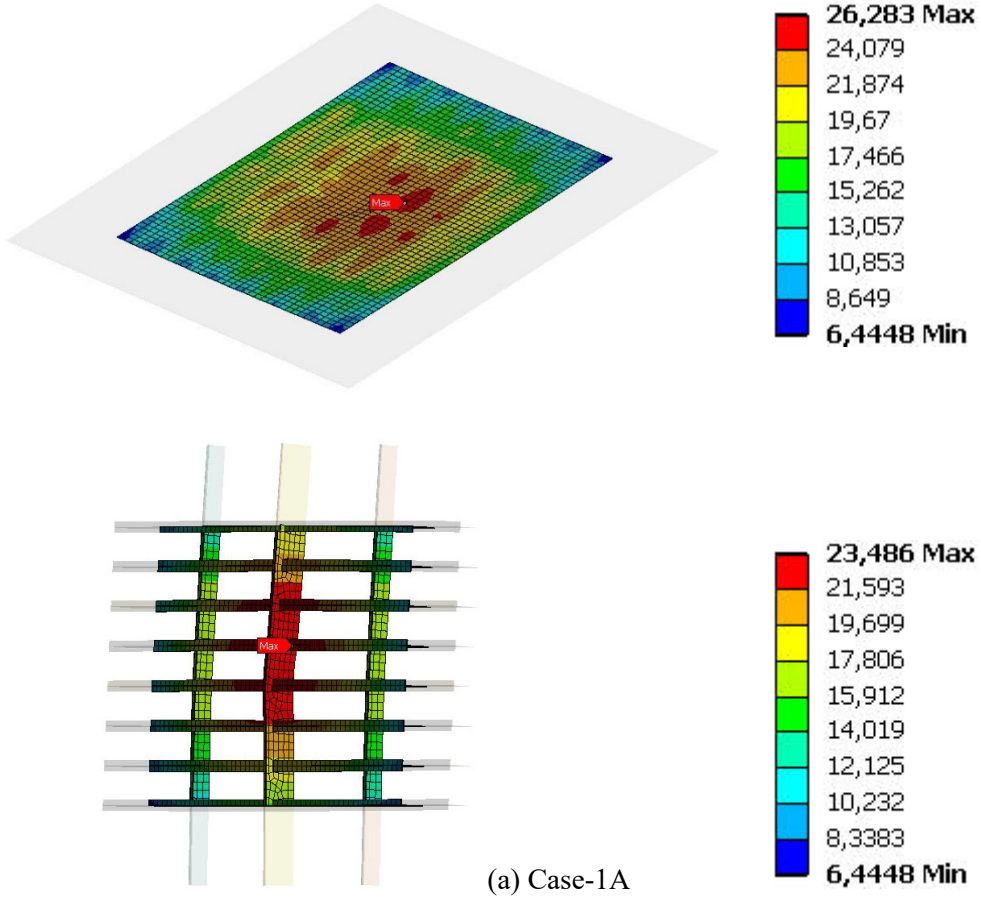

(a) Case-1A

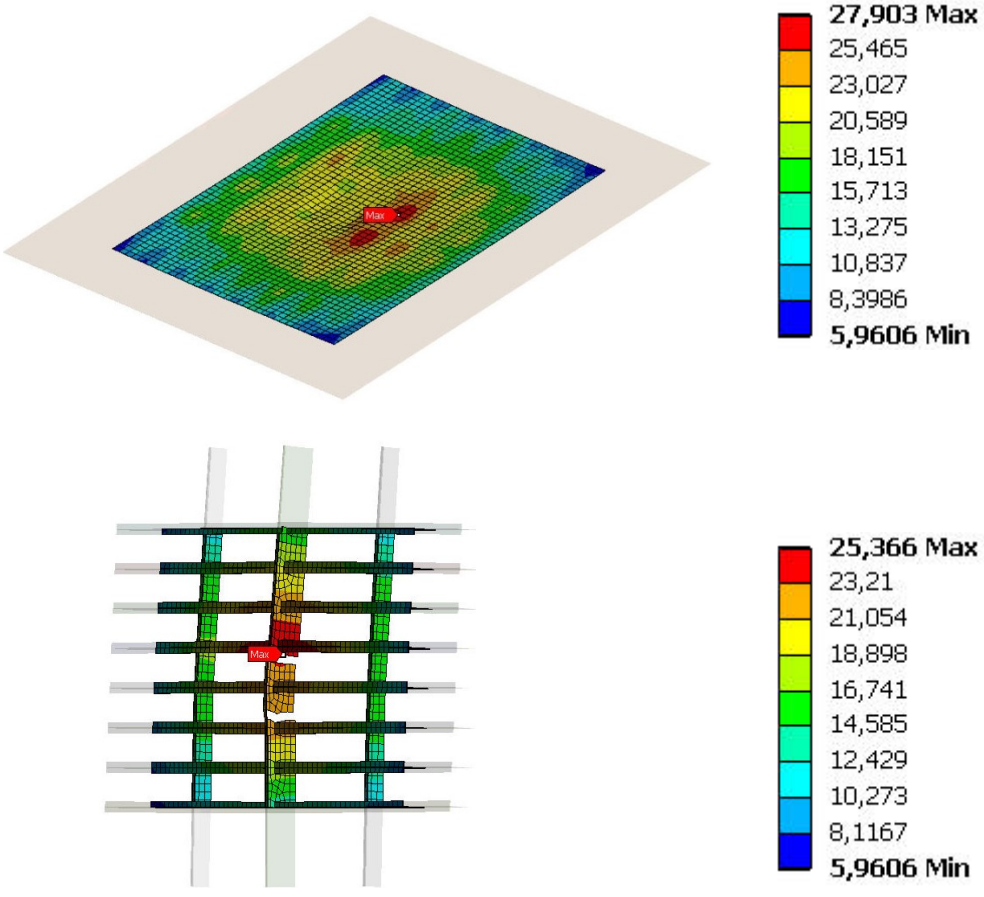

(b) Case-2A

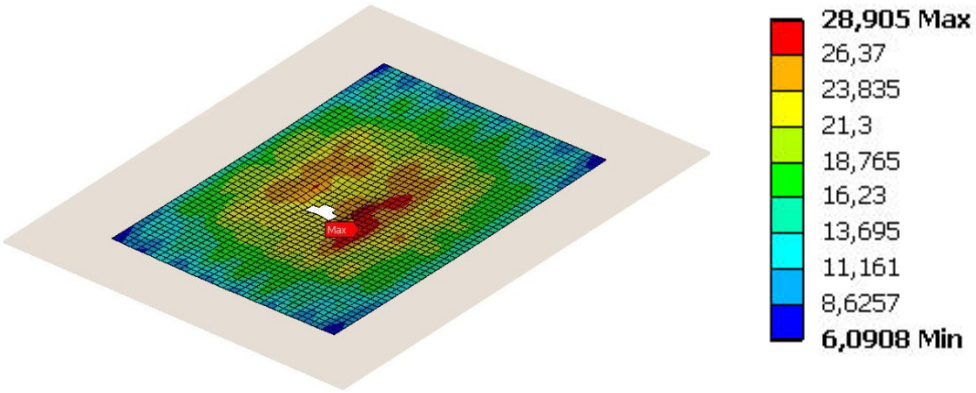

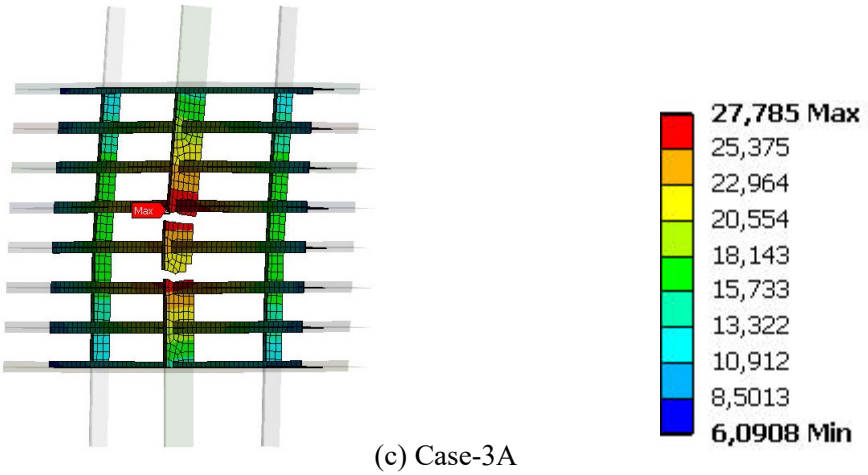

(c) Case-3A

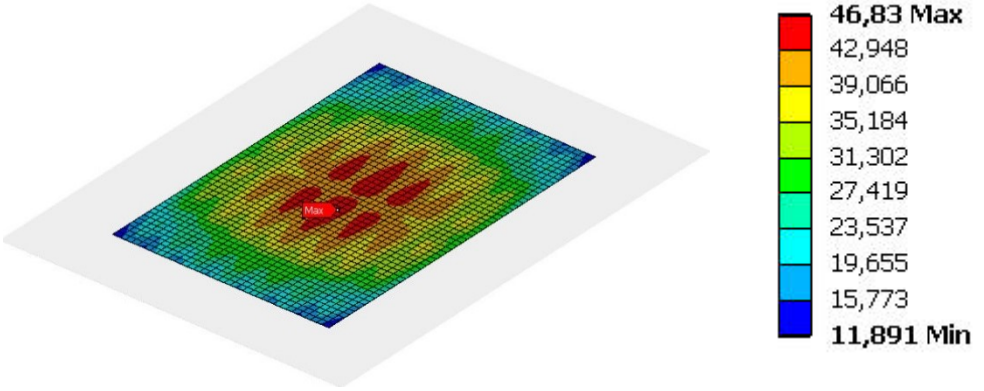

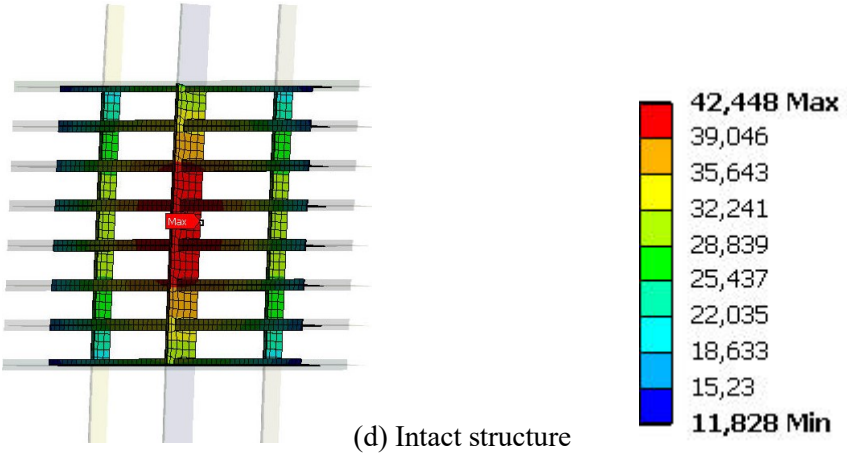

(d) Intact structure

Figure 5.5: Deformation results

5.3.2 Equivalent Stress Results

The equivalent stress results, which are also illustrated in Fig. 5.6 and Fig. 5.7, confirm that stress values occur within the plate of the damaged hatch covers almost twice as high as intact hatch cover. Stiffeners of the intact structure are also showing better performance under the design load, whereas under the collapse load, results are slightly different. Moreover, stress concentrations are observed around the damage areas, while intact structure forms homogenous stress distribution, as it can be seen in Fig. 5.8.

When Case-1A and Case-2A are compared for the element erosion effect, especially under lower load Case-1A experiences higher stresses than Case-2A, however when the load is increased, results converge. A possible explanation could be that in Case-1A elements with high stress due to the impact are kept within the structure and it leads higher results in static analysis.

The comparison of two cases with element erosion Case-2A and Case-3A reveals that bigger damage exposes the structure to high stress magnitudes.

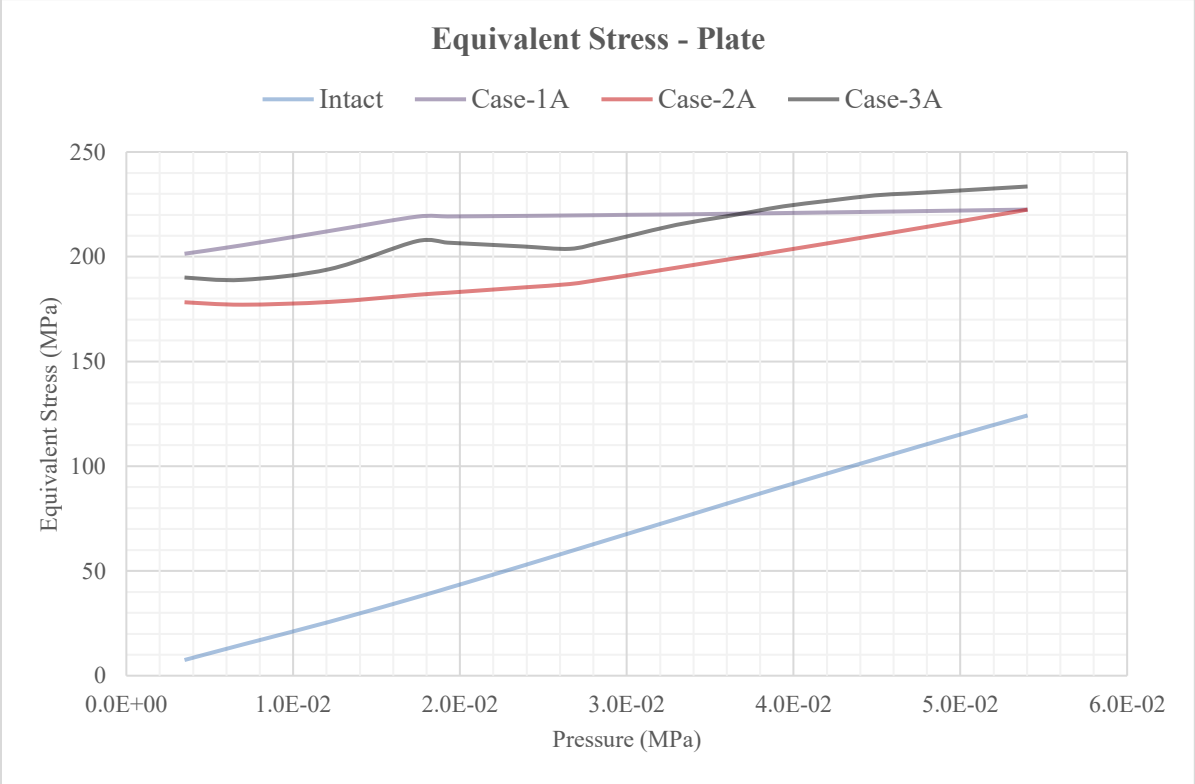

Figure 5.6: Equivalent stress results of the plate

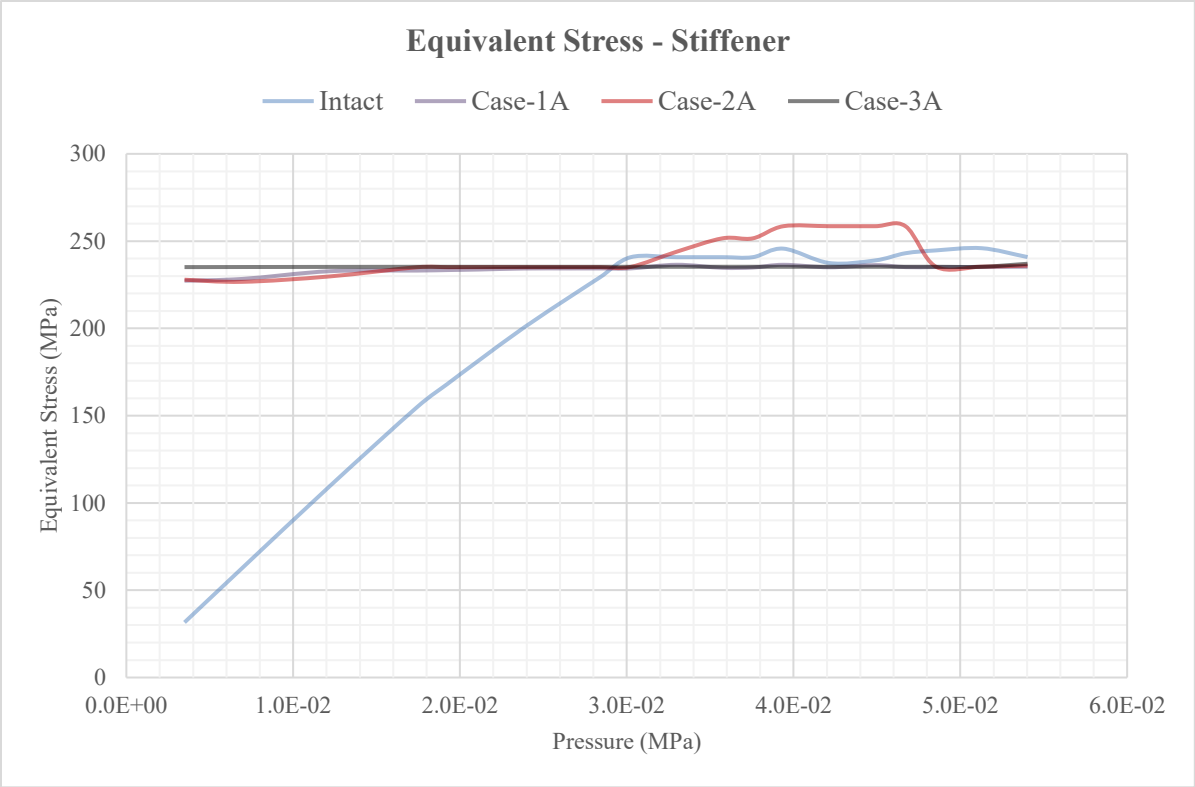

Figure 5.7: Equivalent stress results of the stiffeners

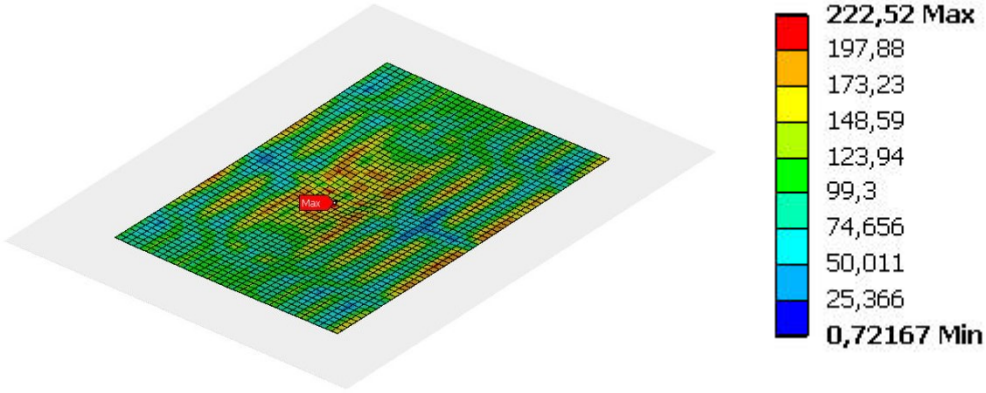

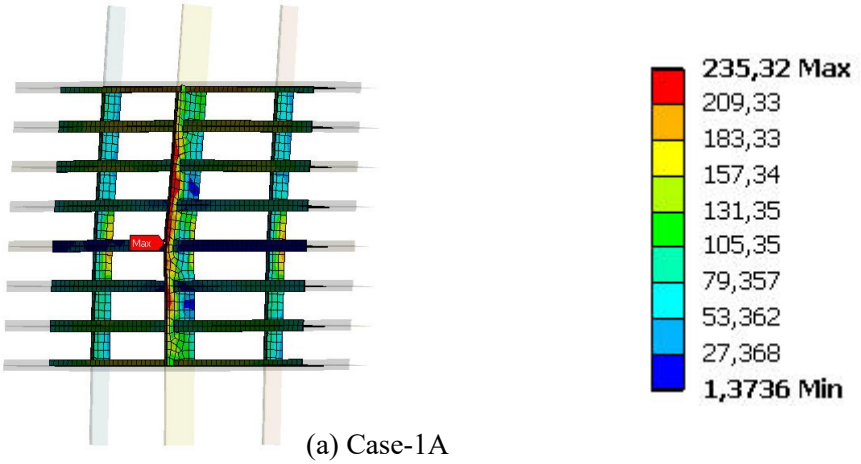

(a) Case-1A

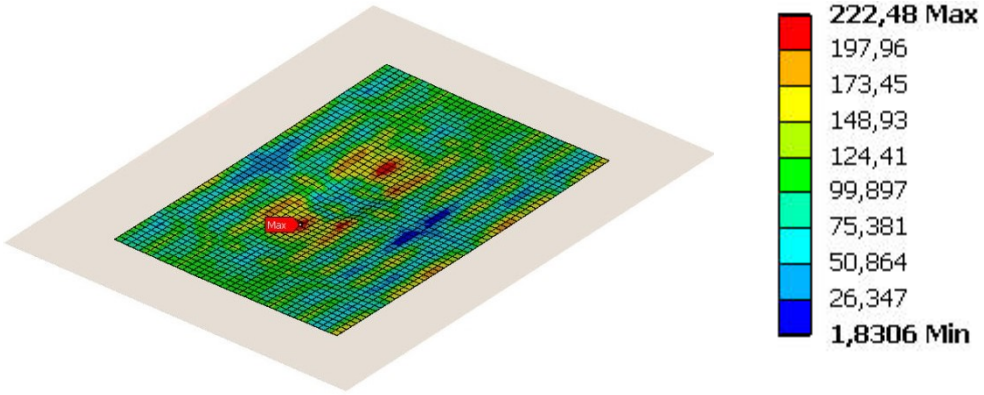

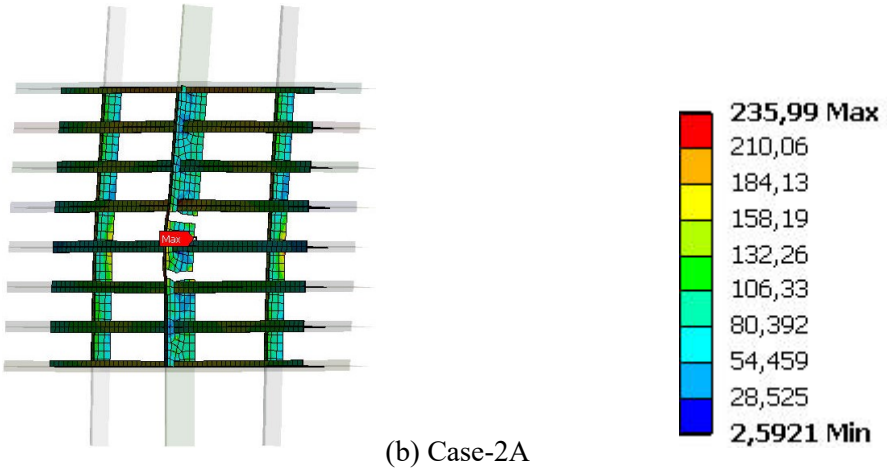

(b) Case-2A

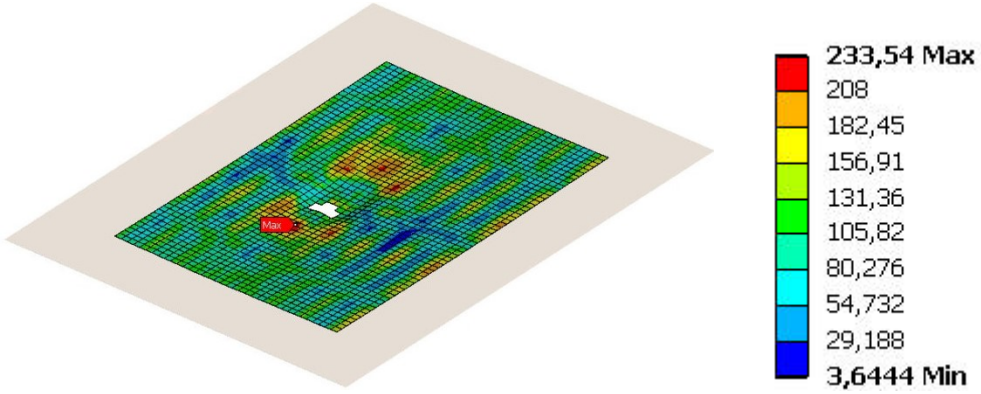

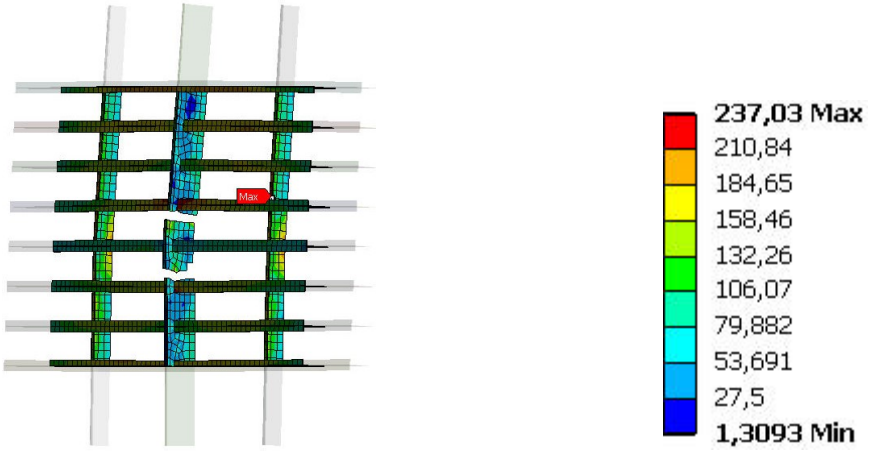

(c) Case-3A

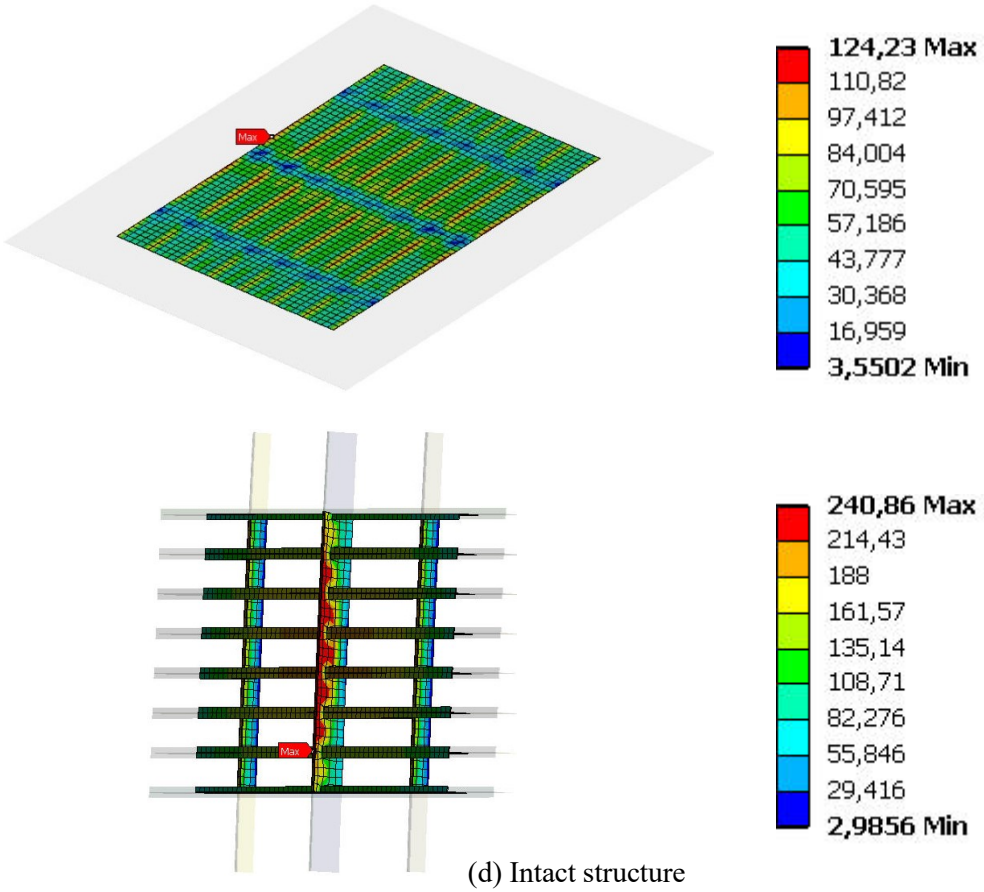

(d) Intact structure

Figure 5.8: Eqivalent stress results

5.3.3 Equivalent Total and Plastic Strain Results

By comparing the strain values presented in Fig. 5.9, Fig. 5.10, Fig. 5.11 and Fig. 5.12, it can be observed that the performance of intact structure is better than the damage structures. Particularly for the plate, no plastic strain occurs in the intact structure. Preserving the elements with high stress and strain values in Case-1A, causes worse performance in comparison to Case-2A which exposed to the same accidental case, but with removal of the failed elements. Furthermore, comparison of damaged structures in Case-2A and Case-3A, with element erosion, leads to similar conclusion that severe deformation affects the performance of the structure negatively. The strain results in the graphics below confirm this argument. However, a noticeable disagreement is evident in stiffener strain results of Case-2A. The reason for this rather contradictory result can be attributed to the preserved elements in the accident simulation, which have plastic strain values very close to but not equal to the failure limit. Although those elements are almost failed, due to the slight divergence from the exact failure value, they are kept. They constitute a relatively instable structure in the damage area and they are separate from the rest of the structure and not supported by the neighbour elements due to the erosion.

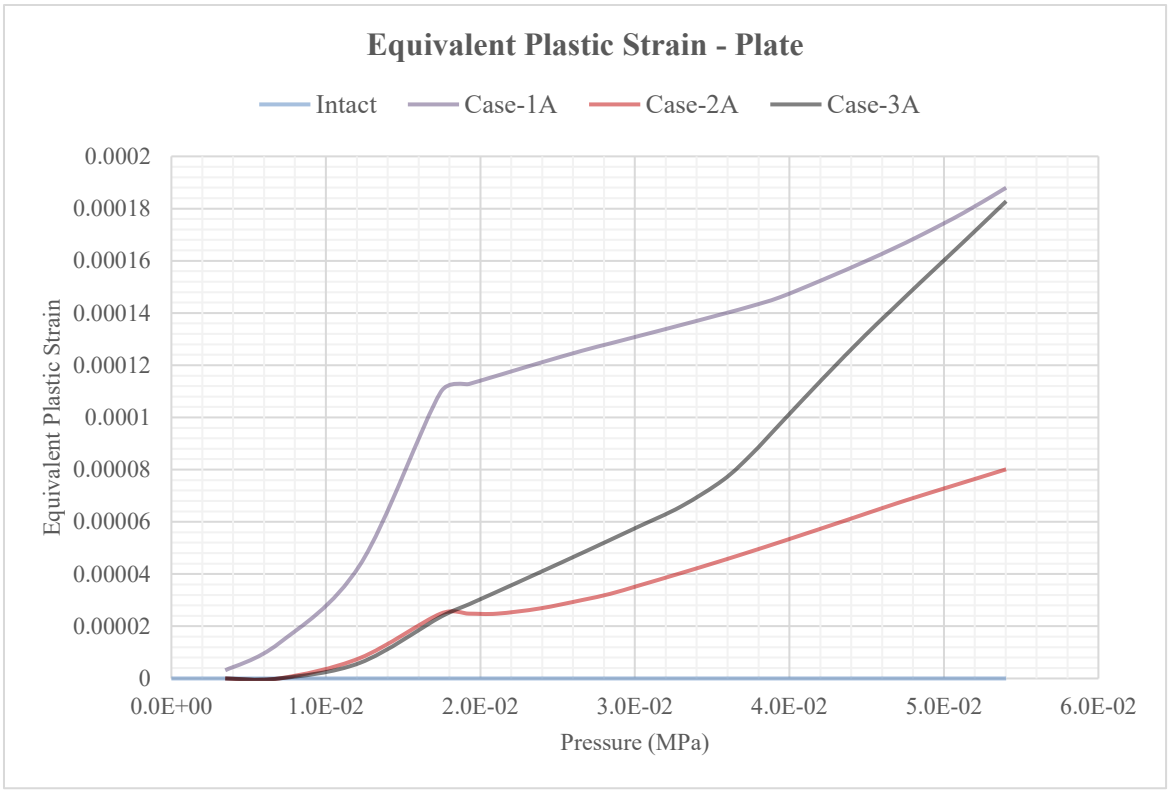

Figure 5.9: Equivalent plastic strain results of the plates

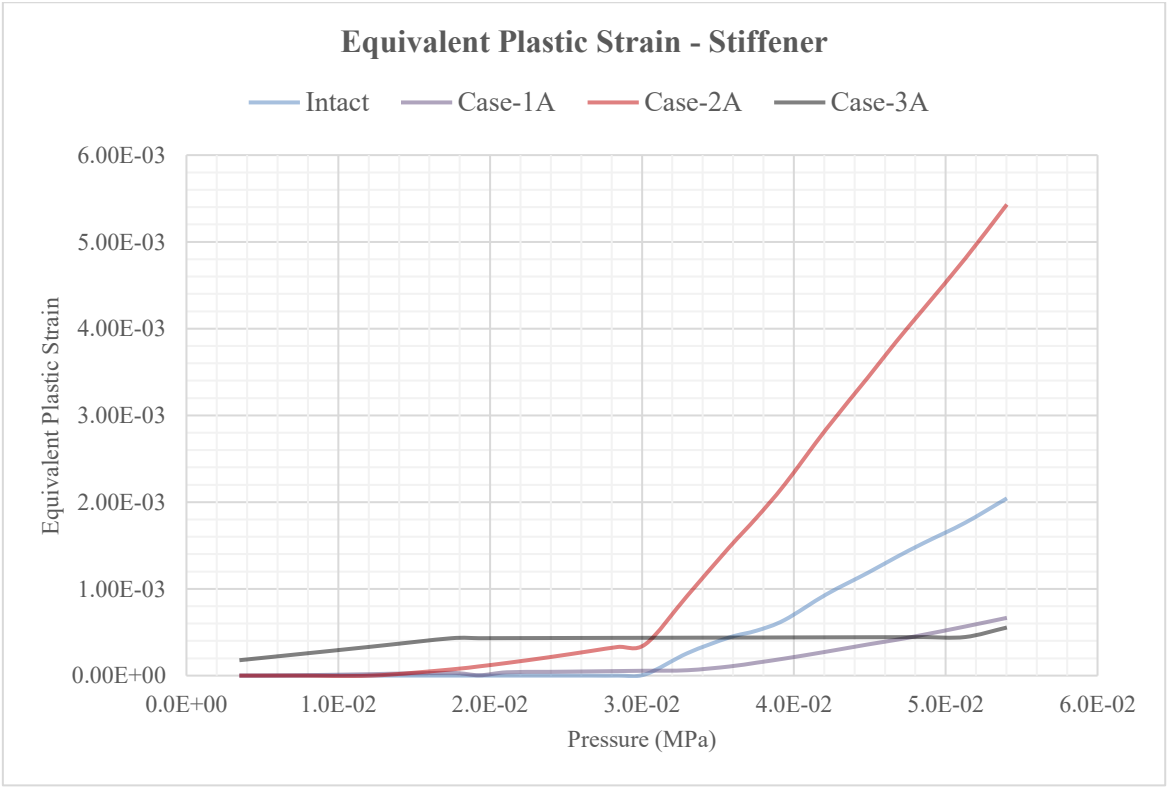

Figure 5.10: Equivalent plastic strain results of the stiffeners

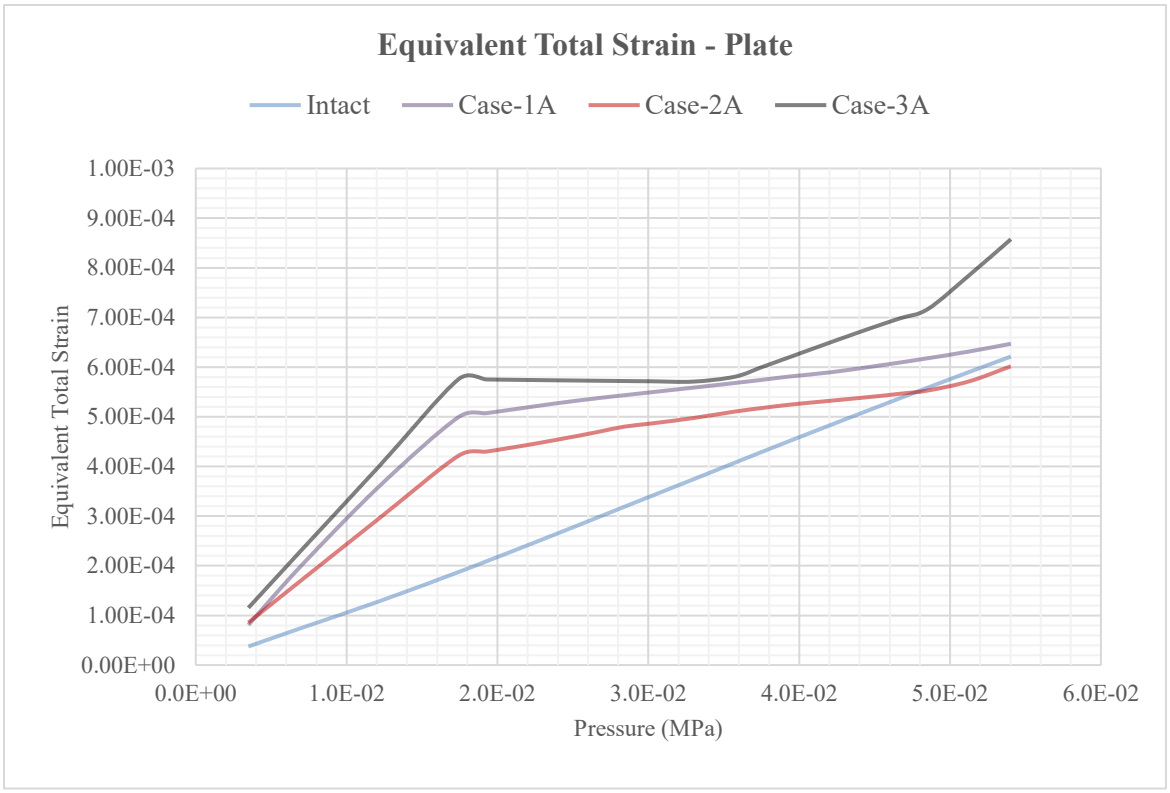

Figure 5.11: Equivalent total strain results of the plates

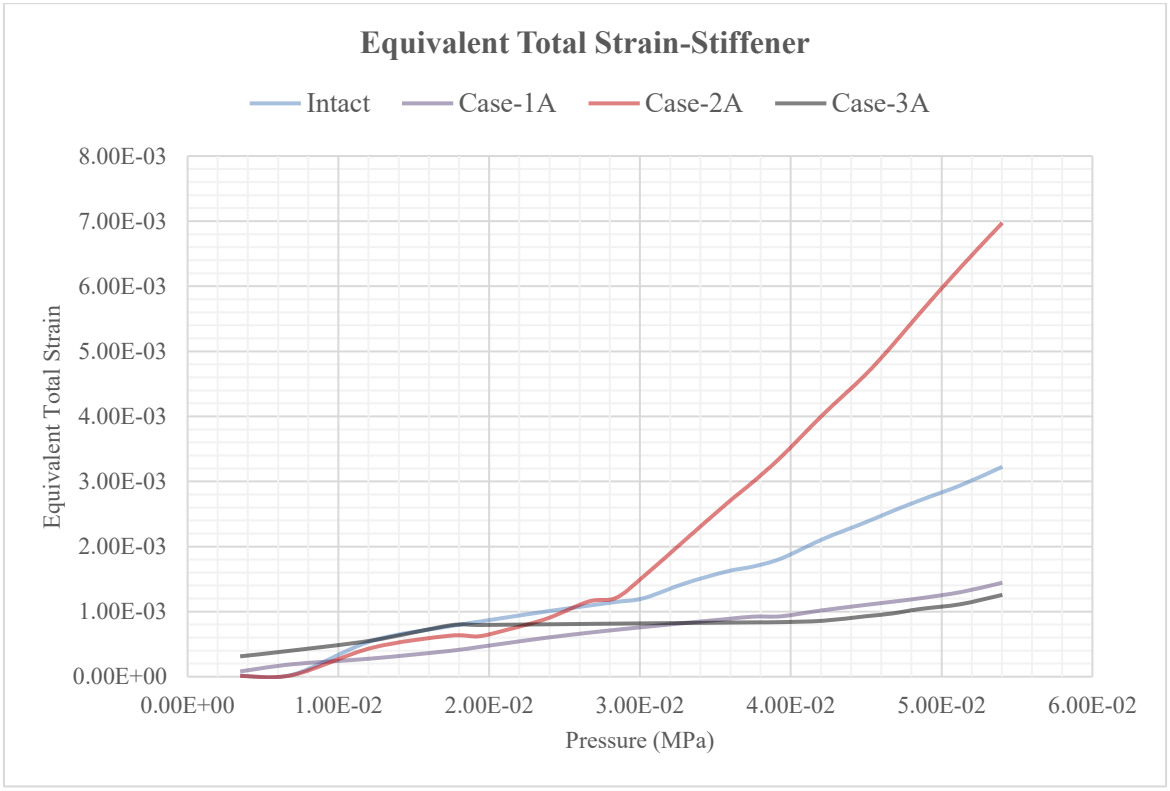

Figure 5.12: Equivalent total strain results of the stiffeners

The detailed configuration of the structures with equivalent plastic strain distribution can be seen in Fig. 5.13.

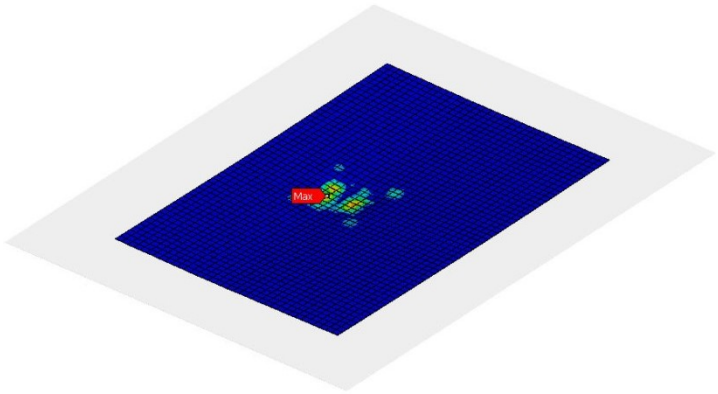

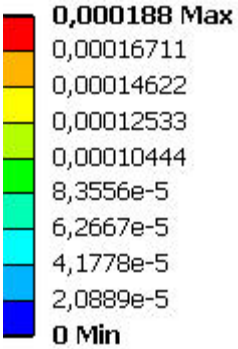

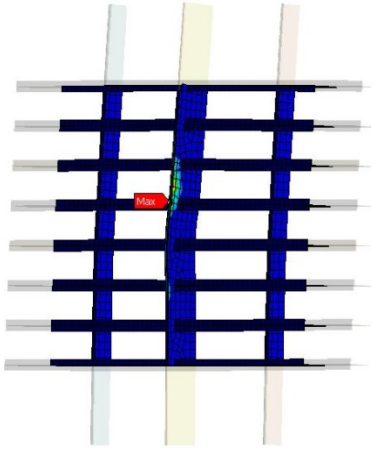

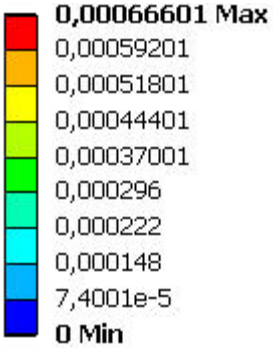

(a) Case-1A

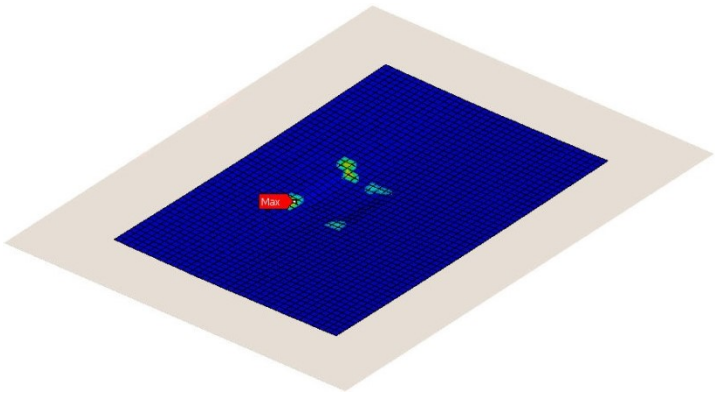

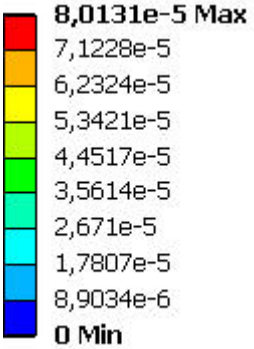

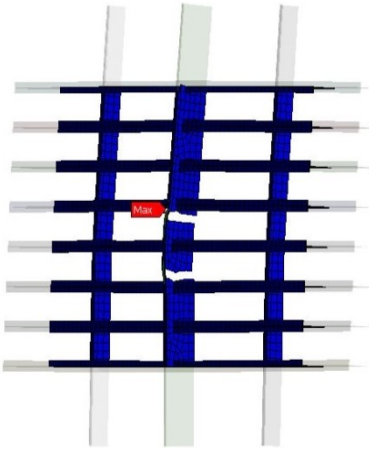

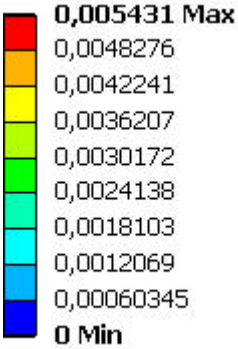

(b) Case-2A

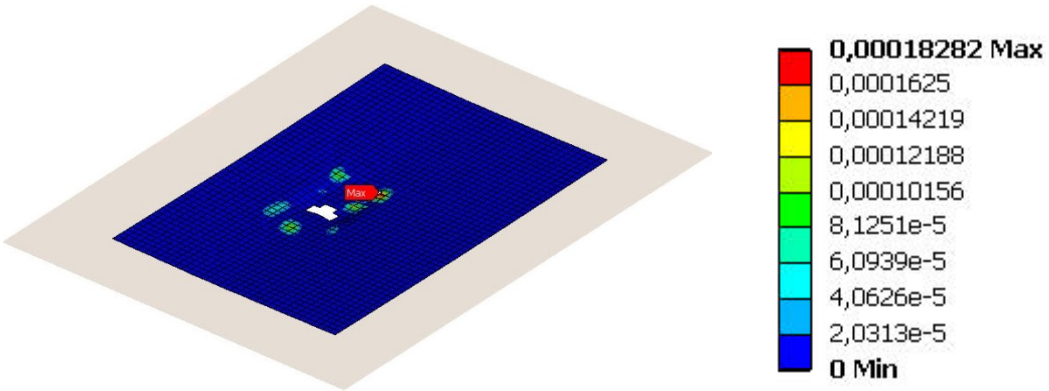

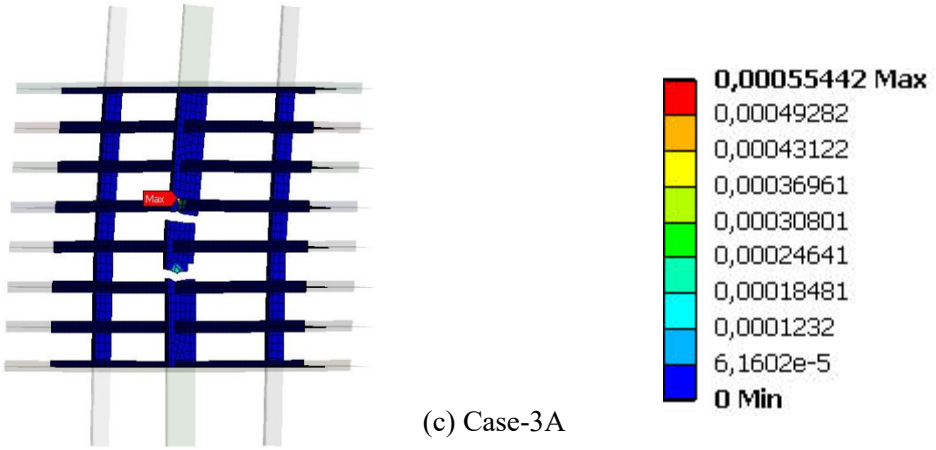

(c) Case-3A

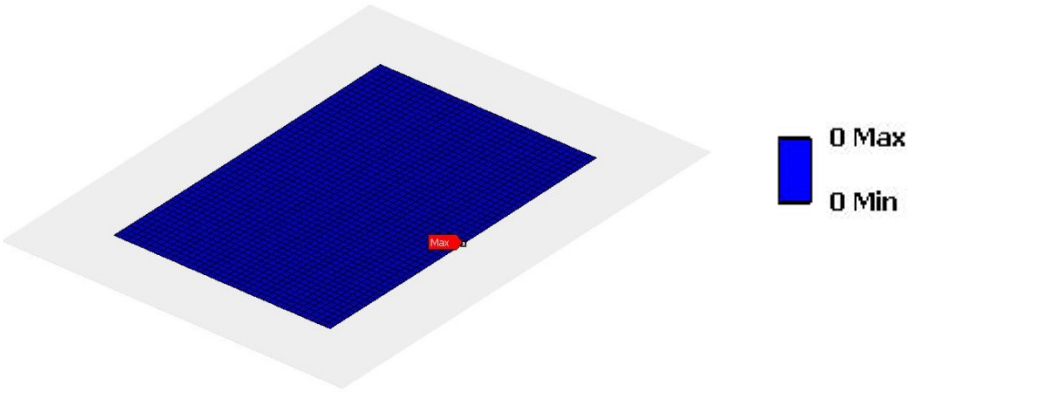

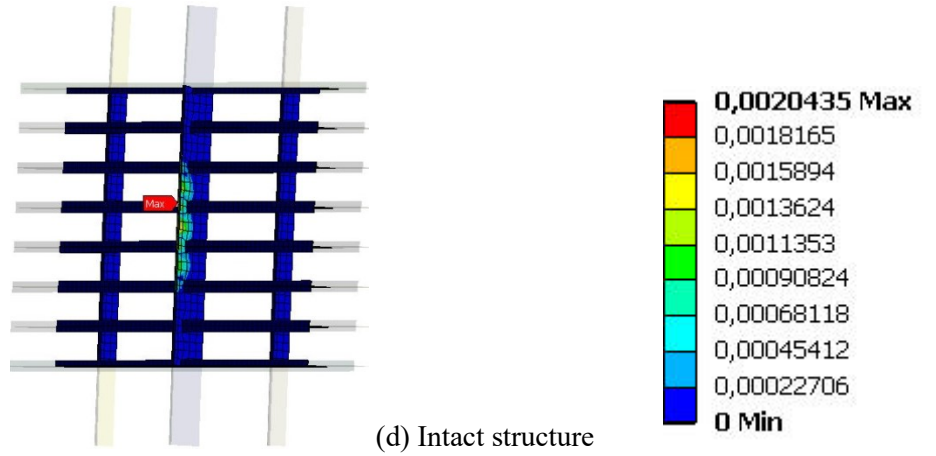

(d) Intact structure

Figure 5.13: Equivalent plastic strain results

6. A NEW HATCH COVER DESIGN PROPOSAL

As it is indicated in previous chapters, hatch covers are crucial structural components in means of vessel integrity and cargo safety. In addition, the type and operation method of the hatch cover are among the factors which determine the duration of loading and unloading operations in the ports. On that account, it can be stated that, hatch covers have an indirect influence on the operation costs. From the financial perspective, another aspect is that cost of hatch covers is around 2-3% of total ship cost, for an ordinary bulk carrier, during the fabrication phase [31].

Therefore, hatch cover design is an interesting topic in the shipbuilding industry. Primary considerations for the design can be listed as follows [31]:

- Hatchway dimensions
- Deck space and clear height for stowage
- Coaming height
- Loading conditions on the cover
- Operation mechanisms and requirements
- Water tightness and cleating
- Weight
- Cost, fabrication, material
- Maintenance and repair

Improvement of the hatch cover design has been also widely studied by many researchers. The majority of those studies are focused on weight reduction by using different materials or optimising the design features [19,20,21,22, 23,63]. Weight reduction is an important target to achieve in hatch cover design, due to its direct effect on vessel performance in many aspects. By reducing the weight of hatch covers, which might occupy up to 80% of the overall breadth of the vessel, it is possible to [22,23,31]:

- Decrease the CoG which leads to improved stability
- Decrease the fuel consumption
- Decrease manufacturing costs
- Increase the freight capacity

However, weight and strength of a steel structure are usually inversely correlated. While reducing the weight, the strength of the hatch cover must be preserved.

Catastrophic consequences of hatch cover structural failure are explained in Chapter-3 and the importance of structural performance after accidental cases, as well as under design conditions, are clearly demonstrated in Chapter-4 and Chapter-5. Bearing those aspects in mind, the aim in this study is to propose an innovative hatch cover structural configuration which has higher strength together with impact load resistance, while ensuring weight reduction, maintenance ease and cost efficiency.

6.1 Previous Hatch Cover Design Optimisation Studies

There is a considerable amount of literature which is focused on the improvement of hatch cover design. While many studies investigated different material alternatives, some authors have discussed optimising the configuration of steel structure.

6.1.1 Alternative Materials

Although traditionally hatch covers are composed of stiffened steel plates, different material alternatives have been investigated and implemented in parallel with the developments in material technology. Composites are the most common alternative materials for hatch cover construction.

Li et.al [19] compared steel and FRP composite hatch covers from the mechanical and financial perspective. By using composite alternative instead of original steel hatch covers of a 230000 DWT ore carrier, 54% weight reduction is achieved. However, the manufacturing cost of composite hatch cover is higher than steel ones. The study concluded that FRP composite hatch cover could be still competitive in cost efficiency during the operational life, considering that less weight could allow less fuel consumption and more cargo capacity. In addition, composite material needs less routine maintenance due to better corrosion resistance in comparison to steel.

Tawfik et.al [20] aimed to achieve weight reduction and strengthening of steel hatch covers of an 82221 DWT bulk carrier by replacing steel with E-Glass composite material. The results showed that it is possible to reduce the weight by 44.32% while preserving structural performance at the same level as the original hatch cover. On the other hand, when the weight is kept same, better structural performance is observed in composite hatch cover. Compliantly with previous studies, the paper demonstrated that the acquisition cost of composite hatch covers is higher than steel hatch covers, while suggesting that life cycle cost of composite material is more advantageous.

Another alternative for steel hatch covers is Sandwich Plate System (SPS) which is composed of two steel face plates and an elastomer core in between. In the literature, there are few studies on implementations of SPS in ship structures. A preliminary analysis was conducted by Boersma [64] to investigate the use of SPS as impact protection for offshore deck structures. However, the results remained insufficient to prove the advantages of SPS over steel structure.

Markulin [65] considered the possibility of using SPS instead of corrugated bulkheads in a Handymax bulk carrier. The study demonstrated that only double sandwich panel can achieve equivalent strength of corrugated bulkhead. By this way, weight reduction is ensured however, the new bulkhead configuration occupies more space which is disadvantageous in terms of cargo capacity. Moreover, the structural performance was assessed only to a very limited extent because the study is based on many simplifications, while dynamic analyses were not included.

6.1.2 Alternative Configurations

In the construction of steel hatch covers, typically L- or T-profile stiffeners are commonly used. In order to strengthen the plate panels, increasing the dimensions of stiffeners is generally a more efficient method than increasing the plate thickness [40].

On the other hand, stronger supporting members can be needed when the lateral loads or out of plane bending are the main load cases such as for hatch covers. For this purpose, alternative shapes of girders such as rectangular box or trapezoidal box can be employed, as presented in Fig.6.1 (b) [40].

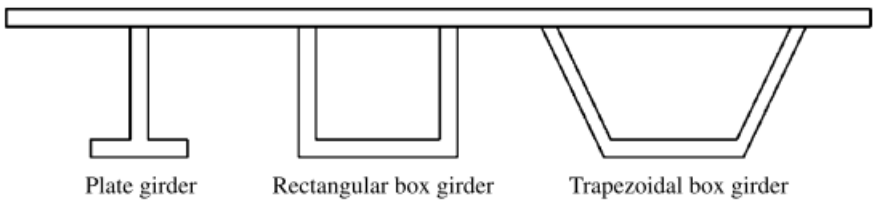

Figure 6.1: Stronger support members [40]

As an innovative approach for the improvement of hatch cover design, trapezoidal box girders, so-called “U-Profiles”, were proposed and patented in Japan, China and Korea in 1997 and currently in use of 950 vessels [21]. U-profiles have been used for top plates of hatch covers, as shown in Fig.6.2 in bulk carriers and container ships.

Figure 6.2: U-profiles of hatch cover top plate [21]

U-Profiles are considered advantageous due to the following aspects [21]:

- Lighter weight in comparison to equivalent traditional angle type (L-Bar) stiffener
- Less accumulation of dust of cargo in bulk carriers
- Reduced weld length and related deformations
- Easier surface treatments and maintenance due to better access possibilities

Um and Roh developed an optimisation program by using C++ programming language to determine optimal dimensions of U-profiles for lightening the structure. The program is able to reduce the weight of hatch cover of an 180000 DWT bulk carrier by 8.5% [22].

Ultimate strength of U-profiles was investigated by Shi and Gao who proved that panels with U-profiles have ~27-28% higher ultimate strength in comparison to panels with bulb (HP) profiles with the same cross-sectional area [23].

6.2 New Hatch Cover Design Concept

This thesis proposes a unique hatch cover design concept, which provides improved structural performance under both static and dynamic loads, while assuring weight reduction and maintenance ease.

A corrugated steel panel is proposed for the new hatch cover design. It is a quite common concept for marine structures and the prime examples of corrugated structures are cargo bulkheads in bulk carriers and tankers as shown in Fig 6.3. Due to the high bearing capacity of corrugated panels against lateral loads, it is considered as a very good alternative configuration for hatch cover structures.

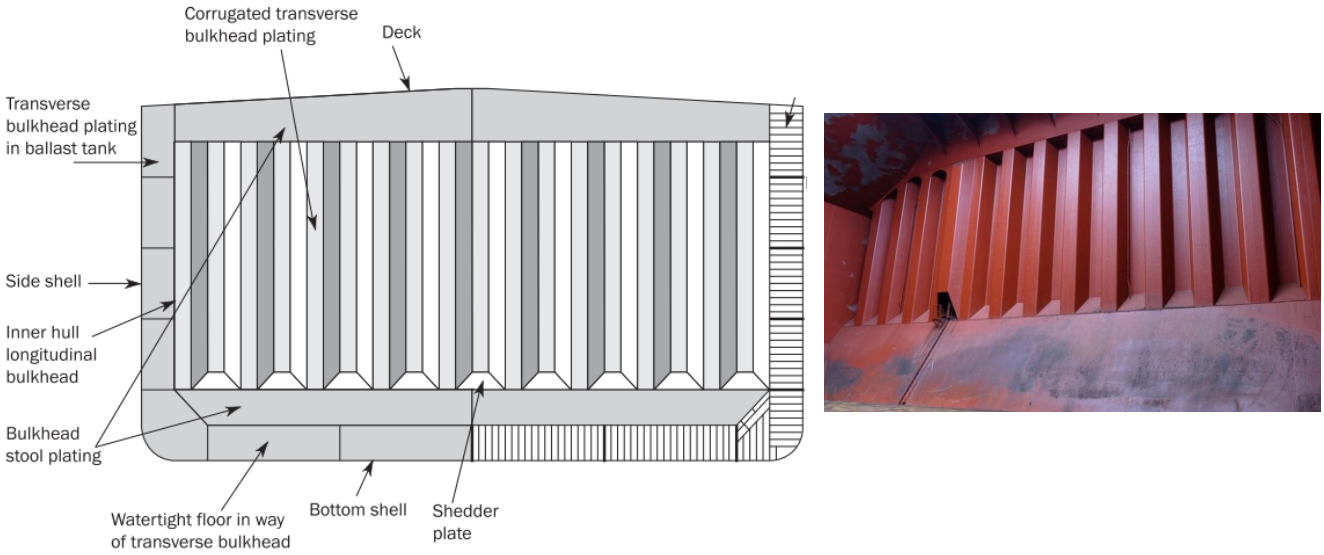

Figure 6.3: Corrugated bulkhead [66,67]

Despite the similarity of the trapezoidal shape with previously developed U-type stiffened plate, in this study the idea is beyond the optimisation of stiffeners of a conventional steel hatch cover. The corrugated structured is not used as a supporting member, but it is directly used as a primary load carrying structure, which makes the concept unique. A 3-D sketch of the proposed corrugated hatch cover concept is seen in Fig. 6.4.

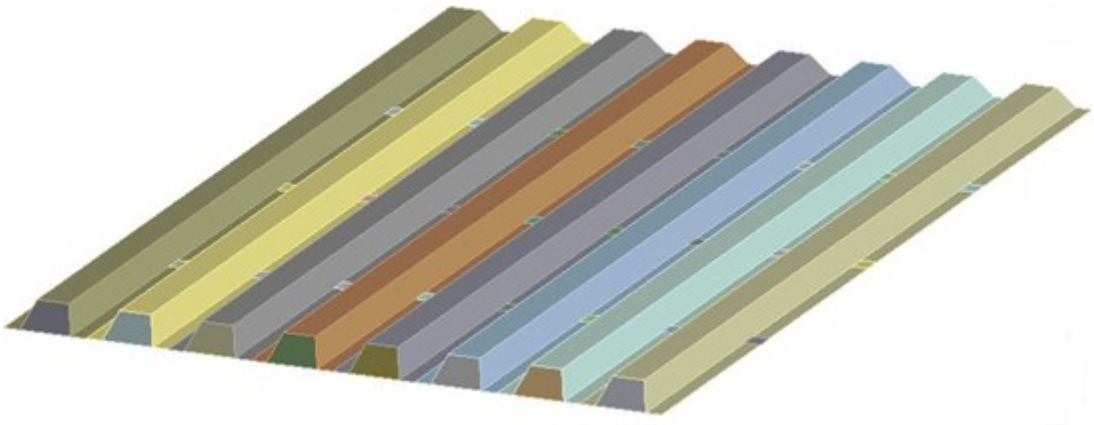

Figure 6.4: 3-D sketch of the corrugated cover concept

However, the trapezoidal configuration causes water accumulation problem on the hatch cover. For the solution of the problem, covering the steel structure with a solid PVC foam material is proposed as the initial idea, which would require enhancement in further studies. The corrugated hatch cover with PVC foam on top of it is illustrated in Fig. 6.5. The only purpose of the PVC structure is to provide a flat surface against water accumulation, thus homogenous load distribution is enabled. However, it does not have any contribution to

stiffness and strength of the hatch cover structure. Moreover, three flat bars of 300x10.5 mm, as seen in Fig. 6.5 are attached transversely to the lower side of the corrugated structure, also as an initial idea to reinforce the structure against overall bending. Although this could be omitted while increasing the section modulus of the corrugation in the future studies.

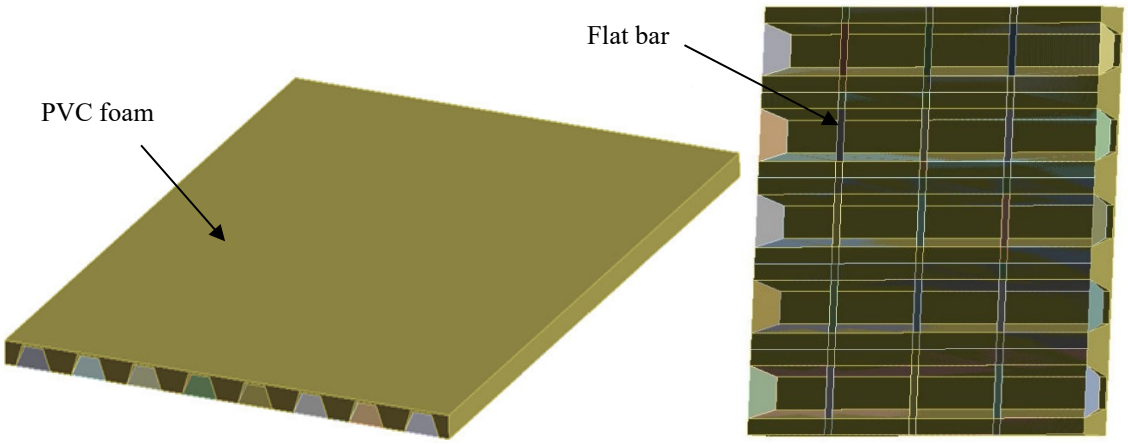

Figure 6.5: Corrugated hatch cover with PVC foam

6.2.1 Structural Properties of Corrugated Plates

It is a well know aspect through the previous studies [68,69] that strength of corrugated panels is very high, especially under lateral loads. Moreover, due to its maintenance ease and low cost, corrugated panels are chosen as structural members in many different industries from aviation to marine.

In shipbuilding, corrugated plates are mainly used for watertight cargo bulkheads in bulk carrier and tanker vessels. Therefore, the regulations [66,70] related to corrugated panels are concerned with bulkhead design. However, it is considered as a proper base and taken as a reference for the new hatch cover design in this study.

The main dimensions and their representation are given in Fig. 6.6 according to DNV Rules for Classification [70].

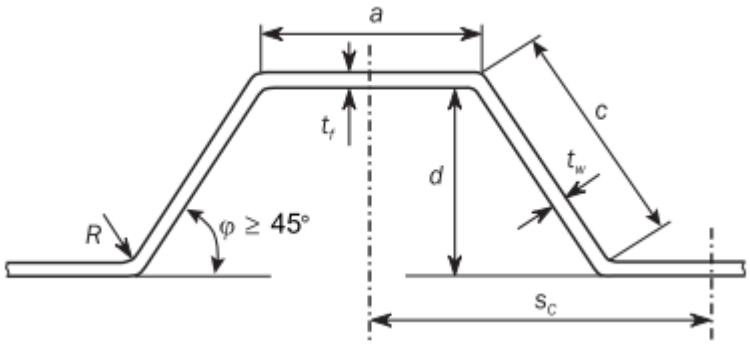

Figure 6.6: Corrugated bulkhead main dimensions [70]

Φ, the corrugation angle should not be less than 55°, however in some specific cases, the angle between 45° and 55° might be accepted.

The section modulus of a corrugation segment can be calculated by Eq. (6.1) [70].

$$Z = \left[\frac{d(3at_f + ct_w)}{6}\right] 10^{-3} \ cm^3 \tag{6.1}$$

Caldwell [68] and Paik et.al [69] conducted experimental studies to investigate ultimate strength of corrugated panels. The authors concluded that the behaviour of a single central corrugation segment can represent the behaviour of the whole structure under uniform lateral load. From the study of Paik et.al [69], a typical collapse pattern of a corrugated panel under lateral load is presented in Fig. 6.7. Considering this behaviour, the ultimate strength of a corrugated panel, under lateral pressure loads (p) can be estimated by calculation of a single corrugation beam as shown in Fig. 6.8.

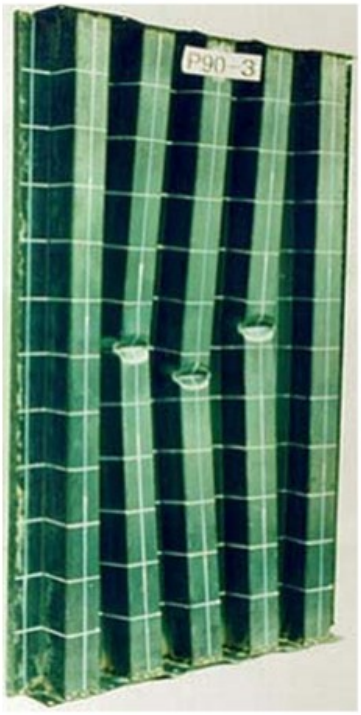

Figure 6.7: Collapse pattern of a corrugated panel [69]

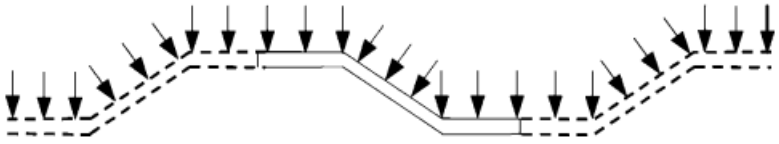

Figure 6.8: Single Corrugation under Lateral Pressure [69]

6.3 Geometric Details of the Proposed Hatch Cover

Corrugated panels are proposed as an innovative hatch cover concept idea in this study. To validate the claimed advantages such as higher structural performance, a number of static and dynamic analyses are conducted in the following sections.

However, while modelling the structure, the main challenge is that no standards or regulations exist for the scantling of corrugated hatch covers yet. Therefore, a section modulus-based parametric approach is applied to find out the optimum dimensions. For this purpose, M/V Derbyshire pontoon hatch cover is chosen as the reference, thus it is also possible to compare the results of the original structure and the new concept. Main geometric properties of M/V Derbyshire original hatch cover (Hold 1) are given in Table 6.1 and the cross-section of the one-bay plate-stiffener combination is illustrated in Fig. 6.9.

Table 6.1: Geometric properties of the hatch cover

Length	14680 mm
Breadth	11000 mm
Stiffener spacing	994 mm
Stiffener dimensions	T 635x10.5x280x25 mm
Section modulus	5246.989 cm^3
Weight	31.503 t

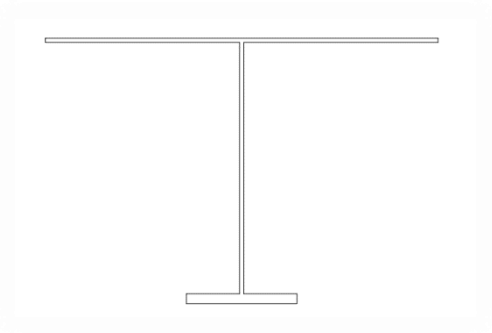

Figure 6.9: One-bay model cross-section

As the new concept, four corrugated hatch covers with different scantlings are modelled and their structural behaviours under design load are compared, in order to determine the optimum dimensions. In this parametric study, the main dimensions (length and breadth) of M/V Derbyshire hatch cover are chosen as design constraints. By this way, performance comparison becomes more coherent and the new hatch cover configuration can be proposed as an alternative to the original structure. While assigning the dimensions to the new design, the target is to obtain a section modulus equal or higher than the original structure`s and achieve a better performance under the design load. Deformation magnitude is taken as the indicator of the structural performance. Bearing those considerations in mind, 4 different corrugated profiles are generated. Previous studies [68,69] have proved that one segment of the corrugation can represent the behaviour of the whole structure in strength calculations. Therefore, it is considered convenient to compare the section modulus of the one corrugation

segment to the one-bay plate-stiffener combination of the original structure. Details of the four different segment cross-sections are given in Table 6.2.

Table 6.2: Cross-sections of corrugated segments

Cross-Section	**Geometric Properties**
Profile-A 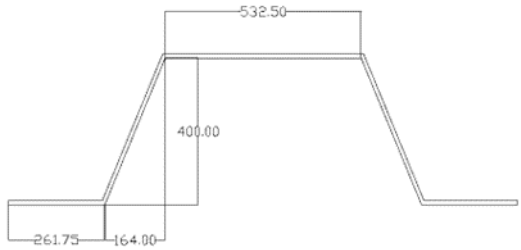	Segment length = 1375 mm Segment number = 8 Thickness =10.5 mm Section modulus = 2713.923 cm^3 Segment weight =2.385 t
Profile-B 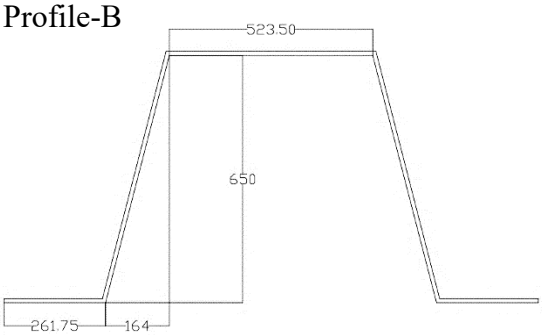	Segment length = 1375 mm Segment number = 8 Thickness =10.5 mm Section modulus = 4984.243 cm^3 Segment weight = 2.974 t
Profile-C 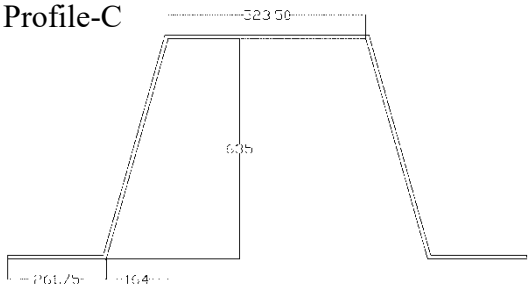	Segment length = 1375 mm Segment number = 8 Thickness =10.5 mm Section modulus = 4835.666 cm^3 Segment weight = 2.938 t
Profile-D 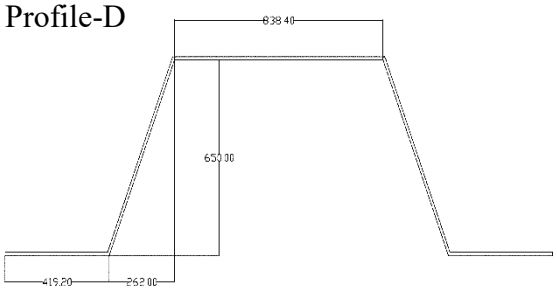	Segment length = 2200.8 mm Segment number = 5 Thickness =10.5 mm Section modulus = 7168.832 cm^3 Segment weight = 3.879 t

As indicated before, weight reduction is one of the main advantages that the proposed design offers. Therefore, it is aimed to achieve better structural performance and less weight at the same time. Table 6.3 summarises deformation results as a structural performance indicator and weights of whole hatch cover structures to be able to determine the optimum dimensions. In the table, "Panel Weight" indicates the weight of the whole steel corrugated hatch cover structure with the dimensions of L= 14720 mm and B= 11000 mm and composed of the profile segments which are explained above. On the other hand, "Total Weight" represents the weight of the steel corrugated structure together with the PVC foam on top. Although, the PVC foam is suggested as a temporary solution to obtain a plain surface on top of the corrugation and requires further investigation for improvement; it is considered meaningful to take into consideration for total weight comparison. Likewise, the graphical deformation results of the whole hatch cover models with different profile types are illustrated in Fig. 6.10.

Table 6.3: Comparison of different design options

	Profile-A	**Profile-B**	**Profile-C**	**Profile-D**	**Original**
Deformation [mm]	58.968	19.800	20.857	22.657	13.828
Panel Weight [t]	19.085	23.795	23.507	19.399	31.503
Total Weight [t]	22.1854	28.511	28.126	24.155	31.503

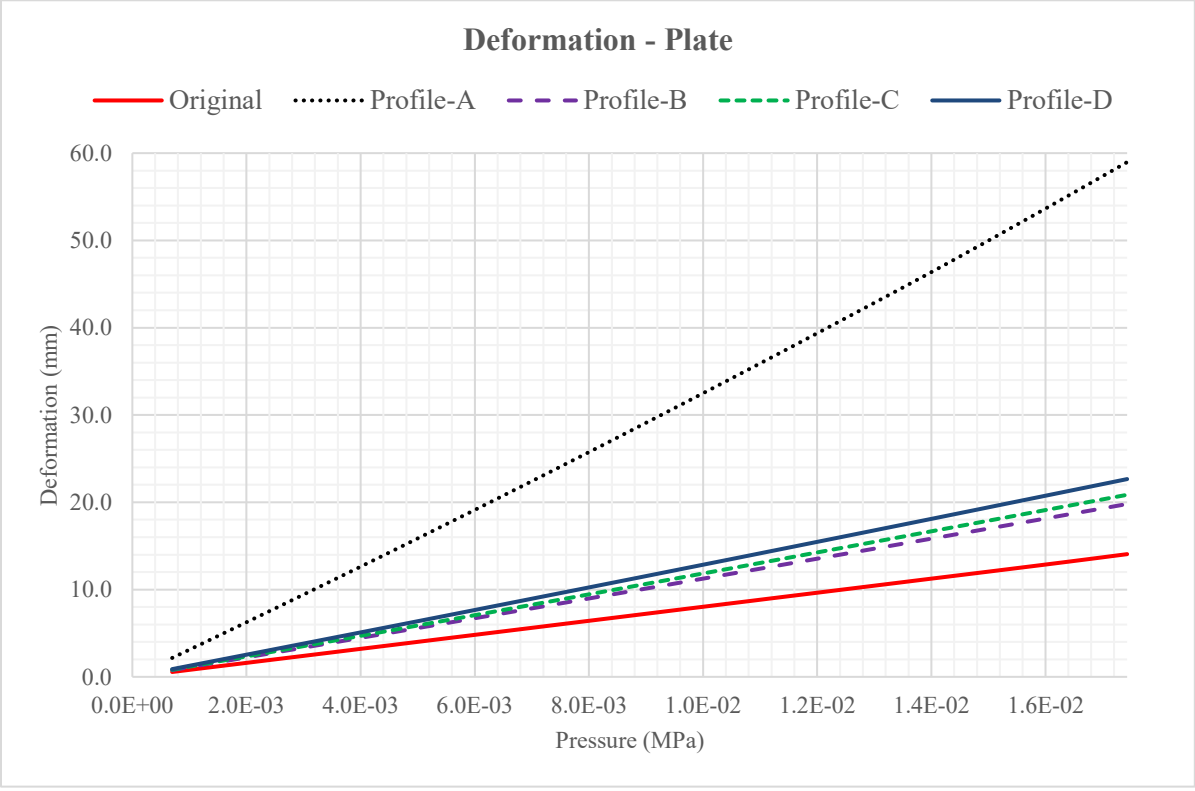

Figure 6.10: Deformation results of different design proposals

After the assessment of the parametric study, it is concluded that Profile-D is the optimum choice, which secures 38% panel weight reduction. Thus, the corrugated hatch cover model which composed of Profile-D segments is employed in the following sections to analyse the structural behaviour under impact load and its post-accident performance.

6.4 Structural Behaviour under Impact Load

By the implementation of the new hatch cover design, a remarkable weight reduction can be achieved. However, it must be ensured that the structure does not compromise its strength while reducing the weight. The strength of the structure is analysed under static design load and satisfying results are obtained, in the previous section.

In this part, the response of the structure against impact load is investigated, coherently with the general frame of this thesis. For this investigation, Drop Case-3 in Chapter-4 is taken as a reference, due to its severe results. Same boundary conditions are applied to the corrugated hatch cover and the dropped object is modelled with the same physical properties and position. Material model and mesh properties are assigned as described in previous chapters.

It should be noted that although the PVC foam and flat bars are included in the simulations, only the results of the steel corrugated panel are presented, since it is the concerned structural strength component. The results show that the original structure reaches high deformation levels due to the element erosion in the plate, whereas deformation of corrugated structure remains very low. Equivalent stress graph patterns are quite similar; while plastic strain results are lower in corrugated hatch cover. Table 6.4 gives explicit dynamic analysis results of corrugated hatch cover, as maximum values over time during the simulation.

Fig. 6.11, Fig 6.12 and Fig. 6.13 compare the deformation, equivalent stress and plastic strain plots of the original and the corrugated structure and present the comparative illustrations. Maximum values over time, which occur right after the impact, are given.

Table 6.4: Analysis of drooped object case – Corrugated hatch cover

	Deformation [mm]	**Equivalent Stress [MPa]**	**Equivalent Plastic Strain [-]**
Corrugated hatch cover	541	264.23	0.0664

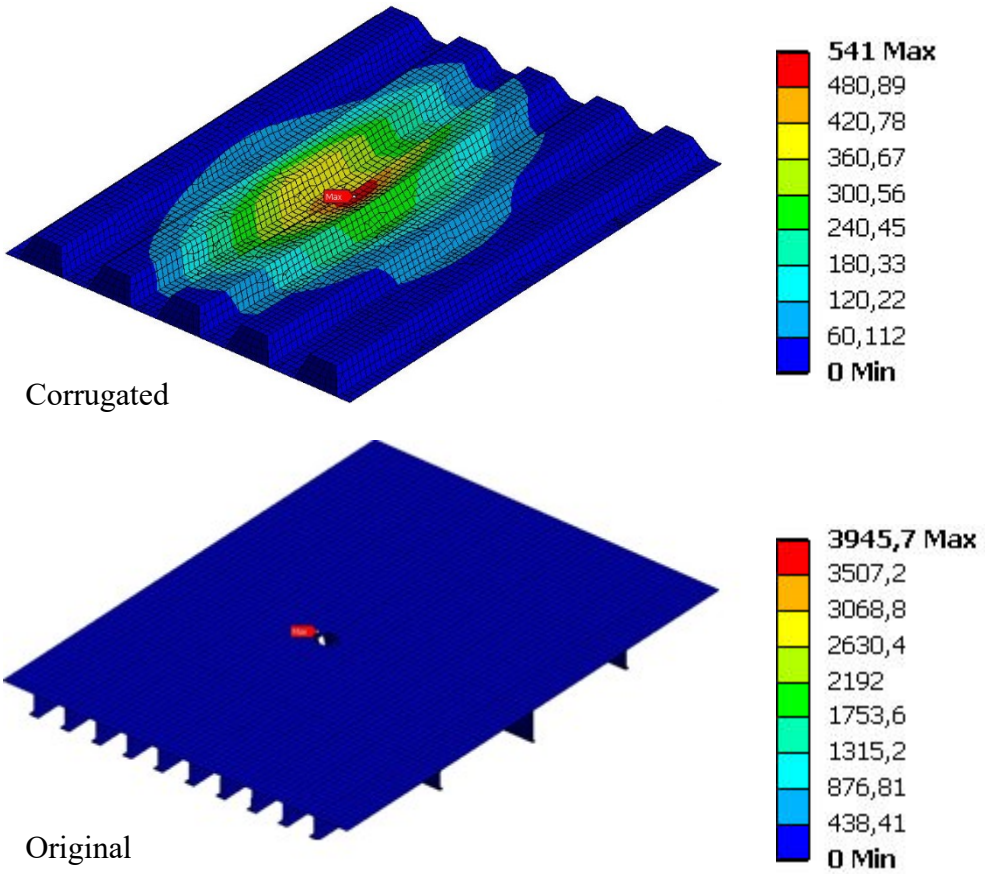

(a) Overall maximum deformation

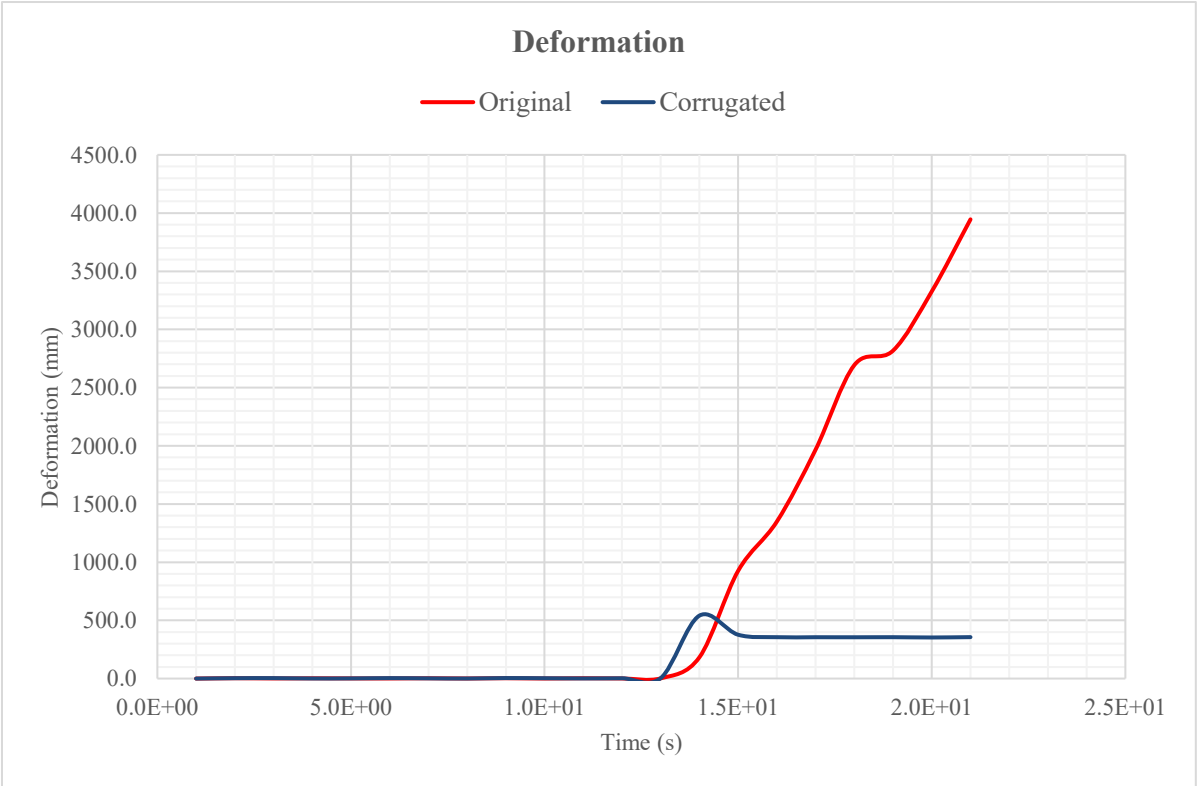

(b) Maximum deformation at each time step

Figure 6.11: Comparative deformation results under impact load

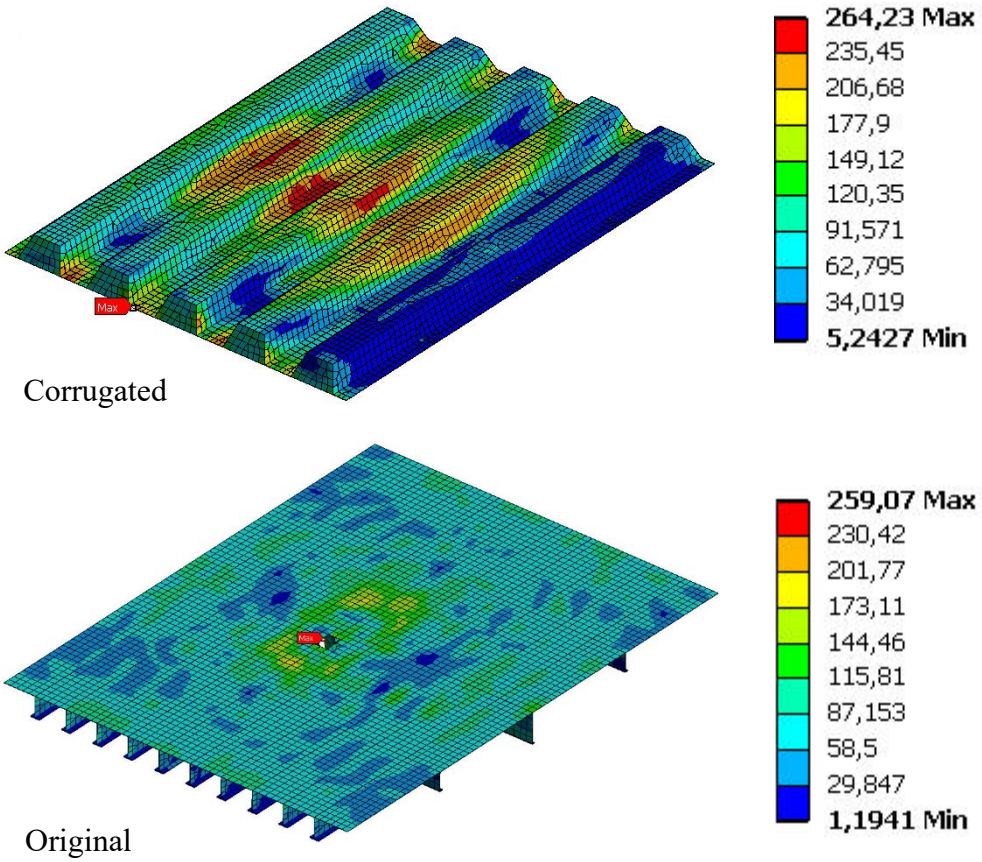

(a) Overall maximum equivalent stress

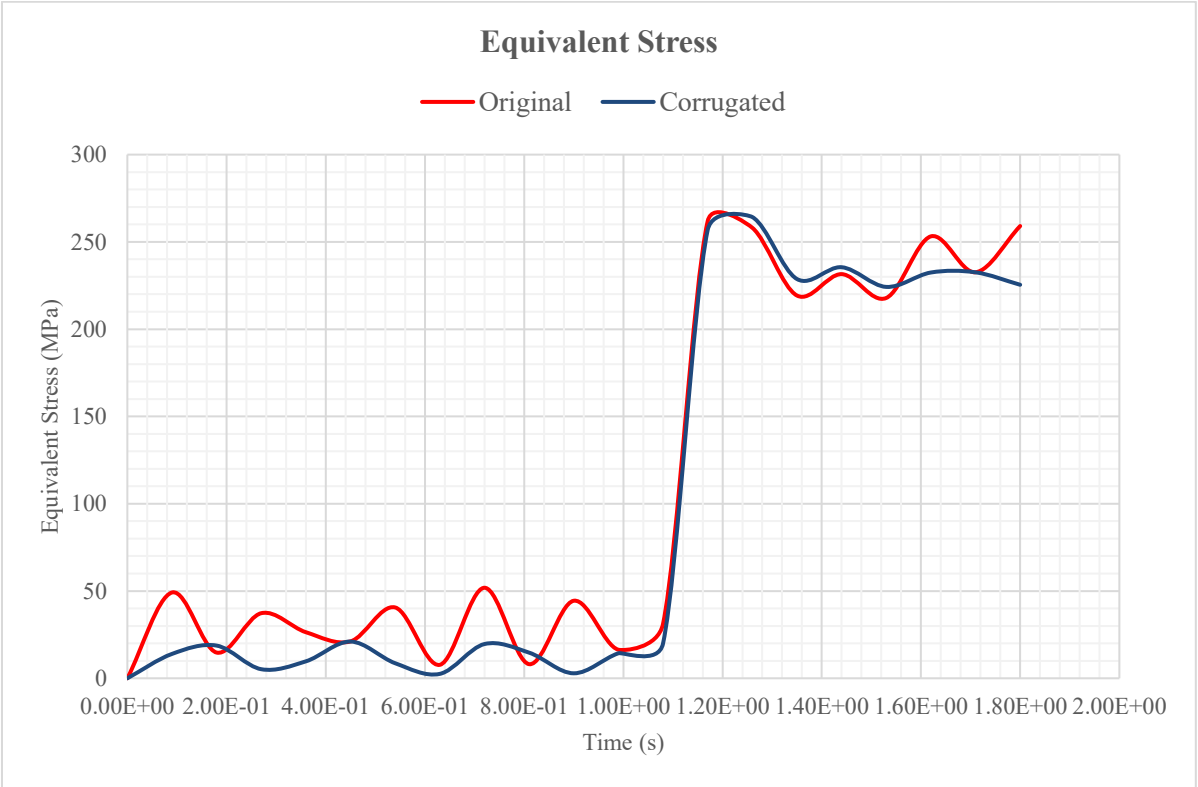

(b) Maximum equivalent stress at each time step

Figure 6.12: Comparative equivalent stress results under impact load

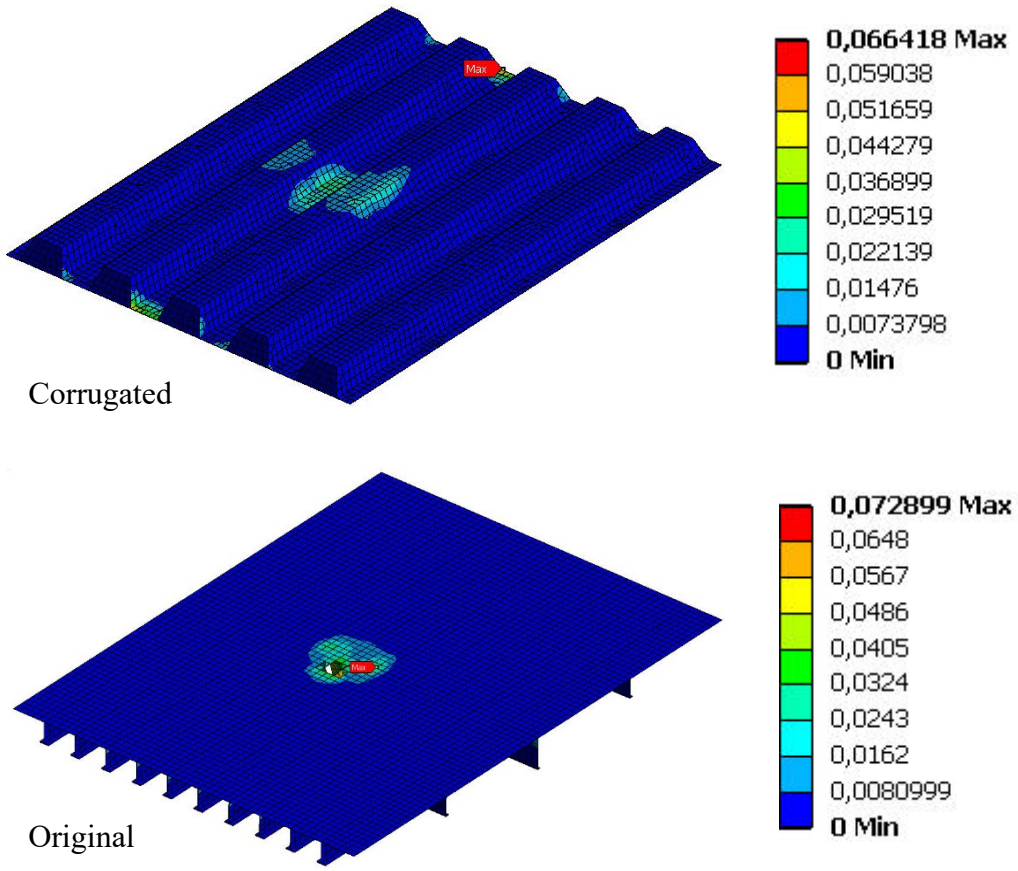

(a) Overall maximum equivalent plastic strain

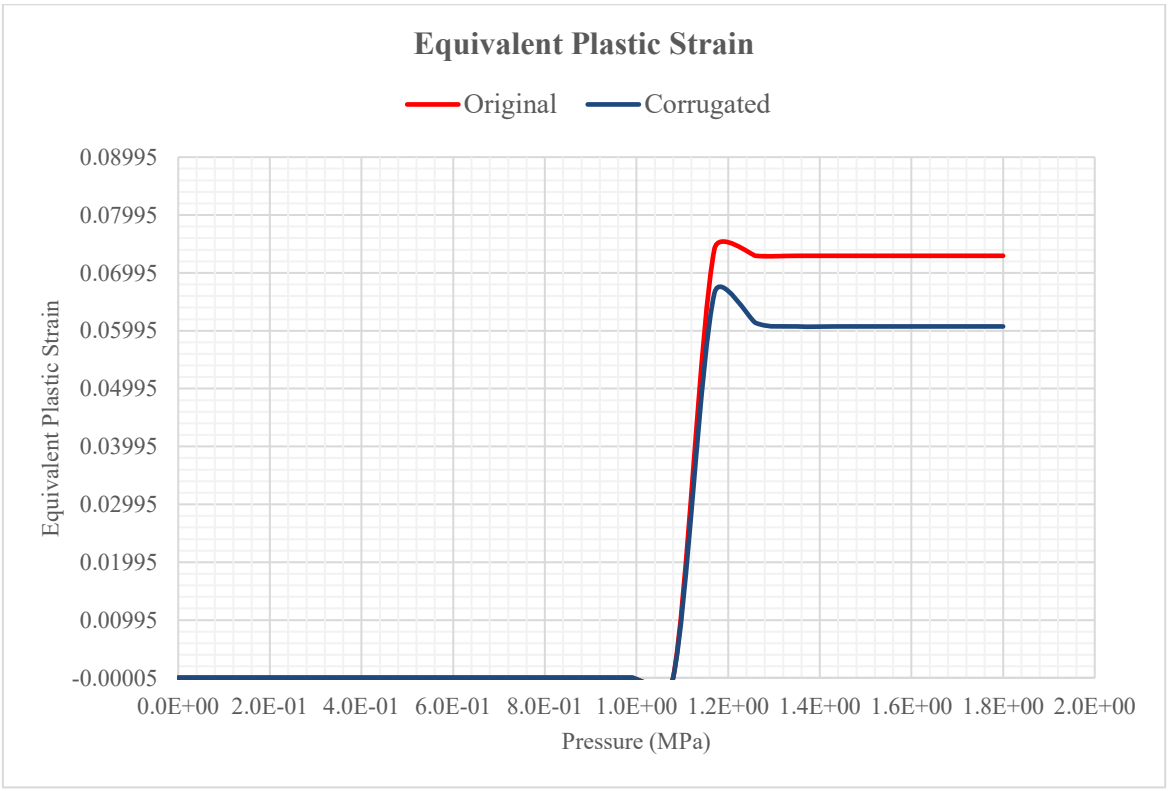

(b) Maximum equivalent plastic strain at each time step

Figure 6.13: Comparative equivalent plastic strain results under impact load

6.5 Post-Accident Performance

It has been confirmed that the corrugated hatch cover is at least as resilient as the original structure under impact load. Subsequently in this section, post-accident performance of the corrugated hatch cover is analysed and compared with the original structure`s. In compliance with the procedure in Chapter-5, Case-3A is implemented on the new design. Namely, the deformed structure is transferred from the dynamic analysis system to the static system and the residual stresses due to impact are imported. Boundary conditions are kept same and the collapse load 0.05403 MPa is applied as lateral pressure gradually.

The comparative post-accident performance results of corrugated and original hatch cover are presented in Table 6.5 As explained in Chapter-5, in order to avoid the influence of boundary conditions, the maximum values are detected within the area 2 meters inside from the edges of the hatch cover models. Overall deformation distribution and deformation results of mid-node are given in Fig. 6.14, in order to present the total displacement resulting from the sequential analyses as explained in the section 5.3.1.

Fig. 15, Fig.16 and Fig. 17 present equivalent stress, equivalent plastic strain and equivalent total strain results. The distribution of the results under maximum load 0.05403 MPa are given in illustrative form, while the graphics show the maximum values within the structure during the load application in five steps.

According to the obtained results, damaged corrugated hatch cover performs significantly better than the damaged original structure under lateral static pressure.

Table 6.5: Post-accident performance comparison

0.05403 MPa	**Original**	**Corrugated**	**Difference**
Deformation [mm]	28.905	5.176	82%
Eqv. Stress [MPa]	233.54	211.830	9%
Eqv. Plastic Strain [-]	1.83e-4	4.989e-7	99%

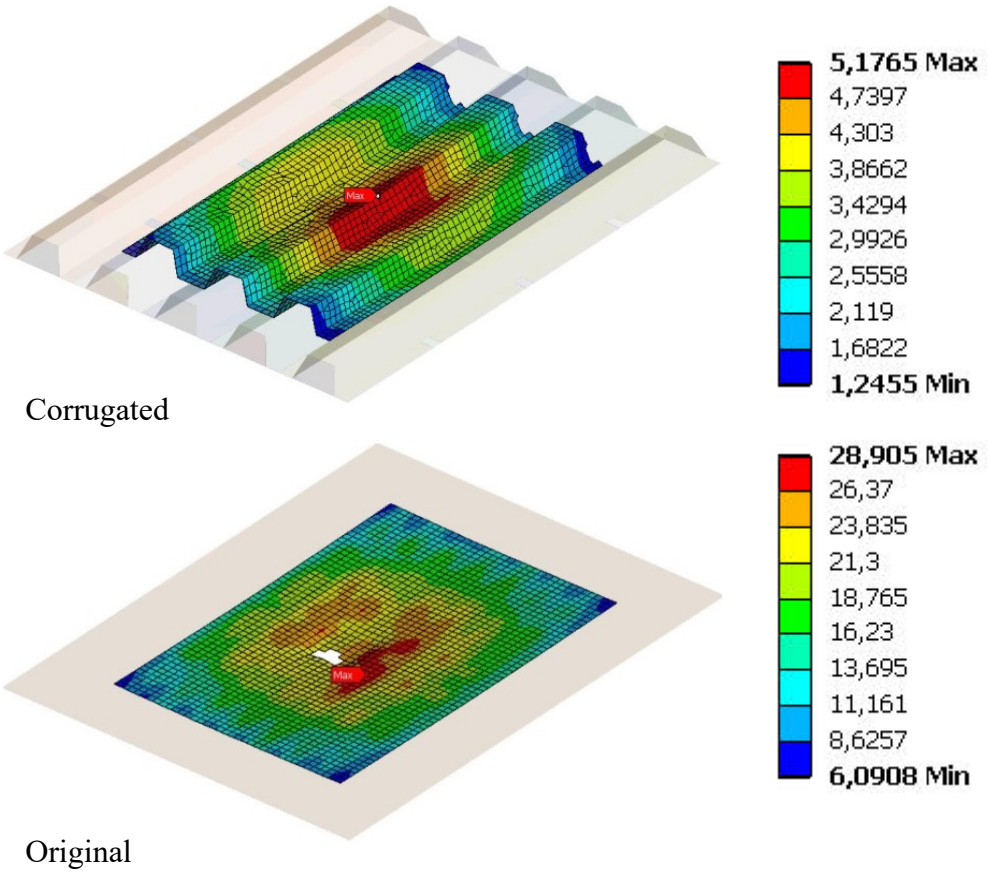

(a) Overall deformation distribution at maximum load

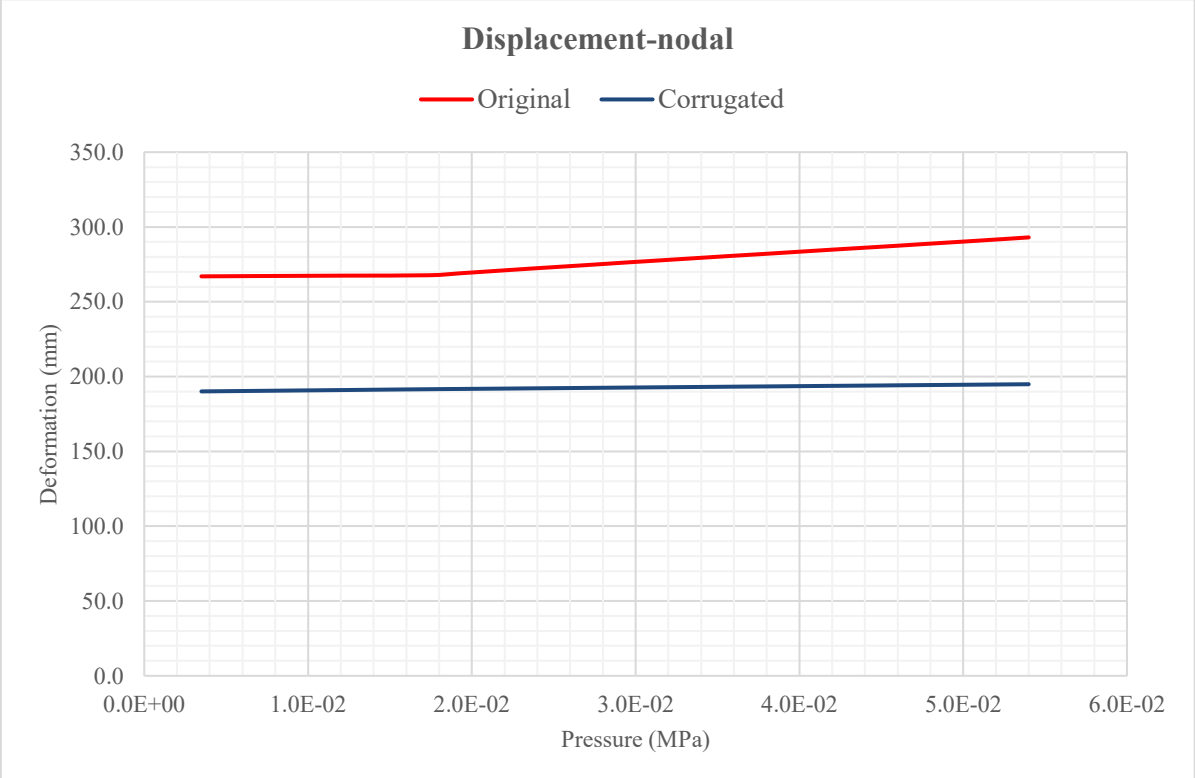

(b) Maximum mid-node displacement during load application

Figure 6.14: Post-accident deformation results

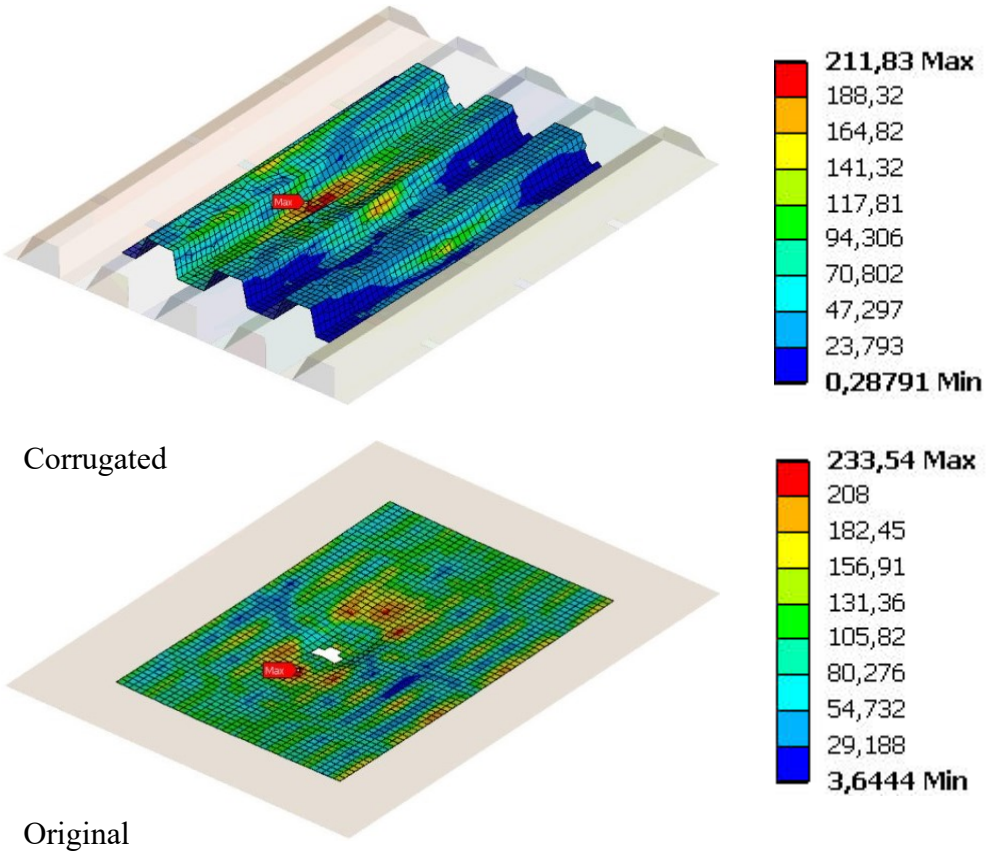

(a) Overall equivalent stress distribution at maximum load

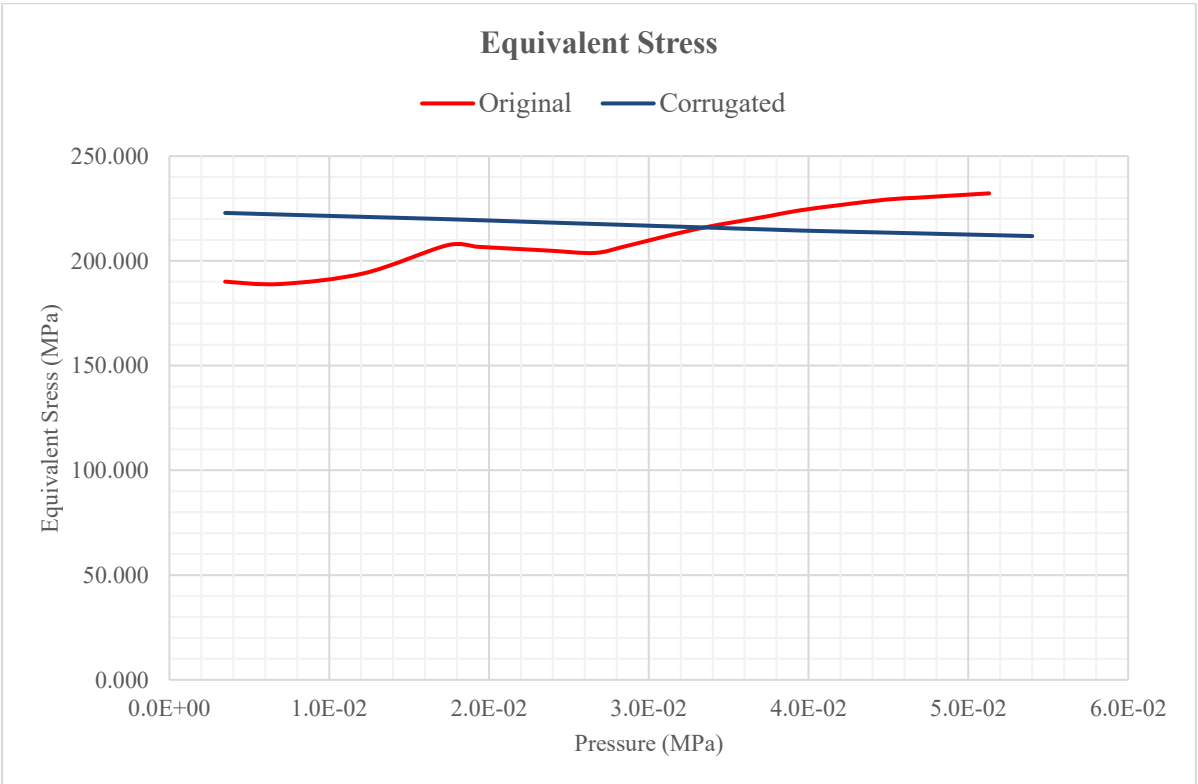

(b) Maximum equivalent stress during load application

Figure 6.15: Post-accident equivalent stress results

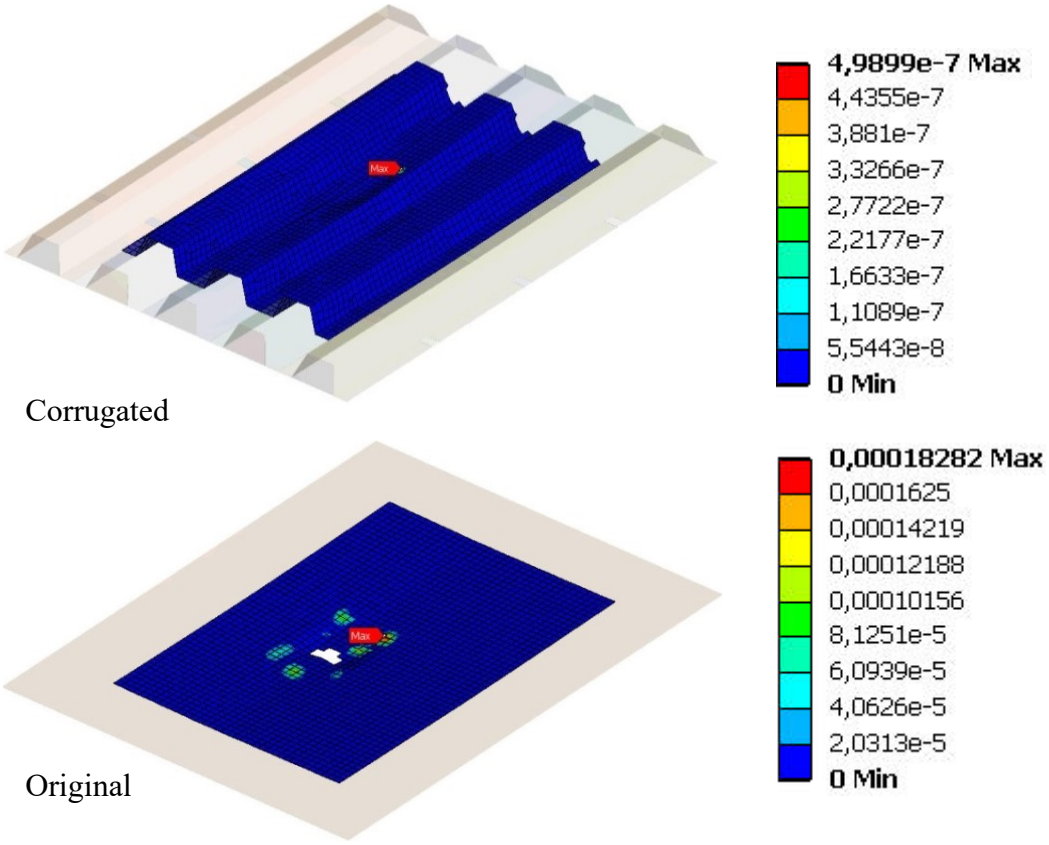

(a) Overall equivalent plastic strain distribution at maximum load

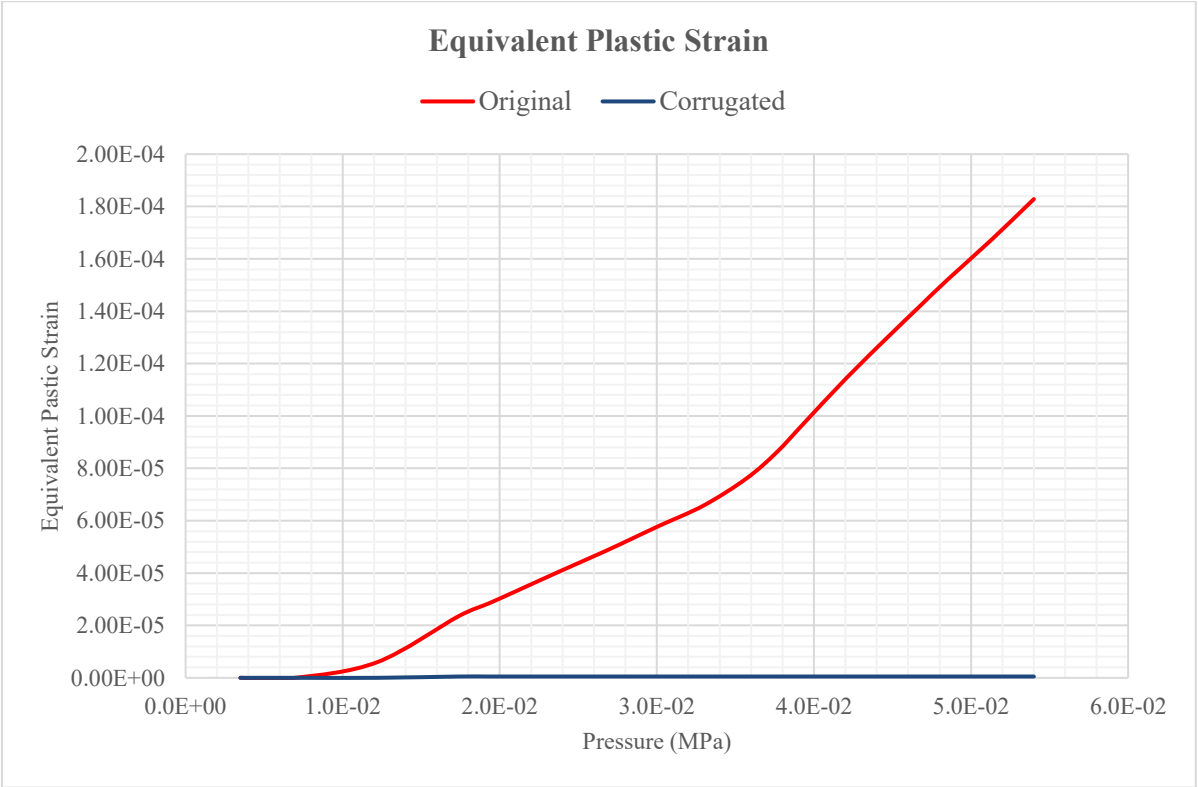

(b) Maximum equivalent plastic strain during load application

Figure 6.16: Post-accident equivalent plastic strain results

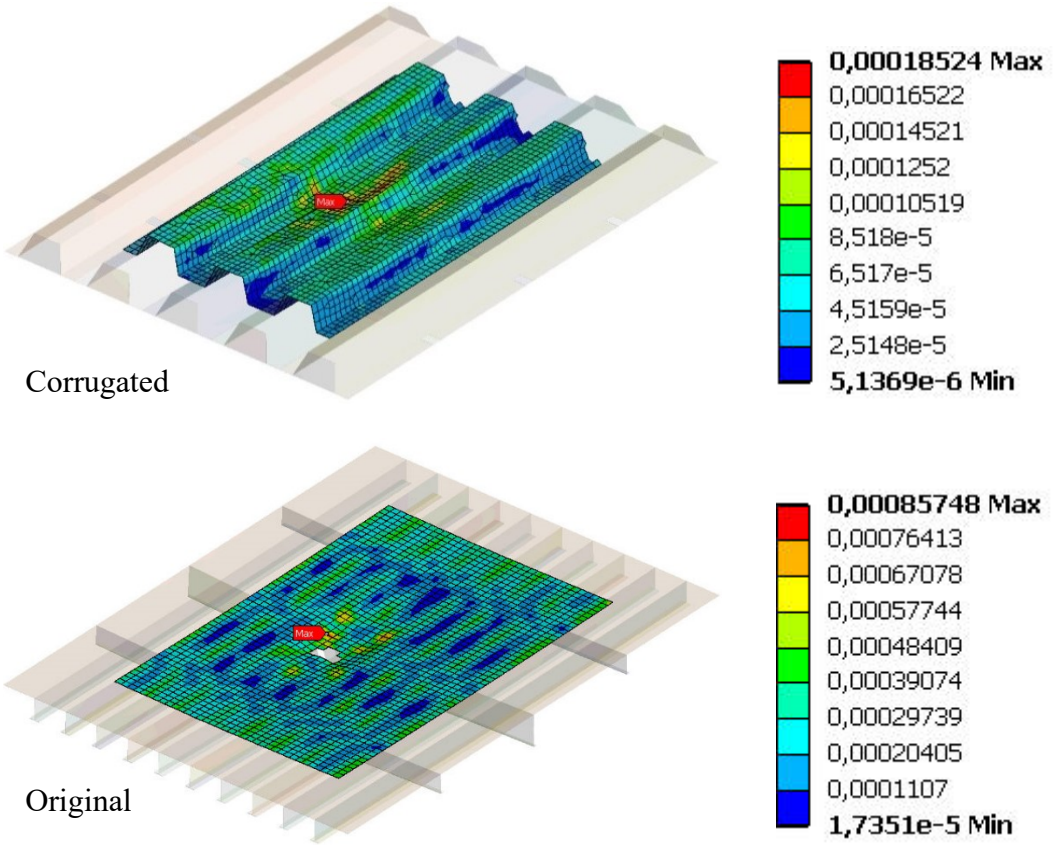

(a) Overall equivalent total strain distribution at maximum load

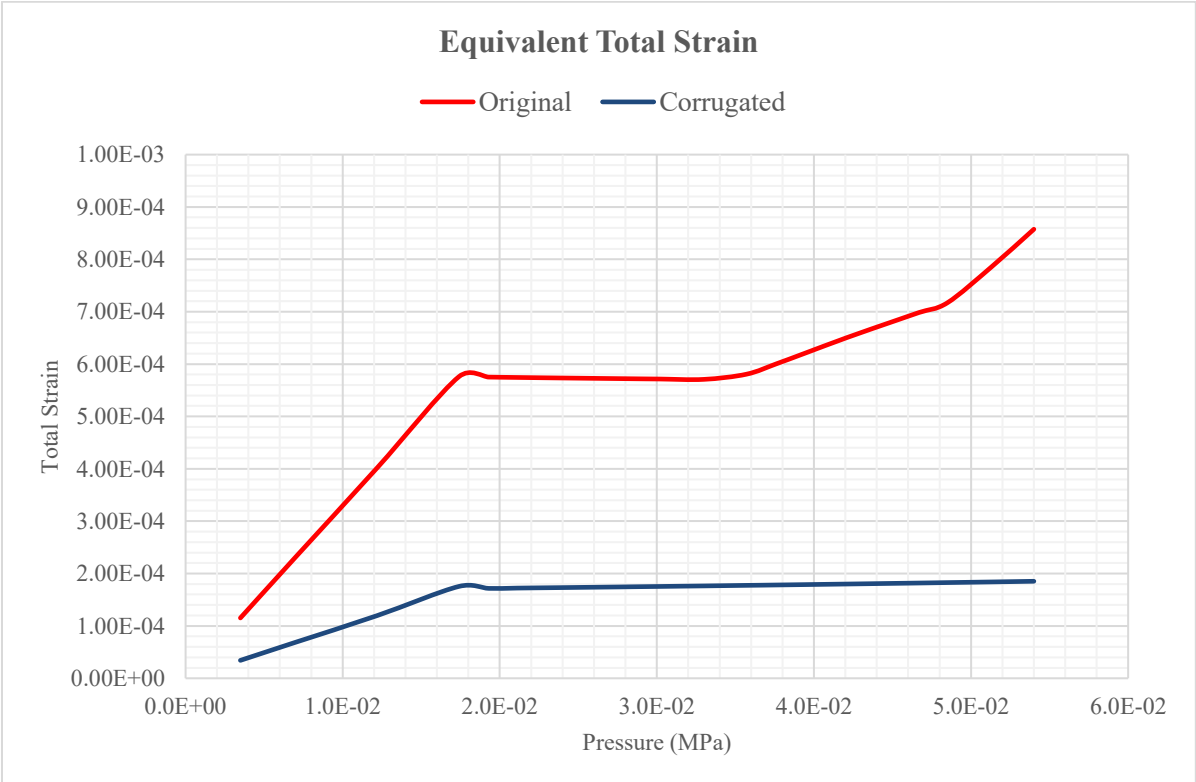

(b) Maximum equivalent total strain during load application

Figure 6.17: Post-accident equivalent total strain results

6.6 Review and Discussion

Regarding the operational and financial benefits of hatch cover weight reduction, it is aimed to propose a lighter and still resilient new hatch cover design. The structural configuration with the optimum weight-performance result is selected among four different options which are generated based on section modulus approach. The structural response under impact load and post-accident performance of the new design are investigated and compared with the original structure.

Although the new hatch cover design experiences higher deformation under static design pressure; its performance is satisfactory, considering the advantage of 38% weight reduction. Explicit dynamic analysis results confirm that the response of the new design against impact load has similar pattern with the original structure's and an even better plastic strain range is achieved. Moreover, significantly better results are obtained in post-accident simulations of the new hatch cover configuration.

The findings of this study suggest that the proposed hatch cover design could be an optimal alternative to the customary hatch covers; when its competitive structural performance, maintenance ease and advantages of weight reduction are taken into account.

7. CONCLUSION AND FUTURE WORK

This thesis has three main goals as set out in Chapter-1; investigating post-accident load carrying capacity of a damaged hatch cover due to impact forces, verifying the capabilities of selected engineering environment for such sophisticated simulation chains and proposing an alternative hatch cover design concept.

The analyses and comparative studies that are undertaken within the framework of the thesis, lead the following conclusions:

- Ansys Explicit Dynamics analysis system is employed for dropped object simulation which is chosen as the accidental case. Chapter-2 is dedicated for the verification of the tool and the method through a comparative work with previous experiments [24]. The satisfactory agreement between the results of experiment and simulation, confirms the validity of the method and the preferred engineering environment.
- Impact forces, such as in dropped object cases, may cause catastrophic consequences within the exposed structures. Especially in nonlinear analysis in plastic range, in which structural failure is of interest, it is crucial to simulate the case properly without unnecessary simplifications. The explicit dynamic analyses in this thesis show that, employing element erosion function of the tool based on the relevant failure criteria leads to notable differences in damage form. Additionally, the comparison between the simulations of dropped object with free-fall pattern and projectile motion, emphasises that modelling the type of impact is highly important. The results of impact with projectile motion demonstrate that the structure loses its watertightness which is one of main functions of hatch covers, due to the rupture on the top plate.
- Traditionally post-accidental load carrying analyses of damaged structures are conducted via simple damage modelling techniques, such as removal of the assumedly deformed region or application of different slenderness ratios. Nevertheless, there are some researches which focus on simulating the damage and considering residual stresses. This thesis takes one step further by exploring more realistic damage modelling techniques and considering not only residual stresses but also residual plastic strains. The post-accidental simulations indicate that including residual plastic strains is not highly effective on deformation and stress results of further static analyses. On the other hand, plastic strain results seem to be influenced strongly. Therefore, it is recommended to handle residual plastic strain parameter sensitively,

according to the nature and the purpose of the analyses. Moreover, the simulations in this thesis demonstrate the cruciality of the accurate and sufficiently detailed damage modelling for post-accident evaluations. Simplifications such as neglecting the impact pattern or preserving failed elements within the structure could lead to deceptive results.

- The applicability of the selected engineering environment for such sophisticated analyses is verified by successfully conducting a chain of analyses that constitutes dynamic damage simulations, transfer of the deformed geometry together with residual stresses-strains and nonlinear static analyses. Thus, a practical, accurate and prompt approach is presented for post-accident evaluations.
- Due to their function for vessel/cargo safety and influence on production and operation costs hatch covers can be considered as one of the critical parts of ships. By means of the proposed hatch cover design concept, it is possible to achieve 38% weight reduction and a competitive structural performance, in addition to production and maintenance ease, while ensuring cost efficiency. The findings of this thesis support the idea that the new concept could be an innovative alternative to the conventional pontoon hatch covers.

Although, a substantive work is presented in this thesis, it is recommended that further research should be conducted for the following aspects:

- The influence of residual plastic strain on post-accidental performance is investigated in this thesis. Further research should validate these initial findings and establish a precise conclusion.
- The post-accident load carrying performance of the damaged hatch cover is evaluated under the calculated design and collapse load according to ICLL 1966 [29] regulations. Determination of the real collapse load could be an important question to resolve for future studies.
- A new hatch cover design is proposed as a concept in this thesis. Next studies could focus on the elaboration of the concept, optimum scantling, production cost assessment and applicability in the industry.

REFERENCES

[1] UNCTAD. 2020. Review of Maritime Transport 2020.

[2] EMSA. 2021. Annual Overview of Marine Casualties and Incidents 2021.

[3] UK Parliament Commons Debates. 2000. MV Derbyshire. Vol:356.

[4] Paik JK & Thayamballi AK. 1998. The Strength and Reliability of Bulk Carrier Structures Subject to Age and Accidental Flooding. *Society of Naval Architects and Marine Engineers*, Vol:106: 1-40.

[5] Paik JK, Thayamballi AK & Yang SH. 1998. Residual Strength Assessment of Ships After Collision and Grounding. *Marine Technology*, Vol: 35(1): 35-54.

[6] Paik JK, Kim DK, Park DH & Kim HB. 2012. A New Method for Assessing the Safety of Ships Damaged by Grounding, *RINA Transactions*, Vol: 154, Part A1.

[7] Underwood JM. 2013. Strength Assessment of Damaged Steel Ship Structures. *PhD Thesis,* University of Southampton.

[8] Alie MZM, Sitepu G, Sade J, Mustafa W, Nugraha AM & Saleh ABM. 2016. Finite Element Analysis on the Hull Girder Ultimate Strength of Asymmetrically Damaged Ships. *Proceedings of ASME 2016 35th International Conference on Ocean, Offshore and Arctic Engineering*, Busan, South Korea, Vol:3: 161-175.

[9] Soares CG, Luis RM, Nikolov P, Downes J, Taczala M, Modiga M, Quesnel T, Toderan C & Samuelides M. 2008. Benchmark Study on the Use of Simplified Structural Codes to Predict the Ultimate Strength of a Damaged Ship Hull *International Shipbuilding Progress*, Vol:55(1-2): 87-107.

[10] Eldeen SS, Garbatov Y & Soares CG. 2016. Ultimate Strength Analysis of Highly Damaged Plates. *Marine Structures*, Vol:45: 63-85.

[11] Witkowska M & Soares CG. 2015. Ultimate Strength of Locally Damaged Panels. *Thin-Walled Structures*, Vol:97: 225-240.

[12] Smith CS & Dow RS. 1981. Residual Strength pf Damaged Steel Ships and Offshore Structures. *Journal of Constructional Steel Research*, Vol:1(4): 2-15.

[13] Nikolov P. 2008. Collapse Strength of Damaged Plating. *Proceedings of ASME 27th International Conference on Ocean, Offshore and Arctic Engineering,* Estoril, Portugal, Vol:2: 79-88.

[14] Cai J, Jiang X & Lodewijks G. 2015. Ultimate Strength of Damaged Stiffened Panels Subjected to Uniaxial Compressive Loads Accounting for Impact Induced Residual Stress and Deformation. *Proceedings of ASME 2015 34th International Conference on Ocean, Offshore and Arctic Engineering,* Newfoundland, Canada, Vol:3.

[15] Faulkner D. 1998. An Independent Assessment of the Sinking of the MV Derbyshire. *SNAME Transactions*, Vol:106: 59-103.

[16] Dallinga R & Gaillarde G. 2001. Hatch Cover Loads Experienced by M.V. Derbyshire During Typhoon "Orchid". *Glasgow Marine Fair And International Workshop On Safety Of Bulk Carriers,* Glasgow, Scotland.

[17] Yao T, Magaino A, Koiwa T & Sato S. 2003. Collapse Strength of Hatch Cover of Bulk Carrier Subjected to Lateral Pressure Load. *Marine Structures*, Vol:16: 687-709.

[18] Mohammadrahimi A & Sayebani M. 2020. Failure Probability and Reliability of Hatch Cover of Bulk Carrier Subjected To Lateral Pressure Load. *International Journal of Innovative Technology and Exploring Engineering*. Vol:9(8).

[19] Li J, Wu N, Tang Y, Zhao C, Li D, Lin W & Liang F. 2012. Application of Composite Materials to Large Marine Hatch Cover. *Advanced Materials Research* Vol:560-561: 809-815.

[20] Tawfik BE, Leheta H, Elhewy A & Elsayed T. 2016. Weight Reduction and Strengthening of Marine Hatch Covers by Using Composite Materials. *International Journal of Naval architecture and Ocean Engineering,* Vol:9(2): 185-198.

[21] MacGregor. Cargo Handling Book.

[22] Um TS & Roh MI. 2015. Optimal Dimension Design of a Hatch Cover for Lightening a Bulk Carrier. *International Journal of Naval Architecture and Ocean Engineering*, Vol:7(2): 270-287.

[23] Shi GJ & Gao DW. 2020. Ultimate Strength of U-Type Stiffened Panels for Hatch Covers Used in ship Cargo Holds. *Ships and Offshore Structures*, Vol: 16(3): 280-291.

[24] Kim KJ, Lee JH, Park DK, Jung BG, Han X & Paik JK. 2016. An Experimental and Numerical Study on Nonlinear Impact Responses of Steel-Plated Structures in an Arctic Environment. *International Journal of Impact Engineering*. Vol:93: 99-115.

[25] Nelson T & Wang E. 2004. Reliable FE-Modeling with Ansys. *International ANSYS Conference*, Pittsburgh, USA.

[26] ANSYS INC. 2021. Workbench User`s Guide Release 2021 R1.

[27] Babicz J. 2015. Wartsila Encyclopaedia of Ship Technology. *Wartsila Corporation*, Helsinki, Finland.

[28] MacGregor. MacGregor History and Milestones. Retrieved in February 2021. https://www.macgregor.com/about-us/history/

[29] IMO. 1966. International Convention on Load Lines.

[30] IACS. 2011. Requirements Concerning Strength of Ships S21A.

[31] Buxton IL, Daggitt RP & King J. 1978. Cargo Access Equipment for Merchant Ships. *MacGregor Publications*, London, UK.

[32] Marine Radio Museum. Merchant Navy Casualties in World War II. Retrieved in January 2022 http://www.mrmsw.co.uk/not%20forgotten.html

[33] Paik JK, Seo JK & Kim BJ. 2008. Ultimate Limit State Assessment of the M.V. Derbyshire Hull Structure. *Journal of Offshore Mechanics and Arctic Engineering*, Vol: 130(2).

[34] Akkus Ö. 2011. Longitudinal Strength Analysis of Bulk Carriers During Loading and Unloading Operations. *MSc Thesis*, Istanbul Technical University (in Turkish).

[35] Tarman D & Heitmann E. Case Study II: Derbyshire Loss of a Bulk Carrier. *Ship Structural Commitee*.

[36] DNV GL AS. 2017. DNVGL-RP-C204 Recommended Practice - Design Against Accidental Loads.

[37] Akkus Ö & Kaeding P. 2019. Impact Analysis in an Engineering Environment. *Ships and Offshore Structures*, Vol:14(1): 231-238.

[38] Zhang L. Egge ED & Bruhns H. 2004. Approval Procedure Concept for Alternative Arrangements. *3rd International Conference on Collision and Grounding of Ships*, Tokyo, Japan.

[39] ANSYS INC. 2022. Element Reference Release 2022 R1.

[40] Paik JK & Thayamballi AK. 2003. Ultimate Limit State Design of Steel-Plated Structures. *John Wiley and Sons*, Chichester, UK.

[41] Paulling JR. Principles of Naval Architecture.

[42] DNV GL AS. 2019. DNVGL-OS-A101 Offshore Standards - Safety Principles and Arrangements.

[43] Madenci E & Güven I. 2015. The Finite Element Method and Applications in Engineering Using ANSYS. *Springer New York,* USA.

[44] DNV GL AS. 2016. DNVGL-RP-C208 Recommended Practice – Determination of Structural Capacity by Non-Linear Finite Element Analysis Methods.

[45] ANSYS INC. 2022. Ansys Explicit Dynamics Analysis Guide Release 2022 R1.

[46] Beidokhti HN, Janssen D, Khosgoftar M, Sprengers A, Perdahcioglu ES, Boogard TV & Verdonschot N. 2016. A Comparison between Dynamic Implicit and Explicit Finite Element Simulations of the Native Knee Joint. *Medical Engineering and Physics,* Vol:38: 1123-1130.

[47] ANSYS INC. 2021. Material Reference 2021 R1.

[48] Ceylan I. 2008. Finite Element Analysis of Plastic Deformations Determined by Material Laws for Metals. *MSc Thesis*, Istanbul Technical University (in Turkish).

[49] Cowper GR & Symonds PS. 1957. Strain-Hardening and Strain-Rate Effects in the Impact Loading of Cantilever Beams. *Technical Report No:28*, Division of Applied Mathematics, Brown University.

[50] Paik JK & Chung JY. 1999. A Basic Study on Static and Dynamic Crushing Behavior of a Stiffened Tube. *KSAE Transactions,* Vol: 7(1): 219–238.

[51] Liu K, Liu B, Soares CG & Wang Z. 2016. Experimental and Numerical Analysis of a Laterally Impacted Square Steel Plate. *Proceedings of the 3rd International Conference on Maritime Technology and Engineering,* Lisbon, Portugal.

[52] Scharrer M, Zhang L & Egge ED. 2002. Final Report MTK0614, Collision Calculations in Naval Design Systems, Report Number: ESS 2002.183, Version 1/2002-11-22, *Germanischer Lloyd*, Hamburg.

[53] Ehlers A, Broekhuijsen J, Alsos HS, Biehl F & Tabri K. 2008. Simulating the Collision Response of Ship Side Structures: A Failure Criteria Benchmark Study. *International Shipbuilding Progress*, Vol: 55(1-2): 127-144.

[54] Ehlers S. 2010. A Procedure to Optimize Ship Side Structures for Crashworthiness. *Proceedings of the Institution of Mechanical Engineers*, *Part M: Journal of Engineering for the Maritime Environment*, Vol: 224: 1-11.

[55] Hughes OF & Paik JK. 2010. Ship Structural Analysis and Design. *The Society of Naval Architects and Marine Engineers*, New Jersey, USA.

[56] Akkus Ö, Kaeding P & Bayraktarkatal E. 2021. Post-Accident Load Carrying Performance of a Deformed Hatch Cover. *6th International E-conference on Engineering, Technology and Management*.

[57] Youssef SAM, Noh SH & Paik, JK. 2017. A New Method for Assessing the Safety of Ships Damaged by Collisions. *Ships and Offshore Structures*, Vol: 12(6): 862-872.

[58] Huh H, Song JH, Kim KP & Kim HS. 2005. Crashworthiness Assessment of Auto-Body Members Considering the Fabrication Histories. *AIP Conference Proceedings*, Vol: 778(1): 167-172.

[59] Kim KP & Huh H. 2003. Collapse Analysis of Auto-Body Structures Considering the Effect of Fabrication. *Key Engineering Materials*, Vol: 233-236: 737-742.

[60] Bathe KU. 1996. Finite Element Procedures. *Prentice Hall, Pearson Education, Inc*. USA.

[61] ANSYS INC. 2021. Theory Reference Release 2021 R2.

[62] ANSYS INC. 2021. Mechanical User`s Guide 2021 R1.

[63] Kunal K, Kannan C & Surendran S. 2010. Hatch Cover Analysis of Capesize Bulk Carriers and Suggestions for Alternate Materials. *Proceedings of International Conference on Marine Technology*, Dhaka, Bangladesh.

[64] Boersma PC. 2017. Sandwich Plate Systems – The Application of Sandwich Plate Systems as Impact Protection in Offshore Structures. *MSc Thesis*. Delft University of Technology.

[65] Markulin M. 2012. Structural Design of Transverse Bulkhead of a Handymax Bulk Carrier Built in Steel Sandwich Panels. *MSc Thesis*. EMSHIP – Erasmus Mundus Master Course.

[66] IACS. 2014. Common Structural Rules.

[67] RBM Hold Solutions. 2020. Can a Load of Petcoke Damage a Ship Hold?. Retrieved in January 2022. https://www.holdsolutions.com/blog/can-a-load-of-petcoke-damage-a-ship-hold

[68] Caldwell JB. 1955. The Strength of Corrugated Plating for Ship`s Bulkheads. *Transactions of the Royal Institution of Naval Architects*, Vol:97: 495-522.

[69] Paik JK, Thayamballi AK & Chun MS. 1997. Theoretical and Experimental Study on the Ultimate Strength of Corrugated Bulkheads. *Journal of Ship Research*, Vol:41(4): 301-317.

[70] DNVGL. 2017. Rules for Classification - Part 3 Hull, Chapter 3 Structural Design Principles.